The effects of nature-based solutions on high- and low flows in the Vecht river basin

Master Thesis

Ivan Leegwater

Enschede, January 2025

UNIVERSITY OF TWENTE.

JCAR ATRACE

Deltares
Enabling Delta Life

The effects of nature-based solutions on high- and low flows in the Vecht river basin

Master Thesis

Enschede, January 2025

to obtain the degree of Master of Science at the University of Twente
to be presented on January 23, 2025

Author:

I. (Ivan) Leegwater ivanleegwater@hotmail.nl

Supervised by:

Dr. Ir. M.J. (Martijn) Booij University of Twente

Prof. Dr. J.C.J. (Jaap) Kwadijk University of Twente & Deltares

Ir. A.C. (Angela) Klein Deltares

UNIVERSITY OF TWENTE.

JCAR ATRACE

Deltares
Enabling Delta Life

Preface

This master's thesis marks the final step in completing my Master Civil Engineering and Management at the University of Twente. The research, titled *The Effects of Nature-Based Solutions on High- and Low Flows in the Vecht River Basin*, was conducted in collaboration with Deltares and is part of the JCAR-ATRACE research programme[1].

During my bachelor's and master's studies in Civil Engineering at the University of Twente, I developed a strong interest and passion for water management, which made choosing this thesis topic during my search for a graduation project an easy decision. Throughout this project, I have benefited greatly from the insightful discussions during the weekly meetings with Angela Klein and Jaap Kwadijk. I would like to sincerely thank them for their guidance and the pleasant experience at Deltares. I would also like to thank Ferdinand Diermanse, Sebastian Hartgring and the colleagues in the Flood Risk Management Department at Deltares for their support and cooperation.

My interest in hydrology was mainly sparked by the courses of my internal supervisor at the University of Twente, Martijn Booij. I really appreciate all our meetings and his valuable feedback, which has greatly improved the quality of this thesis throughout the process.

Working with the hydrological model LISFLOOD-OS, which was new to me, was a challenge I was eager to take on. I would like to thank Julia Kraatz for her support in introducing me to this model and helping me to get to know it better. I am also very grateful to Stefania Grimaldi from the Joint Research Centre for her endless patience in answering my many questions over countless emails. Without your help, it would not have been possible to get this model up and running.

Jeroen van der Scheer from Waterschap Vechtstromen, thank you for sharing your data and knowledge about the Vecht River. Your insights and contributions have hopefully ensured that this work also provides added value to the waterboard. I also want to thank William and Sander for the enjoyable time and great collaboration during our joint graduation work at Deltares. I believe the three of us greatly benefited from working together, and I hope our contributions make a positive impact.

Finally, I would like to thank my parents and family for their endless patience, trust, and interest in my studies over the past years. I also want to express my gratitude to all my (study) friends, club members, housemates, and, most importantly, my girlfriend Welmoed for making my time in Enschede so wonderful. Without your support, I would not have made it this far. A special thanks also goes to the friends and family who offered me a place to stay during my graduation period in Delft, allowing me to start each day well-rested and ready to work.

I hope you enjoy reading this thesis as much as I did working on it!

Ivan

Enschede, January 2025

[1] https://www.jcar-atrace.eu/

Summary

Climate change is leading to increased frequency and severity of extreme weather events worldwide, including intense rainfall and prolonged droughts. These events disrupt water systems, cause significant economic losses and threaten communities worldwide. In Europe, the devastating floods of July 2021 caused widespread damage and fatalities, while recurrent droughts, such as in 2018 and 2022, have severely affected agriculture and water availability. These extremes highlight the urgent need for measures to mitigate the negative impacts of high flows, such as flooding and erosion, and low flows, such as water scarcity. Nature-based solutions (NBS) have emerged as a promising alternative to traditional infrastructure, leveraging natural processes to reduce flood risk and increase resilience to drought. However, large-scale testing of NBS is often impractical, and modelling their effects using hydrological models remains challenging.

This study focuses on quantifying the effects of nature-based solutions on high and low flows in the Vecht catchment, which is located in Germany and the Netherlands. This was done using the distributed hydrological model LISFLOOD-OS, which was calibrated and validated using historical weather and discharge data. Afforestation and soil improvement measures were then parameterised, and potential implementation scenarios were developed based on their feasibility in the Vecht catchment. Finally, their effects on high and low flows were evaluated through changes in flow indicators and water balance components.

Although certain limitations were evident, the LISFLOOD-OS model showed acceptable performance in simulating high and low flows in the Vecht catchment. Calibration was guided by a multi-objective function that included the weighted Nash-Sutcliffe efficiency for high flows, the inverse Nash-Sutcliffe efficiency for low flows, and the relative volume error (RVE), targeting the total water balance, respectively. The model performed better for simulating high flows, while low flows were less accurately represented. Deviations in RVE highlighted inconsistencies in the water balance simulation, with over- or under-estimation varying between sub-catchments. Performance was significantly better in the less regulated German part of the catchment than in the more managed Dutch part.

The simulation of 11 different NBS scenarios in the LISFLOOD-OS model demonstrated clear potential for NBS to mitigate the effects of extreme hydrological events in the Vecht catchment. Afforestation, as parametrised by adjustments to land use, vegetation, and soil parameters in the model, significantly reduced peak flows, particularly during summer rainfall, due to increased infiltration and interception capacity. However, its effectiveness according to the LISFLOOD-OS model was highly dependent on the scale of implementation, with significant reductions observed only when applied over large areas, in contrast to current policy plans to increase forest cover by 10% of the existing forest area. Measures targeted at agricultural land, such as soil aeration and conservation tillage, offered more practical potential given the extensive availability of farmland. These measures, parameterised by adjusting soil hydraulic properties, effectively increased infiltration and reduced surface runoff during high-intensity rainfall events, making them a promising option. Despite these benefits, afforestation and soil improvement measures showed minimal impact on low flows, with only slight increases in baseflow due to limited contributions from deeper soil layers.

Future research should address the uncertainties inherent in the parameterisation of NBS and their representation in hydrological models. Incorporating realistic climate change scenarios in future modelling efforts is also crucial to assess the long-term effectiveness of NBS. While cross-model comparisons can provide valuable insights into the sensitivity of results to model frameworks and assumptions, going a step further with a multi-model ensemble approach could help to leverage the strengths of different models. Such an approach would provide a more robust and comprehensive understanding of the impacts of NBS, thereby contributing to the refinement of implementation strategies and enhancing decision-making processes for integrated water resources management.

Keywords: Nature-based solutions, LISFLOOD-OS, Vecht, hydrological modelling, flood risk mitigation, drought resilience, climate change adaptation, hydrology

Table of Contents

List of Symbols

Symbol	Description	Unit
LISFLOOD-OS calibration parameters		
C_m	Snow melt rate in degree day model equation.	mm/(C day)
b	Exponent in Xinanjiang equation for infiltration capacity of the soil.	-
C_{pref}	Exponent in the empirical function describing the preferential flow (i.e. flow that bypasses the soil matrix and drains directly to the groundwater).	-
T_{uz}	Time constant for upper groundwater zone.	days
GW_{perc}	Maximum percolation rate from upper to lower groundwater zone.	mm/day
T_{lz}	Time constant for lower groundwater zone.	days
$LZ_{threshold}$	Threshold to stop outflow from lower groundwater zone to the channel.	mm
GW_{loss}	Maximum loss rate out of lower groundwater zone expressed as a fraction of lower zone outflow.	mm/day
QsplitMult	Multiplier to adjust discharge triggering floodplains flow.	-
CalChanMan1	Multiplier for channel Manning's coefficient *n* for riverbed.	-
CalChanMan2	Multiplier for channel Manning's coefficient *n* for floodplains.	-
$AdjL_n$	Multiplier to adjust reservoir normal filling (balance between lower and upper limit of reservoir filling).	-
$ResMultQ_{norm}$	Multiplier to adjust normal reservoir outflow.	-
α	Multiplier to adjust lake outflow.	-
Multi-objective function		
n	Total number of timesteps	-
Q_{sim}	Simulated discharge at time step *i*	m^3/s
Q_{obs}	Observed discharge at time step *i*	m^3/s
NS_w	Weighted form of the Nash-Sutcliffe Efficiency	-
NS_{inv}	Nash-Sutcliffe criterion calculated on inverse transformed flows	-
RVE	Relative Volume Error	%
y_{comb}	Multi-objective function for high and low flows	-
LISFLOOD-OS parameters adjusted to integrate effects of NBS		
fracforest	Forest fraction for each grid-cell	-
fracother	Other land cover type fraction for each grid-cell	-
fracwater	Inland water fraction for each grid-cell	-
fracsealed	Urban surface fraction for each grid-cell	-
mannings_forest (mannings_f)	Manning's roughness for forested area	$m^{1/3}\ s^{-1}$
ksat1_forest (ksat1_f)	Saturated conductivity for forested area; first soil layer	mm/day
ksat1_other (ksat1_o)	Saturated conductivity for other area; first soil layer	mm/day
thetas1_other (thetas1_o)	Saturated volumetric soil moisture content for other area; first soil layer	m^3/m^3
ksat2_forest (ksat2_f)	Saturated conductivity for forested area; second soil layer	mm/day
ksat2_other (ksat2_o)	Saturated conductivity for other area; second soil layer	mm/day
thetas2_other (thetas2_o)	Saturated volumetric soil moisture content for other area; second soil layer	m^3/m^3
Indices		
Q_{max}	Maximum daily discharge	m^3/s
MAM7	Minimum average 7-day discharge	m^3/s
Q_{mean}	Average discharge	m^3/s

1. Introduction

1.1. Problem Context

Climate change is altering weather patterns worldwide, increasing the frequency of extreme events such as heavy rainfall and prolonged droughts (Bessembinder et al., 2023). These events cause extreme high and low river flows, disrupting water systems and posing significant challenges to communities worldwide. Such extremes have also been observed in north-western Europe in recent years, with the floods of July 2021 being one of the most devastating natural disasters in the region's recent history (European Centre for Disease Prevention and Control, 2021). Multiple countries, including Germany, Belgium, the Netherlands, and Luxembourg, were severely impacted by the floodwaters, resulting in extensive destruction. Homes, buildings, roads, bridges, and other crucial infrastructure were completely washed away or damaged. Furthermore, the flood resulted in over 200 casualties and forced thousands of individuals out of their homes, leaving them without shelter or basic necessities (Koks et al., 2022).

The July 2021 flood event was not the sole extreme hydroclimatic event that Western Europe has faced recently. In 2018 and 2022, the region experienced significant droughts that had severe consequences (Beillouin et al., 2020; Toreti et al., 2022). These droughts resulted in substantial water shortages, particularly in agricultural areas, leading to crop failures and declining food production. The impact on water supply led to certain regions implementing water usage restrictions (Joint Research Centre, 2022).

The July 2021 flood resulted in approximate damages of 32 billion euros (Mohr et al., 2023). The consequences for businesses have been severe, as many now face financial challenges due to the direct and indirect harm caused. The economic effects of extreme droughts, such as reduced crop yields, remain uncertain (Beillouin et al., 2020). From 1980 to 2020, weather- and climate-related incidents, such as floods and droughts, led to cumulative economic losses totalling 450-520 billion EUR across the 32 member countries of the European Environment Agency (EEA), with the most severe 3% of events contributing to 60% of the damages (European Environment Agency, 2022). Evaluations conducted in various countries concerning these events emphasised the requirement for enhanced water management strategies, as well as measures for disaster preparedness and response measures.

Extreme weather events have shown the importance of effective water resource management in the Netherlands and other European countries (Slager & Kwadijk, 2023). Recent research suggests that climate changes in Europe are happening faster than the global average (Copernicus & World Meteorological Organization, 2022), and highlights a lack of preparedness in our societies (Berrang-Ford et al., 2021). Adapting to these changes will require considerable time. Scientists and the EU stress the need for enhanced cooperation among researchers, practitioners, and policymakers to speed up the adaptation process. This has reignited the call for a more integrated approach to managing river basins at national and regional levels (Slager & Kwadijk, 2023).

It is crucial for the countries involved to adjust and prepare for the changes as effectively as possible. There are various options for adapting to the changing climate and its impacts on the environment (Haasnoot & Diermanse, 2022). The focus of possible solutions is shifting from the traditional grey infrastructure, such as dikes and dams, to more integrative strategies that not only offer protection but also enhance biodiversity and ecosystem services (Van Zanten et al., 2023). These measures are referred to as "nature-based solutions" (NBS). It is essential to ensure that these NBS offer protection against the effects of climate change. However, because of the large scale at which these measures generally must be applied to have an impact and the potential risks involved in implementing such measures, it is impossible to test them at the scale of a river basin. To determine whether NBS have the desired effect on hydrological processes within a catchment, including runoff, their effects must be simulated. This involves using hydrological models to replicate how these measures affect hydrological processes in a river basin. Such modelling helps to understand whether NBS can provide the desired protection against floods and alleviate the adverse effects of prolonged drought and low flows.

1.2 State-of-the-art

1.2.1. Nature-based solutions

The United Nations define nature-based solutions as "actions to protect, conserve, restore, sustainably use and manage natural or modified terrestrial, freshwater, coastal and marine ecosystems, which address social, economic and environmental challenges effectively and adaptively, while simultaneously providing human well-being, ecosystem services and resilience and biodiversity benefits" (United Nations Environment Programme, 2022). From this definition, it already becomes clear that the term "nature-based solutions" is an umbrella term, being broad and vague. Van Zanten et al. (2023) refer to NBS for climate resilience as integrative strategies to reduce climate risks while at the same time enhancing biodiversity and ecosystem services. They can include various measures to prevent or adapt to hazards like flooding, heat stress, droughts, landslides, and erosion. Table 1 shows an overview of groups of NBS identified by Raška et al. (2022). Within each group, multiple types of measures and interventions for adaptation and disaster risk reduction are reported in the literature.

Table 1: Groups of nature-based solutions identified in literature; adapted from Raška et al. (2022).

Nature-based solution groups	
Floodplain retention and polders	Wetlands
River restoration	Nature-based river dams
Spatial water retention in urban areas	Channel alterations and diverging flows
Improving soil conditions	Small retention ponds, pools and lakes
Urban water sensitive buildings	Coastal measures
Improving policies for NBS coordination and planning	Land use & land cover changes

Nature-based solutions face several barriers that limit their use in flood risk management. A significant challenge is the uncertainty of their effectiveness, as the results of NBS vary widely depending on local conditions such as topography, vegetation, soil, and spatial layout (Raška et al., 2022). Conflicting research findings for measures such as improving soil conditions and land use change, add to this uncertainty. For example, while some studies highlight the role of afforestation in reducing flood risks, others show limited effects or significant variation due to factors such as rainfall interception and soil permeability (Bezak et al., 2021; Danáčová et al., 2020; Dunn et al., 2011; Zabret & Šraj, 2015). These uncertainties make it difficult to predict the performance of NBS in different environments, discouraging investment and planning.

Institutional and financial issues, along with the limitations in resources, land and physical capability, further hinder the uptake of NBS. High costs and a lack of financial incentives discourage stakeholders, especially when flood recovery schemes do not cover adaptive measures (Slavíková et al., 2021). In addition, the need for extensive land areas for measures such as river restoration or afforestation poses challenges in densely populated regions, where landowners may resist changes that reduce productive land use. Complex institutional frameworks, unclear responsibilities and limited support for co-designing NBS with communities also limit progress (Snel et al., 2020; Han & Kuhlicke, 2019).

1.2.2. Quantifying effects of nature-based solutions

Overcoming the challenge of uncertainty in the effectiveness of NBS requires robust methods to quantify their impacts on high and low flows. This requires incorporating these measures into model data and parameters, though a standardised methodology remains lacking (Kumar et al., 2021). Kumar et al. (2021) reviewed tools for assessing NBS effectiveness in mitigating hydro-meteorological risks and emphasised that model selection depends on factors such as NBS typology, scale, data availability, and project resources. The scale of NBS is crucial in model choice, as high-resolution models are essential for small-scale interventions but are often less suited for large-scale, catchment-level assessments.

Effective modelling of NBS impacts requires simulating runoff generation influenced by interaction between vegetation, meteorological conditions, groundwater, and surface water (Ávila et al., 2022; Trautmann et al., 2021). To assess the effects of NBS under drought conditions, it is essential that the models can adequately simulate the interaction between unsaturated and saturated flows, as well as the influence of underground water on NBS to maintain subsurface water flows (Ávila et al., 2022). As droughts typically occur at the catchment scale, the models should be capable of evaluating the performance of NBS implemented for drought risk at this scale (Kumar et al., 2021).

Based on his literature review, Cazemier (2024a) has identified several hydrological models that he believes are suitable for modelling nature-based solutions. Recommended hydrological models include: Wflow sbm (Deltares, 2021), VIC (University of Washington Computational Hydrology Group, 2021), LISFLOOD-OS (De Roo et al., 2000), Dynamic TOPMODEL (Beven & Freer, 2001) and WRF-Hydro (Gochis et al., 2020).

1.2.3. Hydrological models

A hydrological model is a simplified representation of real-world hydrological systems, crucial for predicting hydrologic responses in water resource management, flood control, and water quality assessment (Yoosefdoost et al., 2022). As such, these models can be valuable for assessing the potential impacts of NBS on hydrological processes. This study focuses on rainfall-runoff models, a type of hydrological model that simulates the transformation of rainfall into runoff in a catchment (Sitterson et al., 2018). In a rainfall-runoff model, the catchment characteristics are described by the model parameters. Hydro-climatic time series, including data on precipitation, potential evapotranspiration and temperature, are the primary forcing data.

Hydrological models vary in complexity, scalability, and spatial representation. They are commonly categorised by their structure, which describes the extent to which they incorporate physical processes: empirical, conceptual or physically based (Dwarakish & Ganasri, 2015). Empirical models rely on data without considering physical processes, providing quick runoff estimates but limited transparency regarding the physical processes (Jaiswal et al., 2020). Conceptual models use simplified representations of hydrological processes, balancing ease of calibration with more accurate process descriptions (Yoosefdoost et al., 2022). Physically-based models simulate hydrological processes using detailed physical relationships and can incorporate spatial and temporal variability, though they require extensive site-specific data and calibration (Yoosefdoost et al., 2022).

Models also differ in spatial representation: lumped, semi-distributed, and fully distributed approaches (Sitterson et al., 2018). Lumped models treat the catchment as a single unit, averaging inputs across the entire area, which allows quick computations but limits spatial accuracy, especially over large areas. Semi-distributed models account for regional variability by distributing lumped parameters across sub-catchments, enhancing accuracy but still averaging within each region. Fully distributed models divide the catchment into grid-cells, capturing detailed spatial variability, though they demand significant data and computation time (Yoosefdoost et al., 2022).

1.3. Research Gap

The July 2021 floods were not an isolated event, and due to climate change, the likelihood of extreme weather events is increasing worldwide (Chen et al., 2023). The shift in focus from traditional grey measures to nature-based solutions is leading to a demand from policymakers for clarity on the effects of such measures (Van Zanten et al., 2023). The previous discussion has shown a wide range of possible NBS, but there are still several barriers that make implementation difficult in practice. One of the most important barriers is the fact that the exact effects are uncertain (Raška et al., 2022). Existing literature tends to focus on assessing the impact of small-scale NBS instead of the implementation of NBS on a larger scale (Ruangpan et al., 2020).

In addition, much of the literature focuses on the role of NBS in reducing flood risks, while their potential to mitigate the impacts of droughts is less well studied (Ruangpan et al., 2020). This imbalance is increasingly problematic given climate projections that indicate an increasing likelihood of both extreme

high and low flow events (Bessembinder et al., 2023). A scoping study for the Vecht basin highlighted the importance of investigating catchment-scale measures to improve sponge functioning and mitigate both floods and droughts (Klein & Van der Vat, 2024). However, understanding how these measures affect hydrological processes at this scale remains a major challenge. A further challenge lies in accurately representing NBS in hydrological models (Jeuken et al., 2023). Successfully implementing large-scale NBS within hydrological models to quantify their effectiveness can help policymakers in making better-informed choices.

In summary, there is a need for more research into the quantitative effectiveness of nature-based solutions at the catchment scale using hydrological models. This includes assessing their role in flood and drought risk reduction and enhancing the accuracy of their representation in models. Addressing these gaps is essential to support the implementation of NBS in water management strategies.

1.4. Research Aim

This study aimed to quantify the effects of the nature-based solution groups land use & cover changes and improving soil conditions[1] on high and low stream flows[2] in the Vecht catchment under extreme wet and dry conditions[3], using the LISFLOOD-OS distributed hydrological model[4].

[1] Of the groups of NBS within the scope of this study, river restoration, land use & cover changes, and improving soil quality hold significant promise for this research (Leegwater, 2024). Within the time frame for this research, it was unfeasible to model and quantify the impacts of all these groups of NBS. For the land use & cover change and soil improvement groups, it is clear that they can be broadly applied to plots in rural areas. Therefore, only measures within the NBS groups land use & cover changes and improving soil conditions are investigated.

[2] For the quantification of the impacts of nature-based solution measures, both high and low stream flows are considered. It is evident that extreme weather events, including very wet and dry periods, will occur more frequently (Adnan et al., 2023), leading to a higher occurrence of extreme high and low stream flows in the Vecht catchment. Hence, it is crucial to consider not only average discharge rates but also a wider range of possible hydroclimatic conditions (Ji et al., 2023).

[3] Historical weather and discharge data are used to assess the effects of nature-based solutions on high and low stream flows in the Vecht catchment. However, the increasing likelihood of extreme events due to climate changes means that assessing the effectiveness of NBS in a changing climate is crucial. Therefore, this study evaluates the performance of NBS under a range of extreme hydroclimatic conditions, representing both intense rainfall and prolonged dry periods.

[4] For this study the spatially distributed hydrological model LISFLOOD-OS (De Roo et al., 2000) is used. The LISFLOOD-OS model is a grid-based hydrological rainfall-runoff-routing model that is capable of simulating the hydrological processes that occur in a catchment (Joint Research Centre, 2024c). It was selected for this study because of its open-source nature, extensive public documentation, and lack of special licensing requirements, which made it relatively easy to install and access. In addition, LISFLOOD-OS was chosen because of existing examples of its use in modelling land use changes and simulating their effects. In his literature review Cazemier (2024a) concluded that LISFLOOD-OS is a widely used model in Europe capable of implementing nature-based solutions and simulating their effects. Given the need to simulate extended periods for drought analysis, the model is applied with a daily time step to balance computational efficiency and temporal resolution.

1.5. Research Questions

To achieve this research aim, the following research questions were formulated:

The first research question evaluated the LISFLOOD-OS model performance by investigating how well it simulates historical extreme events in the Vecht catchment, characterized by high and low flows.

1. What is the performance of the LISFLOOD-OS model in simulating high and low flows in the Vecht catchment during historical extreme events?

The second research question focused on identifying how measures within the NBS groups land use & cover changes and improving soil conditions affect hydrological processes in the Vecht catchment. Their effects were then parameterised for integration into LISFLOOD-OS.

2. How can measures within the NBS groups land use & cover changes and improving soil conditions be integrated into the LISFLOOD-OS hydrological model?

Finally, the third research question focused on evaluating the effects of NBS on high and low flows in the Vecht catchment through different implementation scenarios.

3. What are the effects of nature-based solutions on high and low flows in the Vecht catchment according to LISFLOOD-OS under extreme wet and dry conditions?

1.6. Research Scope

This study aims to quantify the impact of NBS measures in the Vecht catchment. Not all NBS measures are suitable for application in the Vecht catchment, nor is it possible to evaluate all feasible measures within the time frame of this study. Since this thesis is part of the large-scale transboundary JCAR-ATRACE research programme, the focus is on measures that address catchment-wide issues that regulate river discharge by enhancing water retention, infiltration, and groundwater recharge to reduce the risk of high and low flows.

Based on the literature review by Leegwater (2024), river restoration, improving soil conditions and land use & cover changes are identified as the most promising NBS groups for this study due to their potential to reduce high flows and retain water during low flow periods. Other groups, such as floodplain retention, nature-based river dams, and channel alterations, are less suitable for this study because their effects are more focused on hydraulic processes, which are better represented in hydraulic models than in hydrological models. In addition, river restoration measures are primarily linked to areas near the river, and measures in this group have a greater impact on hydraulic processes in the river, which are not well represented in hydrological models. Therefore, the river restoration group falls beyond the scope of this study. The focus of this study is thus on the NBS groups land use & cover changes and soil improvement measures.

Although climate change is an important driver influencing the hydrological behaviour of river basins, this study does not simulate extensive climate change scenarios. Instead, the analysis relies on historical meteorological data and artificial rainfall events.

2. Study area, model and data description

2.1. Study area

The catchment area of the river Vecht is 4,192 km², with 2,157 km² located in Germany and the other half in the Netherlands (2,035 km^2). Figure 1a gives an overview of the Vecht catchment area and its location. The Vecht river enters the Netherlands close to Emlichheim and flows into the Zwarte Water. From the Zwarte Water, the water flows into the Zwarte Meer, finally leading to the IJsselmeer (Waterschap Drents Overijsselse Delta, 2021). Figure 1b shows an overview of land use in the Vecht basin, which is based on the CORINE land cover dataset (Büttner & Kosztra, 2011). Land use within a river basin plays an important role in shaping hydrological processes. Different types of land use, including agricultural land, forests and urban areas, interact differently with rainfall. These interactions influence how water is absorbed, retained and transported across the landscape. The dominant land use in the study area is agriculture (38%), followed by meadows (32%), forests (18%), urban (10%) and water (3%) (Klein & Van der Vat, 2024).

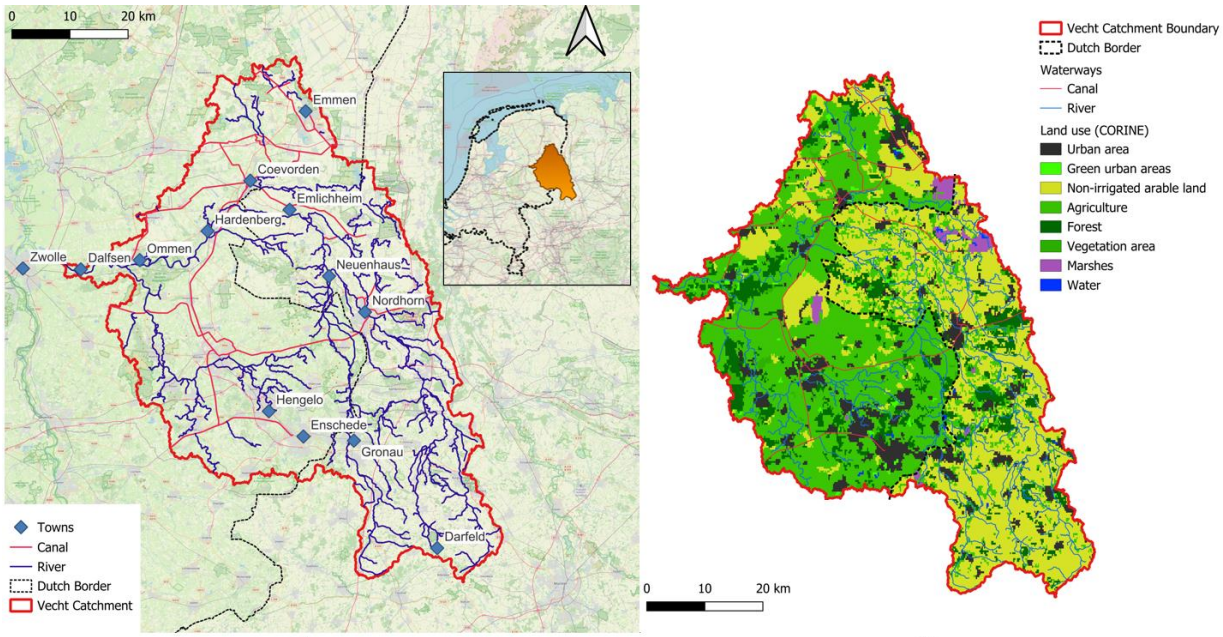

(a) *(b)*

Figure 1: Vecht catchment area, including the border between Germany and the Netherlands (a); Land use in the Vecht basin (CORINE land cover 2018) (b).

Figure 2a divides the Vecht catchment into distinct sub-catchment areas, each corresponding to a discharge station used in this thesis. The included table provides an overview of the sub-catchments and their respective surface areas. Archem is the largest sub-catchment with an area of 1200 km^2, with the Regge river flowing through and originating from this sub-catchment. Together, the sub-catchments of Lage Gesamt and Gronau form the catchment of the river Dinkel. Figure 2b shows the elevation differences within the Vecht catchment. The Vecht has an elevation difference of 70 meters and a slope of 0.4 ‰. The most significant differences in elevation are in the German part of the catchment, while the differences in elevation are minimal in the Dutch part.

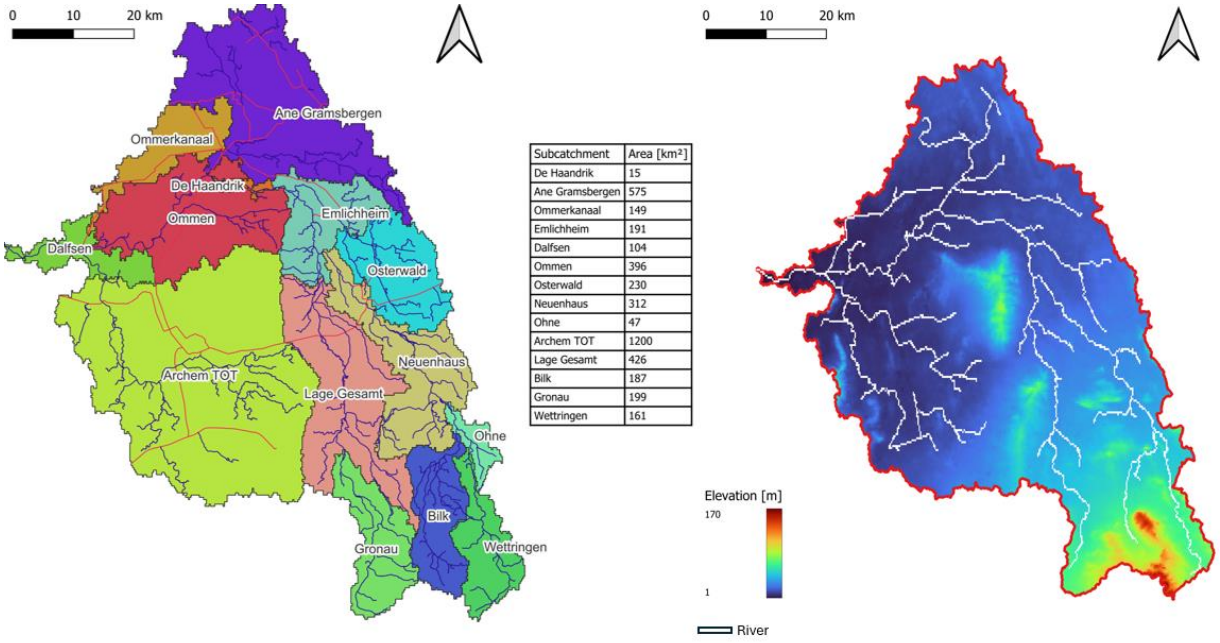

Figure 2: Sub-catchments and corresponding areas; derived using HydroMT-wflow based on the outlet discharge station of sub-catchments (a); Digital Elevation Map (Yamazaki et al., 2019) (b).

The study area has a temperate maritime climate with moderate temperatures. The average annual rainfall in the catchment area is about 835 mm, and there is no clear seasonal pattern. Yearly potential evapotranspiration in the area is about 555 mm (Klein & Van der Vat, 2024). Due to climate change, the adverse effects of low flows during droughts are expected to increase. The same holds for the expected increase in heavy rainfall events with higher precipitation levels leading to increased surface runoff and increased risk of river flooding (Klein & Van der Vat, 2024).

The river Vecht is characterised by its rainfed nature and has a length of 182 km. The average discharge at Dalfsen is 30 m³/s, ranging from 5 m³/s at low flow up to 250 m³/s at high flow. Due to the rain-fed characteristic of the river, its flow dynamics depend on precipitation volumes and water extraction during the summer period. The Vecht's water is discharged rapidly, resulting in notably low base flow during dry periods, which causes a water supply deficit for nature and agriculture (Klein & Van der Vat, 2024). Figure 3 shows the contributions of lateral flows to the discharge at Dalfsen. One-third of the water originates from the Vecht, and the other two-thirds enter the Vecht via the Regge, Dinkel, Afwateringskanaal and Ommerkanaal.

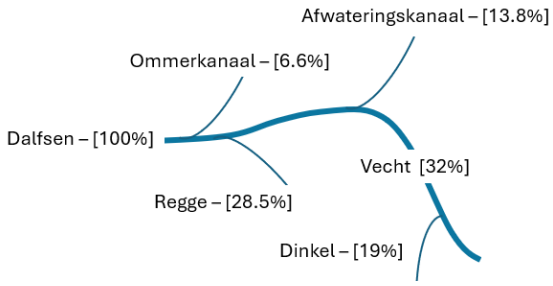

Figure 3: Lateral flows in the Vecht basin under normal conditions compared to discharge observed at Dalfsen.

Human interventions in the study area strongly affected the geohydrology of the region. Historically, the natural flow of groundwater from high to low areas was strongly delayed. However, human activities such as drainage, groundwater abstraction for various purposes (e.g. drinking water, irrigation) and changes in land use have affected both groundwater and surface flow, leading to changes in water levels, flow patterns, and overall hydrological dynamics. In both the Netherlands and Germany, the region has been and continues to be extensively drained to optimise agricultural productivity (Klein & Van der Vat, 2024).

2.2. LISFLOOD-OS hydrological model

The LISFLOOD-OS hydrological model is a distributed rainfall-runoff hydrological model capable of simulating hydrological processes at the catchment scale. The model consists of several modules that simulate surface and subsurface processes at the grid scale (Joint Research Centre, 2024c). The model is designed to be applied across a wide range of spatial and temporal scales. Applications to date have employed grid-cells with sizes ranging between 100 meters (for medium-sized catchments) up to 55 km (for modelling at the global scale). Long-term water balances can be simulated using daily or sub-daily time steps, as can individual flood events using hourly (or smaller) time intervals (Joint Research Centre, 2024a).

2.2.1. Model overview

The standard model setup includes the following components (Joint Research Centre, 2024c):

- a 3-layer soil water balance sub-model (superficial, upper & lower soil layer);
- sub-models for the simulation of groundwater and subsurface flow (using 2 interconnected groundwater zones, each consisting of a linear reservoir);
- a sub-model for the routing of surface runoff to the nearest river channel;
- a sub-model for the routing of channel flow.

The model is driven by meteorological forcing data (precipitation, temperature, potential evapotranspiration, and evaporation rates for open water and bare soil surfaces). At every time step and for every grid-cell, LISFLOOD-OS calculates a complete water balance. The list of simulated processes for each grid-cell includes: interception and leaf evaporation, evapotranspiration, evaporation from soil surface and open water, snow melt, soil freezing, surface runoff, infiltration, preferential flow (bypassing the soil layer), redistribution of soil moisture within the soil profile, sub-surface runoff, drainage of water to the groundwater system, groundwater storage, and groundwater base flow (Joint Research Centre, 2024a). Figure 4 provides a first overview of the processes included in LISFLOOD-OS.

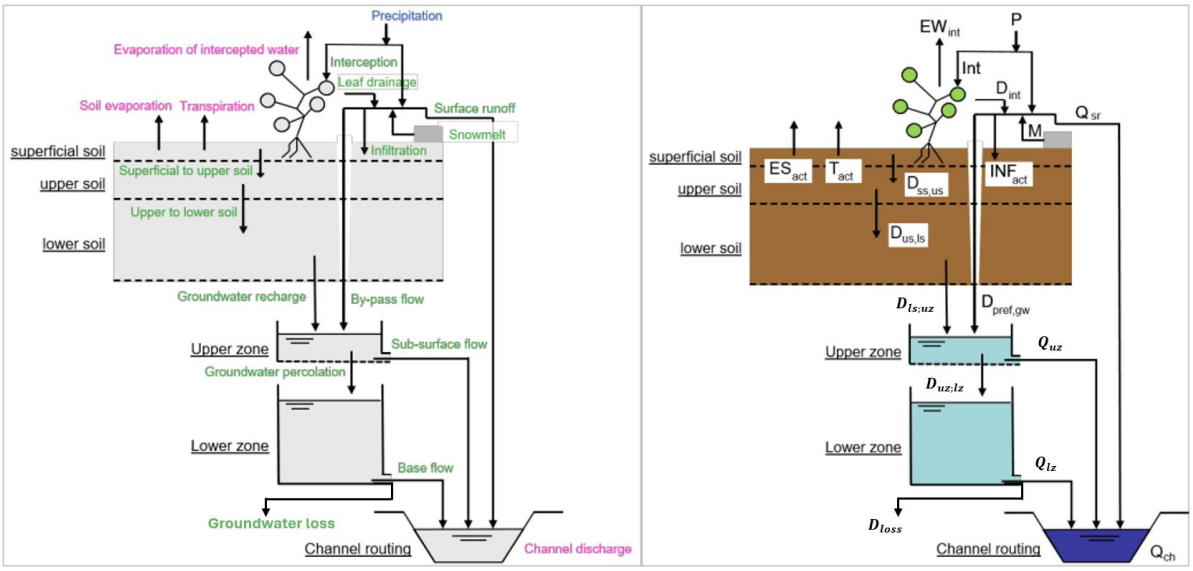

Figure 4: Structure of the processes included in LISFLOOD-OS; adapted from Joint Research Centre (2024a).

The hydrological processes included in LISFLOOD-OS are to some extent modelled using physically based approaches. However, LISFLOOD-OS balances accuracy with computational efficiency. While fully physically based models can be complex and data-intensive, LISFLOOD-OS uses process descriptions that make use of available data, minimising the need for calibration without adding unnecessary complexity (van der Knijff et al., 2010). In Appendix A, each individual process is described in more detail.

2.2.2. Sub-grid variability

The Joint Research Centre originally developed LISFLOOD-OS to support large-scale hydrological applications such as the European Flood Awareness System (EFAS) (Copernicus Emergency Management Service, 2023). The model was designed to handle the coarse spatial resolution required for continent-wide simulations. At the same time, it can effectively model sub-grid variability in land cover, ensuring that land use heterogeneity is reflected in hydrological processes.

In LISFLOOD-OS, a number of parameters are directly linked to land cover classes. To account for the sub-grid variability of land use, the within-grid variability is modelled. In each grid-cell, the spatial distribution and frequency of each class is defined as a percentage of the total represented area of the new grid-cell. This is known as the Hydrological Response Unit (HRU) concept, where land cover classes are combined and modelled to better capture the non-linear rainfall-runoff processes over different surfaces. This approach is used in models such as SWAT (Arnold & Fohrer, 2005) and PREVAH (Viviroli et al., 2009) and has been adapted to a sub-grid scale in LISFLOOD-OS, as shown in Figure 5 (Joint Research Centre, 2024a).

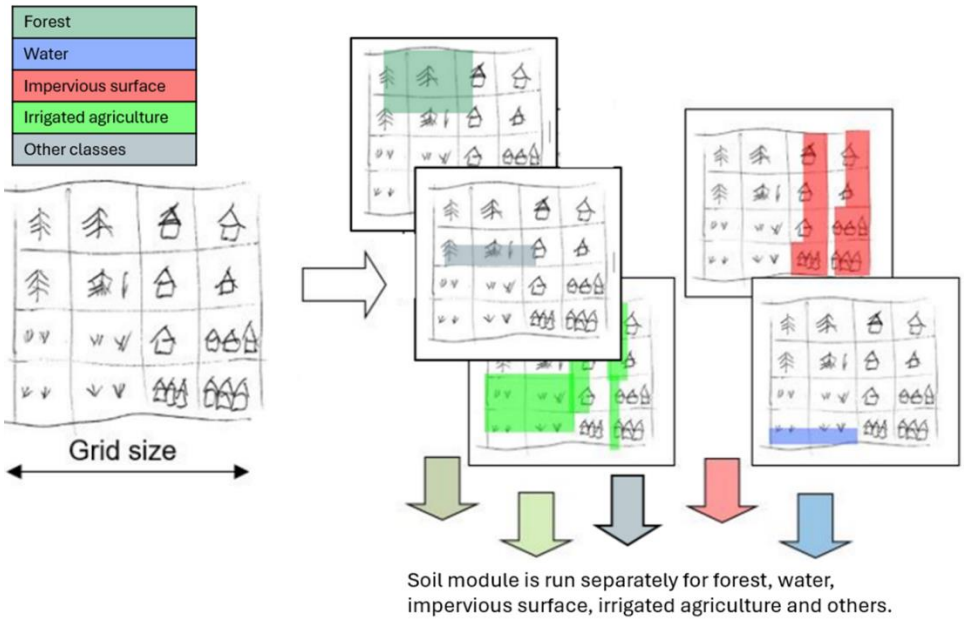

Figure 5: LISFLOOD-OS land cover aggregation by modelling aggregated land use classes separately; adapted from Joint Research Centre (2024a).

In LISFLOOD-OS, built-up areas within a pixel affect the pixel's water balance. The "direct runoff fraction" (f_{dr}) parameter defines the impervious portion of a pixel.

For impervious areas, LISFLOOD-OS assumes:

- Precipitation and snowmelt fill a depression storage, which is emptied by evaporation.
- Excess water contributes directly to surface runoff.
- There is no soil moisture or groundwater storage.

For open water areas (e.g., lakes, rivers), the "water fraction" (f_{water}) parameter defines the water-covered fraction of a pixel. In these water-covered areas:

- Actual evaporation is equal to potential evaporation on open water.
- There is no soil moisture or groundwater storage.

For forests (f_{forest}), irrigated agriculture ($f_{irrigated}$), or other land cover ($f_{other} = 1 - f_{forest} - f_{irrigated} - f_{dr} - f_{water}$), all soil- and groundwater-related processes (evaporation, transpiration, infiltration, and groundwater flow) apply. Although the modelling framework is the same for forests, irrigated agriculture, and other land cover types, they each use distinct map sets for leaf area index, soil characteristics, and soil hydraulic properties. This approach accounts for the non-linear behaviour

of rainfall-runoff processes, leading to more accurate results than averaged parameter values (Joint Research Centre, 2024a). Table 2 summarises the profiles for these four land cover types.

Table 2: Summary of hydrological properties per category; adapted from Joint Research Centre (2024a).

Category	**Evapotranspiration**	**Soil**	**Runoff**
Forest	High level of evapotranspiration (high Leaf area index) seasonally dependent	Large rooting depth	Low concentration time
Impervious surface	Not applicable	Not applicable	Surface runoff but initial loss and depression storage, fast concentration time
Inland water	Maximum evaporation	Not applicable	Fast concentration time
Irrigated agriculture	Evapotranspiration lower than for forest but still significant	Rooting depth lower than for forest but still significant	Medium concentration time
Other (agricultural areas, non-forested natural area, pervious surface of urban areas)	Evapotranspiration lower than for forest but still significant	Rooting depth lower than for forest but still significant	Medium concentration time

2.3. Data description

2.3.1. Meteorological data

Meteorological conditions are a key driver of hydrological processes. LISFLOOD-OS uses the following meteorological input variables: precipitation, potential (reference) evapotranspiration, potential evaporation from open water surfaces, potential evaporation from bare soil surfaces and mean daily temperature. Various precipitation datasets, including those from the Koninklijk Nederlands Meteorologisch Instituut (KNMI), the International Radar Composite (IRC), E-OBS & ERA5 from Copernicus, and RADOLAN from the Deutsche Wetter Dienst, were evaluated for their suitability in a similar study for the Vecht by Cazemier (2024b). Based on this evaluation, E-OBS was selected as the most suitable dataset. E-OBS is a high-resolution, daily gridded dataset for several climate variables, including precipitation and minimum, maximum and mean surface temperatures, derived from measurements that are part of the European Climate Assessment & Dataset project (Cornes et al., 2018).

Daily gridded time series of temperature and potential evapotranspiration were obtained from ERA5. ERA5 provides hourly estimates for a wide range of atmospheric, land and oceanic climate variables, with daily and monthly aggregates also available from the hourly data fields (Hersbach et al., 2024). Table 3 provides an overview of the meteorological datasets that were used to set-up the LISFLOOD-OS model for the Vecht basin and their corresponding resolution.

Table 3: Meteorological datasets used to set-up the LISFLOOD-OS model for the Vecht basin.

Maps	**Dataset**	**Resolution**
Precipitation	E-OBS	~7 km
Potential evapotranspiration	ERA5	~17 km
Temperature	ERA5	~17 km

2.3.2. Discharge data

Historical discharge measurements for the Vecht river basin were requested from the following authorities: Deltares, Rijkswaterstaat, Waterboard Vechtstromen, Waterboard Drents Overijsselse Delta (WDOD), Niedersächsischer Landesbetrieb für Wasserwirtschaft, Küsten- und Naturschutz (NLWKN) and the Landesamt für Natur, Umwelt und Verbraucherschutz Nordrhein-Westfalen (LANUV NRW). In Appendix B, an overview of all the discharge data that was gathered, along with corresponding sources, is provided. Daily measurements were used, and the time series were checked and corrected for inconsistencies or gaps. Negative discharge values were adjusted to zero, while extreme outliers — flows exceeding 1000 m^3/s — were set to NaN to exclude them from the performance metrics calculations and other analyses. All measurement series from the various monitoring stations in the Vecht river basin have been compiled, and the data availability since 1997 is mapped in Figure 6.

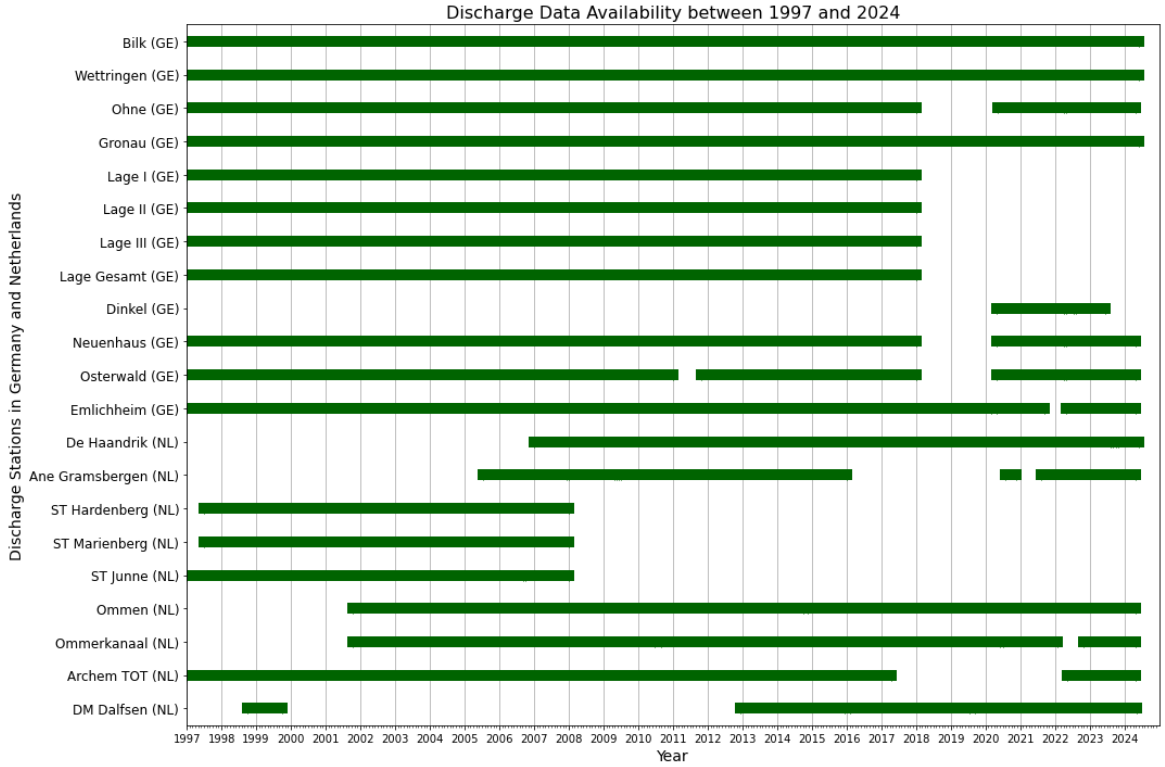

Figure 6: Availability of daily discharge measurements in the Vecht catchment between 1997 and 2024.

3. Methods

An overview of the methods used to investigate the effects of nature-based solutions on high and low flows in the Vecht catchment using LISFLOOD-OS is shown in Figure 7.

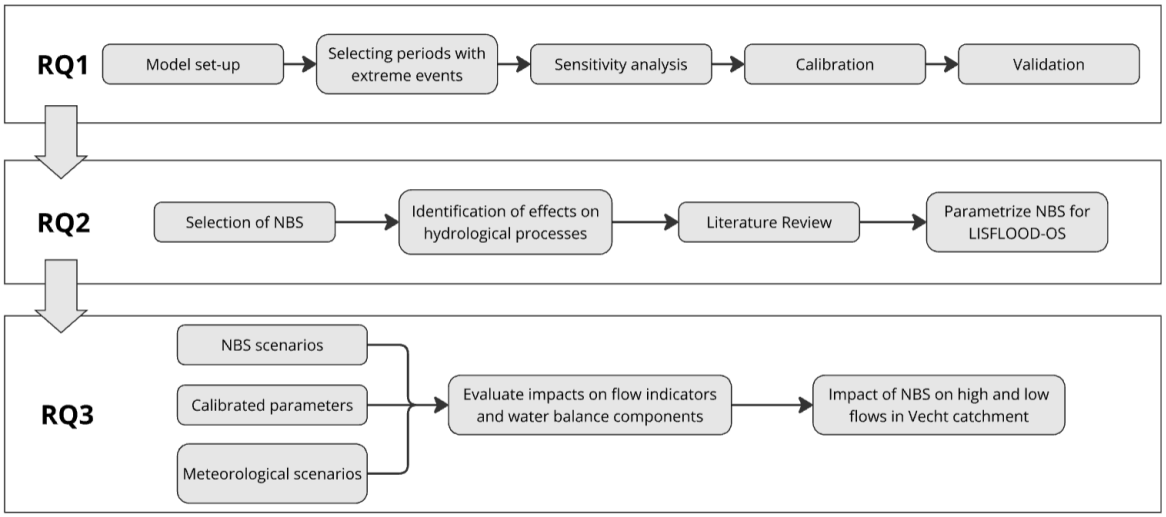

Figure 7: Overview of methodology. The frames indicate to which research question (RQ) each step belongs.

The LISFLOOD-OS model was calibrated and validated to assess its performance in simulating high and low flows during extreme events (RQ1), as described in section 3.1. Specific measures within the NBS groups land use & cover changes and improving soil conditions were then selected, their effects on hydrological processes identified and their parameterisation integrated into the LISFLOOD-OS model (RQ2). Sections 3.2.1 & 3.2.2 present all the steps taken to address RQ2. Finally, the methods for evaluating the impact of the implemented NBS scenarios on high and low flows under different meteorological conditions, using flow indicators and water balance components, are presented in sections 3.2.3 & 3.2.4 (RQ3).

3.1. Determination of the LISFLOOD-OS model performance

Answering the first research question required four steps. First a LISFLOOD-OS model for the Vecht basin was set up, for which static input maps were collected. The second step was selecting extreme historical weather events for model calibration and validation. The third step included a sensitivity analysis of the model parameters, after which the model was calibrated. The fourth and final step is validating the final model to assess the model performance.

3.1.1. Model set up

LISFLOOD-OS requires a considerable number of static input maps and meteorological forcings. To build a LISFLOOD-OS model for a catchment such as the Vecht, a schematisation of the catchment is created by integrating static maps of topography, soil properties, land cover, channel geometry and vegetation. Maps must have consistent resolution and orientation to ensure accurate calculations and must be in NetCDF or PCRaster format to ensure model compatibility. Maps of temperature, precipitation and evaporation are added as meteorological forcing. Finally, the LISFLOOD-OS code links all these maps and inputs to enable the model to simulate hydrological processes.

For the implementation of NBS on agricultural lands it is desirable to have a grid resolution high enough to be able to implement measures on these plots. Average plot sizes of German farms range between 4 and 6 hectares (Heinrichs et al., 2021) and for Dutch farms this is even smaller. Therefore, a grid resolution of approximately 100-200 meters would be preferable. Ultimately, a grid resolution of 200 meters was chosen instead of 100 meters to balance the need for spatial detail with manageable computation times.

General maps

The general maps in the hydrological model include the following: area and land use mask maps and grid-cell length and area maps. Area and land use mask maps in the hydrological model determine where computations should occur and where grid-cells should be skipped. Both are Boolean maps defining model boundaries and the land use calculation domain. To create the mask maps, source data such as elevation or flow direction was reclassified to '1'. Grid-cell length and area maps are used in LISFLOOD-OS to accurately compute areal sums, such as the upstream river area or rainfall over specific grid-cells. The grid-cell area was calculated using the ee.Image.pixelArea() function in Google Earth Engine, which considers the Earth's curvature and applies the required grid resolution (e.g., 1 and 3 arc minutes) along the longitude in meters. The grid-cell length was then determined by dividing the area by its longitudinal resolution in meters.

Other static maps

Topography, land use, land use-dependent parameters, soil hydraulic properties, channel geometry, and leaf area index maps were sourced partly from the European Flood Awareness System (EFAS) (Joint Research Centre, 2024d) and partly from MERIT Hydro (Yamazaki et al., 2019). The EFAS maps that originally covered all European countries were clipped to the catchment area of the Vecht and have a spatial resolution of 1 arc min (approximately 1.5 km). A complete overview of all static maps, including descriptions, units, ranges, and sources, is provided in Appendix C.

The high-resolution model with a grid size of 200 metres primarily uses interpolated EFAS static maps (Joint Research Centre, 2024d). To prepare the high-resolution EFAS maps, two different interpolation methods were used: cubic and nearest neighbour. The cubic interpolation method (Figure 8) was used for continuous data, as it provides smooth transitions between values while maintaining accuracy, making it suitable for variables such as slope gradient. This method offers a balance between producing natural results and maintaining computational feasibility without introducing unnecessary complexity as seen with more advanced methods such as Kriging. In contrast, the nearest-neighbour interpolation method (Figure 9) was applied for maps with discrete data, such as forest fraction per grid-cell, as it preserves the original values without introducing new ones, which is essential for maintaining the integrity of these categorical datasets. The interpolation method per static input map can be found in Appendix C.

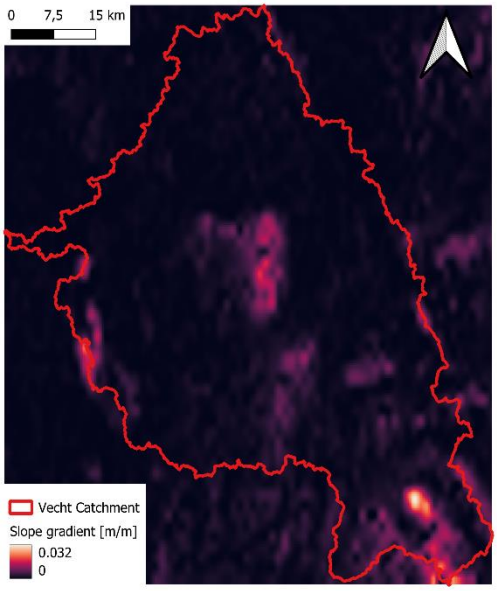

Figure 8: Slope gradient in Vecht catchment.

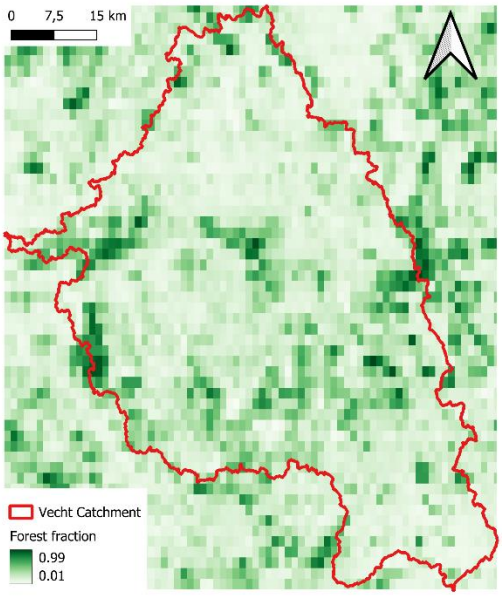

Figure 9: Forest fraction in Vecht catchment.

The local drain direction map and the channel length map could not be interpolated from the EFAS maps; therefore, static maps from MERIT Hydro (Yamazaki et al., 2019), were used. Additionally, it was found that both the EFAS and Wflow sbm maps provided unrepresentative estimations for the

channel bottom and floodplain width maps. Figure 10 shows the EFAS map for channel bottom width, highlighting these inaccuracies. To address these issues, channel bottom width and floodplain width maps were manually generated using the Strahler stream order method (Strahler, 1952), which resulted in the bottom width map shown in Figure 11. This method assigns stream orders based on the hierarchical branching of rivers and is commonly used in hydrological modelling to estimate channel characteristics (Ghorai et al., 2022).

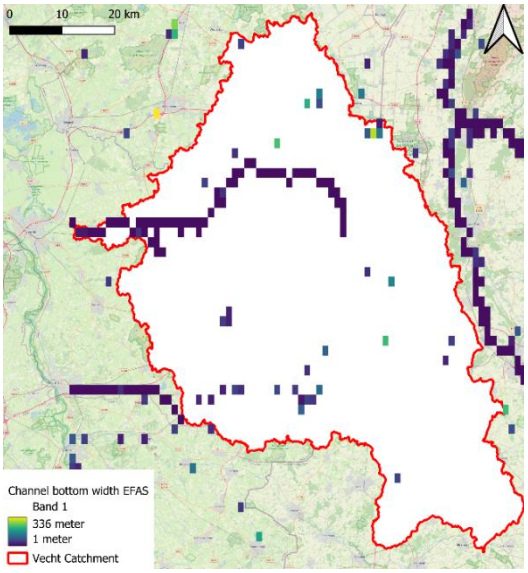

Figure 10: EFAS channel bottom width map.

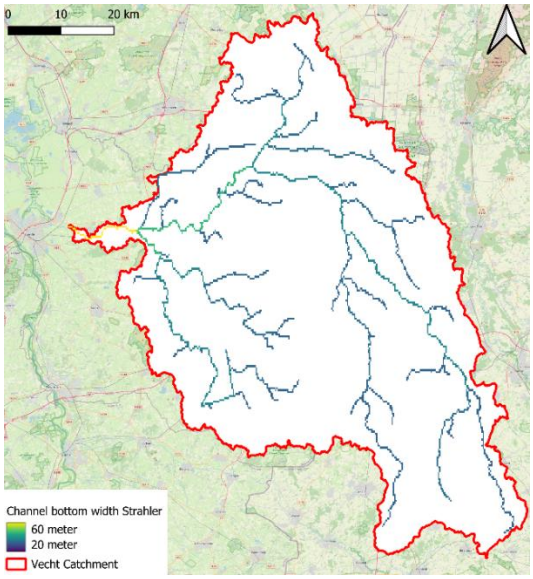

Figure 11: User-defined bottom width map using Strahler method.

3.1.2. Selecting periods with extreme events

To effectively assess the model performance during high and low flow conditions, calibration and validation were carried out using periods representing high flow and low flow events. This approach allowed for a thorough evaluation of the model's ability to simulate both flood peaks and baseflow during periods of prolonged drought.

For the selection of dry periods, the analysis focused on the months from March through October. First, discharge data from each station was examined to exclude years where more than 25% of the summer measurements were missing due to insufficient data. For the remaining years, the total water volume for each summer was calculated. The four summers with the lowest total water volumes were selected to represent dry years, ensuring that the model performance during low flow conditions could be evaluated. Figure 12 provides an example of how the selection procedure was applied, with the selected years of lowest flow volumes highlighted in red.

	'97	'98	'99	...	...	...	...	...
Missing data	8%	2%	5%	13%	0%	10%	32%	0%
Total water volume [Mm^3]	152	131	163	102	148	126	✕	89

Figure 12: Example of the selection procedure of years with extreme dry periods.

For the selection of years with extreme flood peaks, discharge data from each station was analysed to identify the years with the highest daily peak events. Specifically, for each station, the five years with the highest daily peak discharges were selected. These peak years were then compared across stations to identify the years in which most stations experienced one of their top five daily peak events. The three years where the most stations recorded one of their five highest peak discharges were selected for calibration and validation as years with significant peak events. The procedure is illustrated by an example in Figure 13, with blue indicating the years containing one of the five highest single-day peak

discharges at each station, and red highlighting the years with the most common peak years across stations.

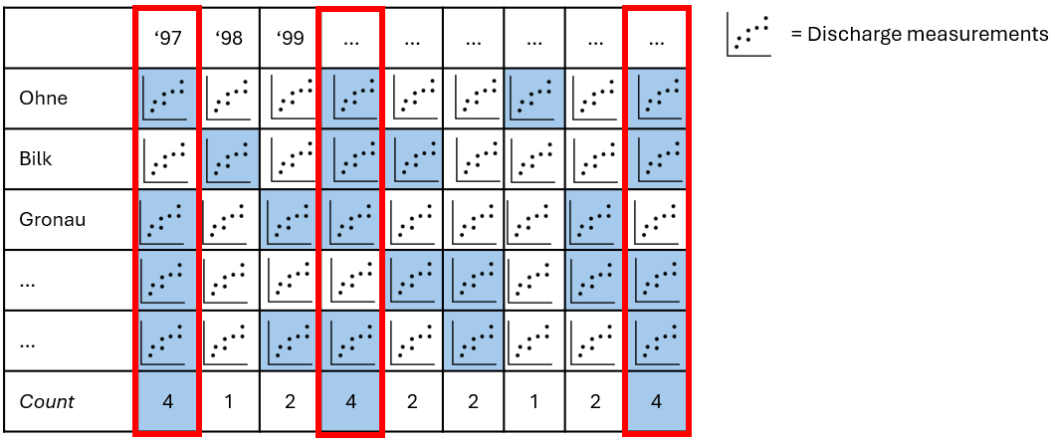

Figure 13: Selection procedure of years with extreme peak discharges.

Figure 14 provides an overview of the years selected for peak discharges and low flows in the Vecht river basin. The selected years for peak discharge events, highlighted in blue, are 1998, 2010, and 2023. These years represent the periods with the most significant peak discharges across the majority of monitoring stations. For extreme droughts, the selected years, marked in red, are 2011, 2012, 2013, and 2018. These years had the lowest total water volumes during the summer months, reflecting low flow conditions. Additionally, Figure 14 indicates the data availability for each station in the selected years, allowing for a clear understanding of which stations contributed to the analysis during these critical periods.

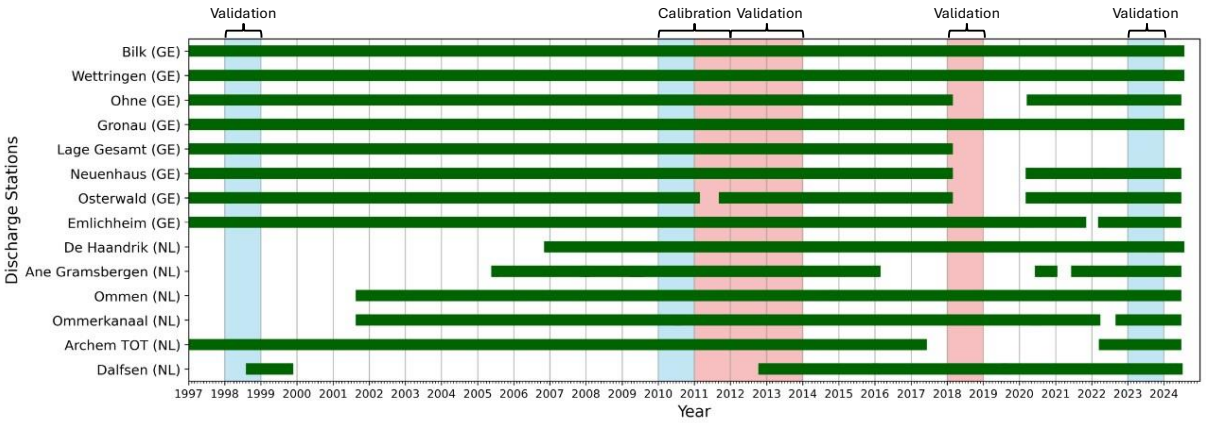

Figure 14: Selected peak flow (blue) and dry (red) years for calibration and validation, including data availability per station.

The years chosen for sensitivity analysis and calibration are 2010 and 2011, as they provide consecutive years with both a high flow event and a dry summer period, allowing a balanced calibration across different flow conditions. Similar calibration durations have been successfully used in previous LISFLOOD-OS studies, such as Feyen (2005) for the Meuse basin. A five-year warm-up period (2007-2011) was used to initialise the model and applied consistently throughout the calibration and validation periods.

3.1.3. Sensitivity analysis

After setting up the model with all the necessary input data, a sensitivity analysis of the model parameters was conducted. This analysis provided valuable insights into the influence of different parameters on the simulated discharges. This information was then used to calibrate the model, which was the next step in the process.

The LISFLOOD-OS model includes 14 parameters that can be calibrated. An overview of these parameters, including their default, maximum, and minimum values, is provided in Table 4. A univariate sensitivity analysis was performed for 10 of these parameters, as not all 14 parameters are relevant to the LISFLOOD-OS model of the Vecht catchment. The 4 parameters excluded from the sensitivity analysis were: C_m, α, $AdjL_n$ and $ResMultQ_{norm}$. These parameters affect hydrological processes related to snow, lakes, and reservoirs, none of which are significant in the Vecht catchment. Furthermore, because there are no large lakes or reservoirs within the Vecht catchment, the lakes and reservoirs modules in LISFLOOD-OS were deactivated.

Table 4: Overview of LISFLOOD-OS calibration parameters with description, influenced fluxes, minimum, maximum and default values; adapted from Joint Research Centre (2024b).

Parameter	**Description**	**Flux**	**Min**	**Max**	**Default**
C_m	Snow melt rate in degree day model equation [mm/(C day)]	M	2.5	6.5	4
b	Exponent in Xinanjiang equation for infiltration capacity of the soil [-]	INF_{act}	0.01	5	0.5
C_{pref}	Exponent in the empirical function describing the preferential flow (i.e. flow that bypasses the soil matrix and drains directly to the groundwater) [-]	$D_{pref,gw}$	0.01	8	4
UpperZone-TimeConstant	Time constant for upper groundwater zone [days]	Q_{uz}	0.01	40	10
GW_{perc}	Maximum percolation rate from upper to lower groundwater zone [mm/day]	$D_{uz,lz}$	0.01	2	0.8
LowerZone-TimeConstant	Time constant for lower groundwater zone [days]	Q_{lz}	40	10,000	100
$LZ_{threshold}$	Threshold to stop outflow from lower groundwater zone to the channel [mm]	Q_{lz}	0	30	10
GW_{loss}	Maximum loss rate out of lower groundwater zone expressed as a fraction of lower zone outflow [mm/day]	Q_{lz}	0	0.5	0
QsplitMult	Multiplier to adjust discharge triggering floodplains flow [-]	Q_{ch}	0	20	2
CalChanMan1	Multiplier for channel Manning's coefficient *n* for riverbed [−]	Q_{ch}	0.5	2	1
CalChanMan2	Multiplier for channel Manning's coefficient *n* for floodplains [−]	Q_{ch}	0.5	5	1
C_m	Snow melt rate in degree day model equation [mm/(C day)]	M	2.5	6.5	4
$AdjL_n$	Multiplier to adjust reservoir normal filling (balance between lower and upper limit of reservoir filling). [-]	Q_{res}	0.01	0.99	0.8
$ResMultQ_{norm}$	Multiplier to adjust normal reservoir outflow [−]	Q_{res}	0.25	2	1
α	Multiplier to adjust lake outflow [−]	Q_{lake}	0.5	2	1

For the 10 parameters in the sensitivity analysis, five runs were performed for each parameter using the minimum, maximum, default, and intermediate values as specified in Appendix D1.

3.1.4. Calibration

The next step in the methodology was to calibrate the LISFLOOD-OS model to ensure that it accurately reflects the hydrological conditions of the Vecht river basin. The default model settings, as determined for EFAS, may not capture the specific characteristics of the sub-catchments in the Vecht basin, so calibration is required to fine-tune the parameters. In this study, a multi-objective function was used to optimise both high flow and low flow scenarios to ensure a balanced performance under different hydrological conditions. An objective function provides a clear quantitative measure to guide the parameter adjustments, making it very useful during model calibration to improve accuracy. The selection of appropriate performance criteria is crucial, as it ensures the model is evaluated against meaningful indicators that reflect its capacity to simulate different hydrological behaviours effectively (Pushpalatha et al., 2012).

Objective function

The multi-objective function used in this study combines different performance metrics to provide a more comprehensive assessment of model performance. In this study, high flows are evaluated using a metric that emphasises peak flow accuracy, while low flows are evaluated using a metric that focuses on base flow representation. This combination ensures that the model is not only calibrated to handle one extreme (e.g., flooding), but is also robust in simulating low flow conditions. The objective function used in this study, inspired by the approach outlined by Akhtar et al. (2009), follows the implementation described by Ten Berge (2024) and is defined in Equation 1. A perfect simulation would result in an NS_w and NS_{inv} of 1, and an RVE of 0, leading to a y_{comb} value of 1. If the score for y_{comb} is 0 or lower, it indicates that the model performs no better than simply predicting the long-term average flow, offering little to no improvement over basic estimates.

$$y_{comb} = \frac{NS_w + NS_{inv}}{2(1 + |RVE|)} \quad \text{[Eq. 1]}$$

In this objective function, NS_w represents the Nash-Sutcliffe efficiency weighted for high flows (Hundecha & Bárdossy, 2004). A weight based on the observed discharge is applied to emphasise peak flows, ensuring the model captures extreme events accurately. Discrepancies between high observed and simulated flows are penalised more heavily, improving peak flow simulation. NS_w ranges from -∞ to 1, with 1 indicating a perfect match. NS_w is computed as described by Equation 2.

$$NS_w = 1 - \frac{\sum_{i=1}^{n}\left[w_i\left(Q_{sim}^i - Q_{obs}^i\right)^2\right]}{\sum_{i=1}^{n}\left[w_i\left(Q_{obs}^i - \overline{Q_{obs}}\right)^2\right]} \; with \; w_i = Q_{obs}^i \quad \text{[Eq. 2]}$$

Q_{sim}^i : Simulated discharge at day i
Q_{obs}^i : Observed discharge at day i
$\overline{Q_{obs}}$: Mean observed discharge over n days
n : Total number of timesteps

NS_{inv} is the inverse Nash-Sutcliffe efficiency as introduced by Le Moine (2008), which focuses on low flows by giving more weight to baseflow conditions (lowest 20% of flows), ensuring that the model performs well during periods of low discharge. NS_{inv} also ranges from -∞ to 1, with 1 indicating a perfect match. NS_{inv} is computed as described by Equation 3.

$$NS_{inv} = 1 - \frac{\sum_{i=1}^{n}\left(q_{sim}^i - q_{obs}^i\right)^2}{\sum_{i=1}^{n}\left(q_{obs}^i - \overline{q_{obs}}\right)^2} \; with \; q^i = \frac{1}{Q^i} \quad \text{[Eq. 3]}$$

RVE is the Relative Volume Error (Equation 4), which measures the discrepancy between the observed and simulated total discharge volumes, thus reflecting the accuracy of the water balance in the system. By incorporating $|RVE|$, the function penalises deviations between the observed and simulated total discharge volumes, ensuring that the overall water balance is accurately represented. The RVE can range from -∞ to ∞, with a perfect water balance at a RVE of 0.

$$RVE = \frac{\sum_{i=1}^{n}\left(Q_{sim}^i - Q_{obs}^i\right)}{\sum_{i=1}^{n}\left(Q_{obs}^i\right)} \quad \text{[Eq. 4]}$$

Calibration parameter selection and range definition

It was important to focus on the most sensitive parameters to streamline the calibration process. The sensitivity analysis results were examined to assess how variations in different parameters affected the objective function. Parameters that resulted in significant changes in the objective function were considered sensitive and were selected for calibration. These parameters influence model performance the most, making them crucial for optimising the objective function.

Reducing the number of parameters involved in the calibration makes the process less computationally demanding and more targeted. Parameters that showed little to no effect on the objective function were deemed less essential and kept at their default values, which were taken from the EFAS model (Joint Research Centre, 2024d). This allowed the focus to remain on the parameters that most impacted the model's ability to simulate high and low flows.

Selecting appropriate ranges for each parameter was equally important. Defining ranges that are too broad could make the calibration less efficient and optimisation more difficult. Therefore, the parameter ranges were also chosen based on the sensitivity analysis results. This approach ensured that the calibration process was efficient and effective in improving the model's representation of hydrological conditions.

Calibration procedure

After determining the parameters and ranges for calibration based on the sensitivity analysis, the next step was systematically calibrating the model for each sub-catchment from upstream to downstream. This approach is common in hydrological modelling, as upstream sub-catchments influence downstream conditions. By calibrating the upstream areas first, the downstream catchments can be adjusted based on already optimised upstream parameters, ensuring that the cumulative effects of flows are effectively accounted for.

The calibration process was structured into five sub-catchment groups, proceeding sequentially from upstream to downstream, as shown in Figure 15. This approach ensured that upstream processes were accurately calibrated before proceeding downstream, as errors in upstream sub-catchments can propagate and affect downstream results.

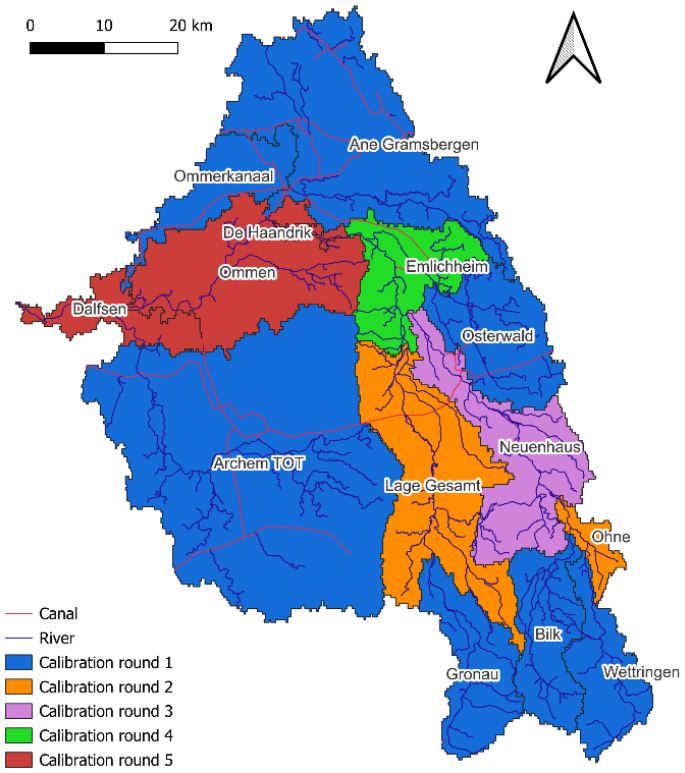

Figure 15: Sub-catchments division per calibration round.

The calibration process started with parameters affecting deeper fluxes, such as groundwater processes, because these parameters set the baseline hydrological conditions. Once these deeper processes were calibrated, the focus shifted to parameters affecting surface fluxes, representing more rapid hydrological responses. This sequence ensured that the calibration of surface fluxes did not mask errors in the representation of deeper fluxes.

For each parameter, 15 calibration runs were carried out, varying the parameter values equally between their minimum and maximum ranges. The optimised value for each parameter in a sub-catchment was then fixed and used in the following calibration steps. Dependencies between parameters were considered by following this sequential approach, ensuring adjustments to one parameter did not overwrite earlier calibration steps. The sequence of parameter calibration is further detailed in the results section.

3.1.5. Validation

Validation evaluates the performance of the LISFLOOD-OS model using the same multi-objective function as during calibration but applied to independent periods not used in the calibration process. This approach assesses the ability of the model to simulate hydrological conditions beyond the calibration period. The validation periods were selected based on extreme events, as shown in Figure 14, capturing both high and low flow conditions to test the model's performance under different hydrological conditions thoroughly. These periods are briefly described below.

In October 1998, the Vecht basin experienced extremely high discharges due to prolonged rainfall. For the German part of the basin, sufficient data is available. The validation period for this event extends from 1 January 1998 to 28 March 1999.

The years 2011, 2012 and 2013 were characterised by prolonged dry conditions, making them valuable for assessing the performance of the model during prolonged low flow periods. To assess this, the period from 1 January 2012 to 28 September 2014 was selected to cover several dry years with sufficient data across the basin. This timeframe allows a detailed analysis of the ability of LISFLOOD-OS to simulate prolonged low flows.

In 2018, another exceptionally dry year occurred due to a significant rainfall deficit, resulting in extremely low flows across the basin. However, data availability for this period was limited, so the assessment could only focus on sub-catchments with sufficient data coverage. The validation period for this year was set from 1 January to 31 December 2018.

Finally, in 2023, heavy rainfall in the Vecht basin during Christmas led to extremely high river flows. This made it an interesting event to test the performance of the model in simulating peak discharges under high flow conditions. The validation period for this event runs from 1 October 2023 to 28 March 2024, covering the peak discharge event and the following months.

3.2. The effects of NBS in the Vecht catchment using LISFLOOD-OS

This section addresses research question 2: *How can measures within the NBS groups land use & cover changes and improving soil conditions be integrated into the LISFLOOD-OS hydrological model?* and research question 3: *What are the effects of the nature-based solutions on high and low flows in the Vecht catchment according to LISFLOOD-OS under extreme wet and dry conditions?* To answer these questions, Figure 16 outlines the steps and the sections in which they are described.

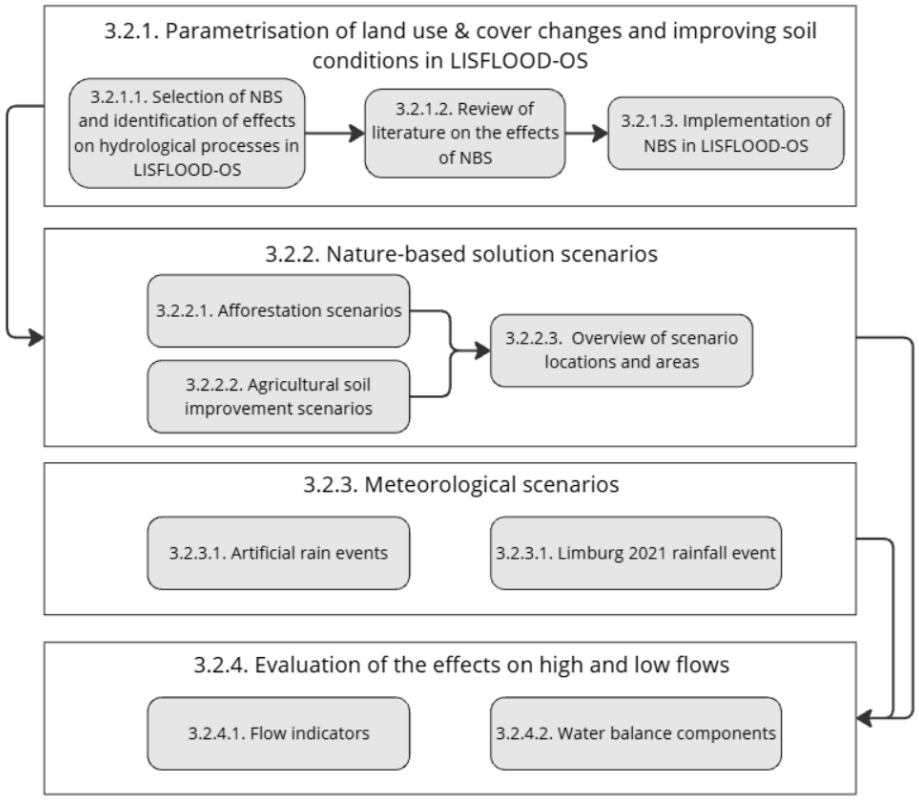

Figure 16: Overview of methodology RQ2 and RQ3, including corresponding sections describing each step.

First, the selected NBS were parameterised by identifying their effects on hydrological processes, reviewing findings from the literature and implementing these effects in the LISFLOOD-OS model (3.2.1). Next, nature-based solution scenarios were defined by determining their spatial distribution and areas of implementation within the Vecht catchment (3.2.2). Subsequently, meteorological scenarios, including artificial rain events and the extreme rainfall event Limburg 2021, were set up to evaluate the NBS under wet and dry conditions (3.2.3). Finally, the impact of the NBS on hydrological dynamics was assessed by analysing its effects on flow indicators and water balance components (3.2.4). Each of these steps is further explained in the following sections.

3.2.1. Parametrisation of land use & cover changes and improving soil conditions in LISFLOOD-OS

This section describes the parameterisation of nature-based solutions (NBS) within the LISFLOOD-OS hydrological model. The aim is to translate the hydrological effects of these NBS into model adjustments that allow their simulation in the Vecht catchment. In section 3.2.1.1, the NBS to be investigated are selected from the broader categories, and the hydrological processes in LISFLOOD-OS that are expected to be affected are identified. In addition, this subsection examines how these processes can be linked to LISFLOOD-OS parameters. In section 3.2.1.2, a literature review provides insight into the documented impacts of the selected NBS on hydrological processes. This knowledge forms the basis for determining parameter adjustments that reflect these impacts. Finally, section 3.2.1.3 summarises the findings from the previous subsections and details the specific parameter changes and model adjustments made to simulate the selected NBS in LISFLOOD-OS.

3.2.1.1. Selection of NBS and identification of effects on hydrological processes in LISFLOOD-OS

To assess the effects of land use & cover changes and soil improvement on hydrological processes in the Vecht catchment, a subset of measures from these NBS categories was selected for further analysis. Table 5 presents the selected NBS, grouped into the two NBS categories. A complete list of all potential NBS considered for both categories is provided in Appendix F1.

Table 5: Selected NBS for further scenario development.

Land use & cover changes	Improving soil conditions
(Re-) forestation	Soil aeration and subsoiling
	Conservation tillage
	Stocking density

The hydrological processes in LISFLOOD-OS expected to be affected by these measures have been identified. These processes are crucial for understanding how NBS can be represented in LISFLOOD-OS. The identified hydrological processes are:

- **Interception**: Rainfall intercepted by vegetation and subsequently evaporated before reaching the ground. This process can significantly reduce direct runoff and infiltration.
- **Soil evaporation**: Water returning to the atmosphere from the soil, playing a crucial role in balancing soil moisture availability.
- **Transpiration**: Evaporation of water from plant leaves, driven by water uptake through roots and atmospheric conditions.
- **Infiltration**: The process by which water enters and moves down the soil profile, influenced by soil structure and surface conditions.
- **Surface runoff**: The portion of precipitation flowing over land or through rivers. Runoff rates are controlled by land cover, slope, and surface roughness.

These processes were used to identify the appropriate LISFLOOD-OS parameters that could be adjusted to represent the effects of the NBS. The following subsections describe the implementation framework, detailing how parameter adjustments can be implemented to simulate the expected effects of the NBS on these hydrological processes.

Land use change

As described in Section 2.2.1, the LISFLOOD-OS model accounts for the distinct hydrological properties of different land uses, particularly regarding evapotranspiration, rooting depths, and runoff generation. These properties are critical for capturing the unique behaviour of various land cover types within the model framework.

In the case of reforestation and improving soil condition measures, land use fractions within affected cells can be adjusted to reflect their dominant land cover class. This ensures that all hydrological calculations within these cells are based entirely on the properties associated with their respective land cover type. A key example of this adjustment is the incorporation of the Leaf Area Index (LAI), which influences evapotranspiration. The LAI values used in the model are derived from separate NetCDF files, which provide 10-day averaged LAI values specific to the dominant land cover type in each grid-cell.

Table 6 provides an overview of the parameters in LISFLOOD-OS that are influenced by adjustments to land use fractions.

Table 6: parameters influenced by changing land use fractions.

Land use depending maps	**Leaf area index maps**
Crop coefficient	LAI for forest
Crop group number	LAI for irrigated crops
Manning's coefficient	LAI for other
Soil depth	
Soil hydraulic properties maps	
Theta saturated	Genu Alpha
Theta residual	K saturated
lambda	

Surface roughness changes

The LISFLOOD-OS model uses Manning's roughness coefficients to account for the resistance to water flow across different land uses, particularly influencing surface runoff. Adjustments to Manning's roughness coefficient can be applied to account for changes in hydraulic resistance. In LISFLOOD-OS, surface roughness is parameterised separately for different land use fractions within each grid-cell. Cells with a high forest fraction are assigned roughness values representative of dense vegetation and ground cover, while cells dominated by the "other" land use fraction (typically agricultural or open land) are assigned lower roughness values. River cells are also treated distinctly, with Manning's coefficients reflecting the hydraulic properties of the river channel.

Enhancing infiltration

Infiltration in LISFLOOD-OS is mainly influenced by input maps with soil hydraulic properties, including saturated hydraulic conductivity and soil moisture content. These parameters are crucial for representing the effects of NBS on infiltration and their subsequent impacts on surface runoff and soil water retention. NBS aimed at improving soil hydraulic properties can be implemented by modifying these maps. Specifically:

- Saturated hydraulic conductivity (ksat in LISFLOOD-OS) reflecting changes in infiltration rates.
- Saturated soil moisture content (thetas in LISFLOOD-OS) reflecting changes in the water-holding capacity of the soil.

Soil layer representation

The LISFLOOD-OS model divides the soil profile into three layers, each contributing differently to infiltration and soil water dynamics. The model captures variations in water retention and flow behaviour across the following three soil depths:

- Layer 1: 0 – 5 cm depth.
- Layer 2: 5 – ±140 cm depth.
- Layer 3: ±140 – ±2800 cm depth.

The model uses separate input maps for each layer, including for parameters such as saturated hydraulic conductivity and saturated soil moisture content. Adjustments to these soil property maps should be made separately for each layer, considering the varying effects of the NBS at different depths.

3.2.1.2. Literature review on the effects of NBS

This section summarises the reported effects of the selected NBS on the hydrological processes in LISFLOOD-OS. The synthesis focuses on the relationships between the identified hydrological processes, the relevant LISFLOOD-OS parameters and the findings from the literature. An overview of these relationships is given in Table 7.

The complete literature review, including specific studies and their reported effects, is provided in Appendix F2.

(Re-) forestation

Forestation enhances infiltration and transpiration through improved saturated hydraulic conductivity and soil water-holding capacity reported in forested soils compared to agricultural land. Increased

interception is driven by the tree canopy intercepting rainfall, while the deeper root systems improve water uptake. The dense vegetation and ground cover slow down the overland flow, reflected in the increased Manning's roughness in the model. This increased hydraulic resistance and increased infiltration rates contribute to reduced surface runoff.

Soil aeration and subsoiling

By mechanically breaking up compacted soils, soil aeration and subsoiling significantly increase saturated hydraulic conductivity in the upper soil layers, allowing higher infiltration rates. These practices improve soil permeability and water retention while reducing surface runoff. However, their effects on interception, soil evapotranspiration and transpiration are negligible because they target soil physical properties rather than vegetation dynamics.

Conservation tillage

Conservation tillage modestly increases saturated hydraulic conductivity and soil water-holding capacity, leading to improved infiltration and reduced surface runoff. However, its effects are typically smaller than those of soil aeration or subsoiling. Changes in interception, soil evapotranspiration and transpiration are negligible as this measure does not significantly alter vegetation or canopy structure.

Stocking density

Reducing livestock grazing reduces soil compaction, which increases saturated hydraulic conductivity, allowing higher infiltration rates. This practice helps to reduce surface runoff but has a negligible effect on interception, soil evaporation and transpiration.

Table 7: Nature-based solutions and their reported effects on hydrological processes.

Nature-based solution	**Description**	**Interception**	**Soil evaporation**	**Transpiration**	**Infiltration**	**Surface runoff**	**Sources**
(Re-) forestation	Planting trees in deforested or non-forested areas	++	+	++	+	-	(Zimmermann et al., 2006) (Ferreira et al., 2021) (Lozano-Baez et al., 2019) (Yao et al., 2015) (Horel et al., 2015) (Eliasson & Larsson, 2006) (Li et al., 2019)
Soil aeration and subsoiling	Breaking up compacted soils	0	0	0	++	--	(Smith, 2012) (Penning et al., 2024) (Drewry et al., 2000) (Burgess et al., 2000)
Conservation tillage	Minimizing soil disturbance	0	0	0	+	-	(He et al., 2009) (Maulé & Reed, 1993) (Fér et al., 2020)
Stocking density	Decrease livestock grazing	0	0	0	+	-	(McCullough et al., 2001) (Dormaar et al., 1989) (Daniel et al., 2002)

3.2.1.3. Implementation of nature-based solutions in LISFLOOD-OS

This section combines the findings from Sections 3.2.1.1 and 3.2.1.2 and summarises how the hydrological processes influenced by the selected NBS were converted into parameter changes in LISFLOOD-OS. Table 8 summarises these adjustments, specifying the parameters influenced by each measure and the applied changes. These adjustments represent how the hydrological processes in LISFLOOD-OS were influenced by implementing specific NBS. Figure 17 complements the table by illustrating where the affected parameters are situated within the LISFLOOD-OS model structure. This figure helps contextualise how the selected NBS measures influence different soil layers.

Multiplication factors were used to modify the soil hydraulic properties maps. Instead of directly replacing values, the existing values in each grid-cell were multiplied by a factor. This approach accounted for the fact that soil hydraulic properties depend not only on the NBS but also on the underlying soil characteristics, which are modified rather than completely transformed by the NBS.

Table 8: NBS and their corresponding parameter changes.

	New fraction			Multiplication factor						New value
	fracforest	fracother	frac(all other)	ksat1_f	ksat2_f	ksat1_o	ksat2_o	thetas1_o	thetas2_o	mannings_f
Land use & cover changes										
(Re-) forestation	1	0	0	3	1,5	-	-	-	-	0,14
Improving soil conditions										
Soil aeration and subsoiling	0	1	0	-	-	3	1,4	1,2	1,05	-
Conservation tillage	0	1	0	-	-	1,5	1,05	1,1	1,02	-
Stocking density	0	1	0	-	-	2	1,02	-	-	-

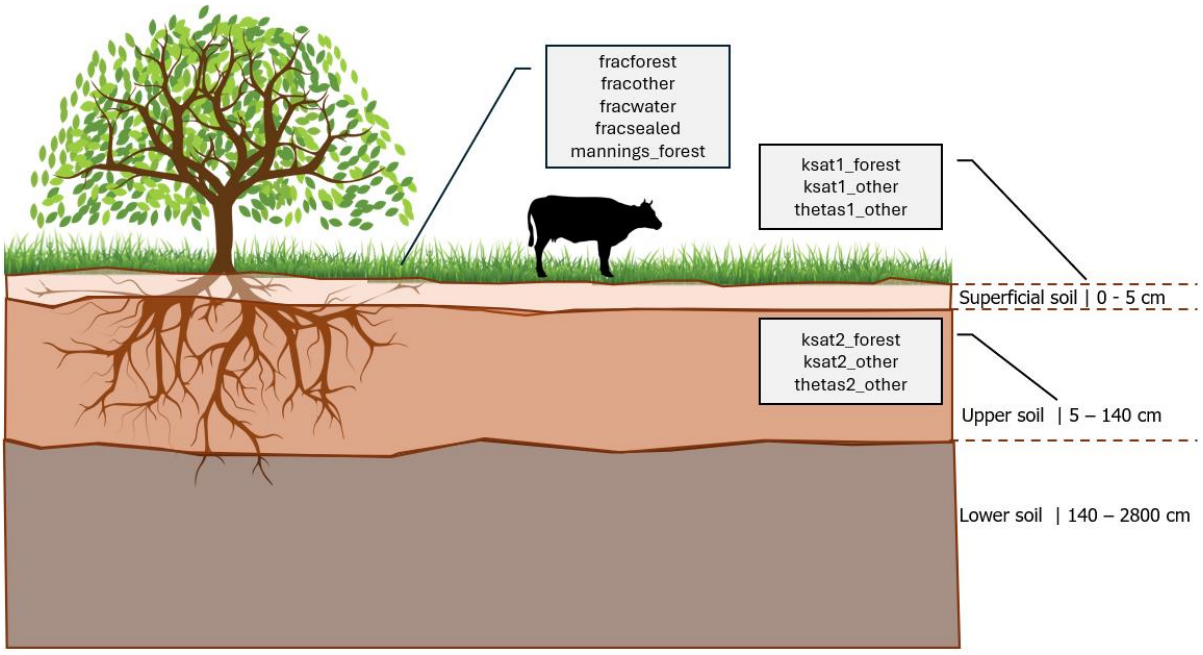

Figure 17: Overview of LISFLOOD-OS soil layer structure and parameters adjusted based on NBS.

3.2.2. Nature-based solution scenarios

To assess the potential impacts of NBS in the Vecht catchment, 11 distinct NBS scenarios were defined. To define these NBS scenarios, adjustments were made to specific areas (and their corresponding grid-cells) based on the parameter changes determined in the previous step. These areas, including their spatial distribution and total hectare coverage, are summarised in Section 3.2.2.3. The scenarios were designed to reflect realistic interventions in the Vecht catchment by following two main principles:

Aligning with current land use

The scenarios have been tailored to be consistent with the existing land use in the Vecht catchment by taking into account the following factors:

- **Exclusion of Urban Areas**: Adjustments were not applied to grid-cells classified as built-up or urban, as it can be assumed that such interventions are unfeasible given the practical challenges and socio-economic implications of altering established urban areas.
- **Agricultural Land Use Differentiation**: Within agricultural areas, a distinction was made between grasslands (typically used for livestock farming) and arable lands. This differentiation helped to determine which NBS were suitable for specific types of agricultural land.
- **Avoiding Redundancy**: Adjustments were avoided in grid-cells where the intended NBS change already aligned with the current land use type, ensurin no unnecessary modifications were made.

Aligning with regional policies

Spatial plans and environmental policies from governmental sources were consulted to identify areas where NBS changes were feasible and realistic within the socio-political context. This ensured the scenarios were consistent with existing land use plans and ecological goals.

By combining these two principles, the defined NBS scenarios represent plausible land use changes that consider both the regional context and practical feasibility, ensuring that parameter adjustments align with the characteristics and policies of the Vecht catchment.

3.2.2.1. Afforestation scenarios

The first set of scenarios focused on afforestation. These include a sensitivity analysis to evaluate the potential impacts of different afforestation levels (25%, 50%, and 75%) and targeted afforestation in specific locations, such as upstream and downstream forested areas. Additionally, three afforestation strategies were developed based on a realistic 10% increase in forest area, guided by governmental objectives.

Overijssel and Drenthe have outlined afforestation strategies that align with the national goal of the Netherlands to increase forest coverage by 10% of the existing forest area by 2030 (Provincie Drenthe, 2021; van Dijk & van Wijk, 2022). This target is based on the forest area as it was in 2020 as described by the Ministry of Agriculture, Nature and Food Quality (Ministerie van Landbouw; Natuur en Voedselkwaliteit, 2020). The province of Overijssel's approach, which first determines the currently existing forest area and then adds 10% extra forest, was adopted for this study. Due to the lack of specific afforestation goals for Niedersachsen and Nordrhein-Westfalen in the German literature, the same 10% increase strategy was applied across all regions.

The existing forest cells in each province and state were counted, and 10% of the current forest area was randomly added to agricultural areas within each region. Table 9 summarises each region's existing forest coverage and corresponding afforestation targets.

Table 9: Forest coverage in 2018 and afforestation targets per region.

Province / State	**Existing forest [ha]**	**+ 10 % afforestation [ha]**
Overijssel	4,400	440
Drenthe	18,200	1,820
Niedersachsen	14,000	1,400
Nordrhein-Westfalen	6,100	610

3.2.2.2. Agricultural soil improvement scenarios

The second set of scenarios examines the application of soil improvement measures within agricultural areas. Each measure is applied to a specific type of agricultural land:

- Soil aeration and subsoiling: applied across all agricultural land.
- Conservation tillage: targeted to arable lands.
- Stocking density optimisation: focused on livestock grazing areas.

Table 10 provides an overview of the proportion of arable and livestock grazing areas within each province or state in the Vecht catchment. These percentages were used to determine the extent of agricultural cells where each NBS measure was applied. In the absence of specific spatial data on agrarian use per cell, the designated percentage of random agricultural cells in each region was adjusted to reflect the proportion of arable or livestock areas indicated in the table.

Table 10: Proportion of arable and livestock grazing areas as a percentage of the total agricultural area per region.

Province / State	**Arable**	**Livestock**	**Source**
Overijssel	11%	89%	(Centraal Bureau Statistiek, 2024)
Drenthe	44%	56%	(Centraal Bureau Statistiek, 2024)
Niedersachsen	72%	28%	(Landesamt für Statistik Niedersachsen, 2023)
Nordrhein-Westfalen	72%	28%	(Information und Technik Nordrhein-Westfalen, 2024)

3.2.2.3. Overview of scenario locations and areas

The selected areas for each scenario, including their spatial distribution and total hectare coverage, are summarised in Table 11. Visual representations of the areas impacted by eight of these scenarios are provided in Figure 18. Scenarios 6, 7 and 8 are not visualised due to the small number of affected cells, which are difficult to distinguish in a compact figure.

Table 11: Overview of developed NBS scenarios.

Scenario nr.	**Description**	**Area type**	**Coverage [ha]**
1	25% afforestation	Forest	± 100,000
2	50% afforestation	Forest	± 200,000
3	75% afforestation	Forest	± 300,000
4	Large upstream forest 50%	Forest	± 200,000
5	Large downstream forest 50%	Forest	± 200,000
6	German afforestation strategy	Forest	2,000
7	Dutch afforestation strategy	Forest	2,300
8	Combined afforestation strategy (GE & NL)	Forest	4,300
9	Soil aeration and subsoiling	All agricultural land	322,480
10	Conservation tillage	Arable area	143,630
11	Stocking density	Livestock area	178,850

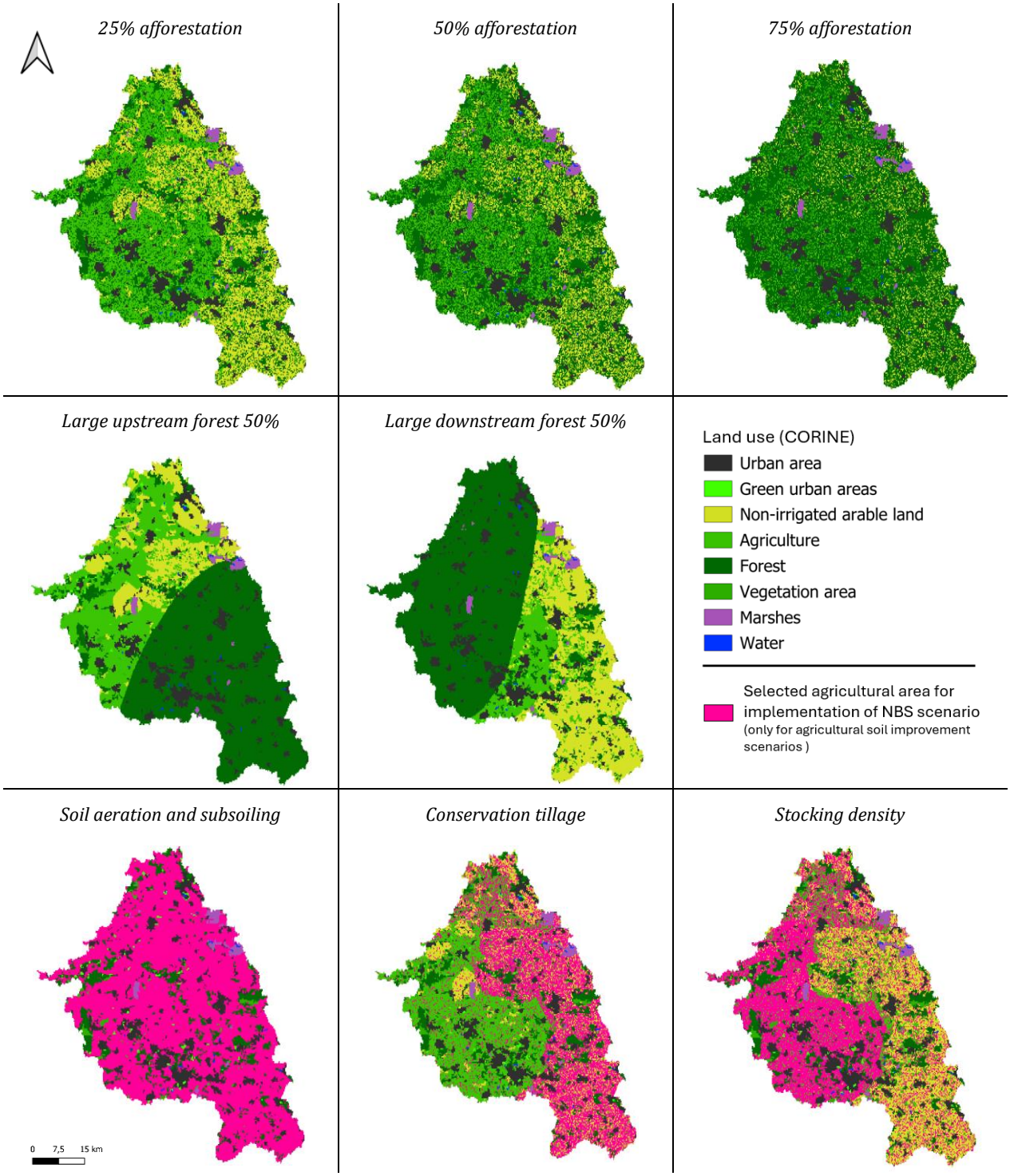

Figure 18: Areas impacted by the different NBS scenarios.

3.2.3. Meteorological scenarios

Two types of meteorological scenarios were used to assess the impact of the NBS: artificial rain events including uniform rainfall events of varying intensity and the Limburg 2021 extreme rainfall event adapted to the Vecht catchment.

3.2.3.1. Artificial rain events

A series of spatially uniform rainfall events were designed to evaluate the effectiveness of NBS under varying rainfall conditions, following a methodology similar to Penning et al. (2024). Three rainfall

scenarios of varying intensities were simulated (80 mm, 150 mm, and 200 mm over two days). These rainfall events were applied under both summer and winter conditions to assess the seasonality of NBS performance.

The rainfall scenarios include three distinct events designed to assess the effectiveness of NBS under varying intensities. The 80 mm scenario represents a 1 in 50-year rainfall event for an average Dutch Waterboard catchment area (Beersma et al., 2019). The 150 mm and 200 mm scenarios are based on stress test protocols developed by Deltares to evaluate extreme and exceptionally intense rainfall events (Bruijn de & Maas, 2023), providing insight into the maximum potential impact of NBS. Penning et al. (2024) emphasise the significant influence of initial conditions on the hydrological response to rainfall events. Therefore, each rainfall event was applied under both summer (July) and winter (March) conditions to account for seasonal variations. A summary of the rainfall events, including their timing and sources, is provided in Table 12.

Table 12: Artificial rain events placed on the Vecht catchment in 2017.

Rainfall intensity [mm/day]	Total volume [mm]	Duration [days]	Start peak event winter	Start peak event summer	Source
40	80	2	1-3-2017	1-7-2017	(Beersma et al., 2019)
75	150	2	1-3-2017	1-7-2017	(Bruijn de & Maas, 2023)
100	200	2	1-3-2017	1-7-2017	(Bruijn de & Maas, 2023)

To assess the performance of NBS during low flows, the meteorological data from the dry year 2018 was repeated for four consecutive years. This repetition of a dry year allowed for an evaluation of the cumulative impacts of NBS on low flow conditions over an extended period.

A warm-up period using meteorological data from 2016 to 2021 was used to establish stable initial conditions. Following this warm-up, the simulation period consisted of two years of historical data (2016–2017) with the rainfall events implemented in 2017, followed by the repeated dry year scenarios (2018a–2018d). Figure 19 illustrates the timeline of the simulation setup, including the placement of the summer and winter rainfall events and the repetition of the dry year for low flow analysis.

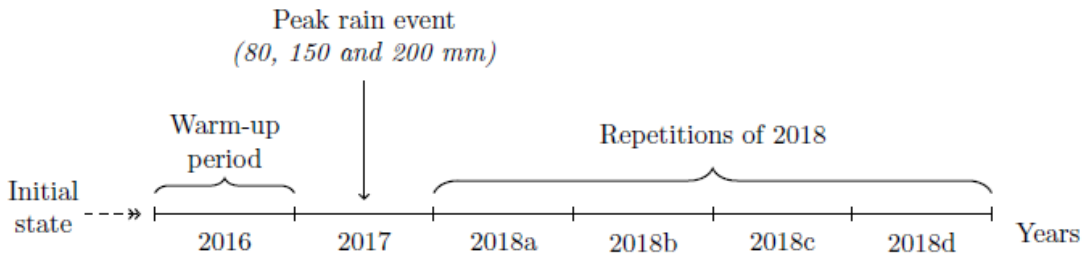

Figure 19: Concept of rainfall series for artificial rain events; 2016 and 2017 are historical series with the peak rain event implemented in 2017; 2018a, b, c and d are repetitions of the dry year 2018 (Cazemier, 2024b).

3.2.3.2. Limburg 2021 rainfall event

To further evaluate the effects of NBS scenarios on high flows, the rainfall data from the severe flooding event in Limburg in July 2021 was applied to the Vecht basin. As highlighted by Bruijn de & Slager (2021), such events could occur elsewhere in the Netherlands due to the increasing frequency and intensity of extreme rainfall driven by climate change (Tradowsky et al., 2023). Using this realistic rainfall scenario helps to estimate the potential effects of NBS under conditions resembling past extreme events.

The RADFLOOD21 precipitation dataset was used for this analysis, which consists of weather radar measurements merged with validated rain gauge data (Journée et al., 2023). This dataset provides precipitation data at an original temporal resolution of 5 minutes for the six days from July 12th to 17th, 2021. To adapt the dataset for use in LISFLOOD-OS, the following modifications were made:

- The coordinate system was adjusted to align with the Vecht catchment.

- Daily precipitation sums were calculated from the high-resolution data.
- The precipitation unit was converted from 0.1 mm to mm.

To account for spatial variability within the catchment, the peak rainfall event (14 July) was centred on three sub-catchments of the Vecht: the Regge (Figure 20a), the Dinkel (Figure 20b) and the main Vecht at Emlichheim (Figure 20c). This placement allows the assessment of NBS effects in different parts of the catchment with varying rainfall intensities.

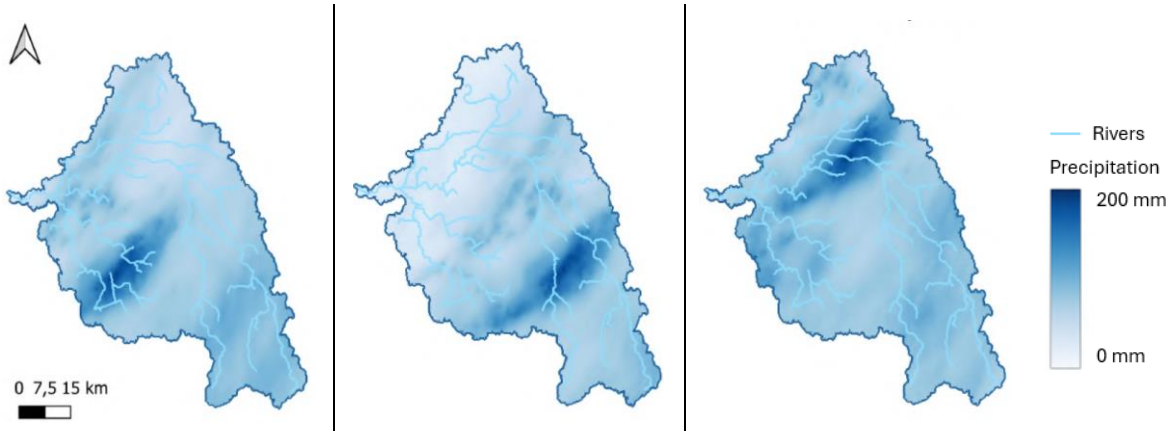

(a) Above Regge *(b) Above Dinkel* *(c) Above Emlichheim*

Figure 20: Locations of 2021 Limburg peak rainfall event; Precipitation in millimetres on July 14th.

The simulation setup used the same initial state and warm-up period (2016-2021) as used in the stress tests, ensuring consistent conditions for comparison. The adjusted RADFLOOD21 dataset was then used in the simulation during the first six days of July (Figure 21).

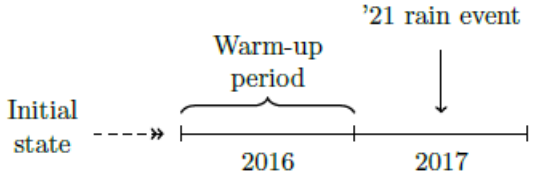

Figure 21: Concept of rainfall event Limburg 2021 evaluation (Cazemier, 2024b).

3.2.4. Evaluation of the effects on high and low flows

This section outlines the methodology used to evaluate the effects of the defined NBS scenarios on high and low flows in the Vecht catchment. The analysis focuses on two main aspects: flow indicators and water balance components. Flow indicators quantify how NBS affect hydrological extremes, such as floods and droughts. Meanwhile, water balance components show what drives these changes. NBS affect water retention and release within the catchment by changing processes like infiltration and evapotranspiration, which directly relate to flow extremes. This connection ensures a comprehensive understanding of how NBS influence both hydrological processes and flow behaviour in the Vecht catchment.

3.2.4.1. Flow indicators

The following flow indicators are used to assess the impact of NBS on high, low and average flows in the Vecht catchment:

Annual maximum daily discharge

The annual maximum daily discharge refers to the highest flow rate recorded in the river during a single day for that year, expressed in m^3/s. This indicator evaluates how NBS influence high flow peaks, which directly relate to flood risk. By analysing the annual maximum daily discharge, it is possible to assess how much water NBS can store or delay before it reaches the river, providing insight into their potential for flood mitigation (Ruangpan et al., 2020).

Minimum 7-day average discharge (MAM7)

The Minimum 7-day Average Discharge (MAM7) captures the lowest average discharge (m^3/s) over any consecutive seven-day period during the simulation (Smakhtin, 2001). This low flow statistic is used to assess drought conditions and water availability during dry periods. By examining MAM7, the effectiveness of NBS in improving water availability during droughts in the Vecht catchment can be assessed.

Average discharge

The average discharge represents the average flow rate (m^3/s) over the simulation period and is a general indicator of the catchment's hydrological response to NBS. It indicates how NBS may influence overall water distribution (Ferreira et al., 2021).

3.2.4.2. Water balance components

To assess the impact of the NBS scenarios on hydrological processes, the water balance components simulated by the LISFLOOD-OS model were analysed. The components considered include actual evapotranspiration, surface runoff, subsurface flow from the upper zone and baseflow from the lower zone. These components provide insights into the effectiveness of the NBS by illustrating their influence on different aspects of the hydrological cycle, an approach similarly taken by Mosbahi et al. (2023) and Hoang & Hughes (2024), who highlight the importance of water balance analysis in assessing land use changes.

Actual evaporation

Evaporation returns water to the atmosphere, reducing soil moisture availability. NBS, such as afforestation, can increase evaporation due to higher vegetation cover, potentially reducing surface runoff and altering the water balance. Therefore, analysis of evaporation is essential for understanding the interplay between vegetation dynamics and water availability.

Surface runoff

Surface runoff is the precipitation that flows directly into streams without infiltrating the soil. NBS, such as afforestation or conservation tillage, can reduce surface runoff by enhancing soil infiltration capacity. Examining surface runoff reveals the extent to which NBS can reduce rapid drainage of water and improve catchment water retention.

Sub-surface flow from the upper zone

Sub-surface flow refers to water infiltrating the soil and moving through the upper zone without percolating into the lower groundwater zone. The amount of sub-surface flow is indirectly affected by the soil hydraulic properties, which are modified by the NBS. Analysing sub-surface flow provides insights into how NBS enhance temporary soil water storage and contributes to delayed water release into streams, helping to reduce peak flows.

Baseflow from the lower zone

Baseflow represents the steady release of groundwater from the lower zone into streams. Improving groundwater recharge through the implementation of NBS could potentially increase resilience to droughts. Evaluating the baseflow provides insight into how effective NBS are in increasing groundwater recharge, ensuring long-term water availability and supporting low flows.

4. Results

4.1. Determination of the LISFLOOD-OS model performance

4.1.1. Sensitivity analysis

The most sensitive parameters were *b*, GW_{perc}, C_{pref} and GW_{loss}. These parameters play a critical role in the hydrological processes simulated by LISFLOOD-OS:

- *b* [-] is an empirical, non-dimensional shape parameter that influences the infiltration capacity of the soil.
- GW_{perc} $\left[\frac{mm}{day}\right]$ represents the maximum percolation rate from the upper to the lower groundwater zone.
- C_{pref} $\left[\frac{mm}{day}\right]$ is an empirical shape parameter that influences the amount of preferential bypass flow towards the upper groundwater zone.
- GW_{loss} $\left[\frac{mm}{day}\right]$ defines the maximum percolation rate from the lower groundwater zone to areas beyond the catchment boundaries or to deeper groundwater systems.

b has the most significant influence on both high and low flows, significantly affecting how water infiltrates into the soil and the ability of the model to simulate flow dynamics under varying conditions. This is clearly illustrated in Figure 22, which shows the objective function values and cumulative discharges at Emlichheim for the five *b* runs, highlighting the strong influence of this parameter. GW_{perc} strongly influences groundwater flow, especially base flow during low flow periods, while C_{pref} plays a key role in the rapid movement of water through the system during high flow events. Finally, GW_{loss} shows considerable sensitivity in controlling baseflow by influencing groundwater storage losses.

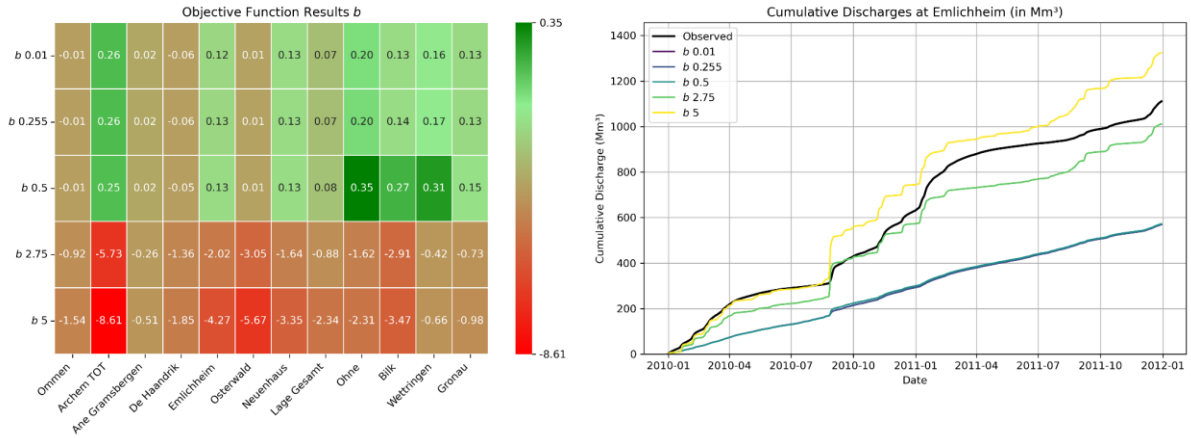

Figure 22: Objective function values and cumulative discharges at Emlichheim for varying b values.

Parameters such as *QSplitMult*, T_{uz} and T_{lz} show a moderate effect on model performance. These parameters influence specific hydrological processes such as floodplain flow, groundwater discharge and long-term groundwater storage and release but did not cause significant variations in objective function values compared to the more sensitive parameters mentioned earlier.

Meanwhile, parameters such as $LZ_{threshold}$, *CalChanMan1* and *CalChanMan2* (Manning's coefficients for riverbed [1] and floodplain [2]) had the least influence, with minimal impact on the overall model results. Detailed results for all parameters, including their respective objective function values and cumulative discharge plots, can be found in Appendix D.

Based on these findings, calibration efforts included the most sensitive parameters - *b*, GW_{perc}, C_{pref} and GW_{loss} - to improve the model's representation of both high and low flows. The calibration procedure was carried out according to a structured approach as described in detail in Section 3.1.4. Calibration began with GW_{loss} to account for groundwater losses, followed by GW_{perc} to refine groundwater percolation. Next, C_{pref} was calibrated to optimise preferential flow within the soil profile, and finally, *b* was adjusted to improve the partitioning between surface runoff and infiltration.

4.1.2. Calibration

Table 13 presents the final calibrated values for each sub-catchment, showing only the parameters included in the calibration: GW_{loss}, GW_{perc}, C_{pref}, and b.

Table 13: Calibrated parameter values for each sub-catchment.

Sub-catchment		GW_{loss} [mm/day]	GW_{perc} [mm/day]	C_{pref} [-]	b [-]
Wettringen	**GE**	0.56	0.8	2.07	1.39
Bilk	**GE**	0.63	0.73	5.21	0.54
Gronau	**GE**	0.63	0.8	4.04	0.97
Ohne	**GE**	0.88	0.37	0.89	0.015
Neuenhaus	**GE**	0.56	0.49	3.64	0.015
Lage Gesamt	**GE/NL**	0.56	0.73	0.5	0.015
Osterwald	**GE**	0.38	0.8	2.46	1.07
Emlichheim	**GE**	0.19	0.73	2.46	0.015
De Haandrik	**GE**	0.46	0.8	1.68	0.015
Ane Gramsbergen	**GE/NL**	0	0.8	2.07	2.5
Ommen	**GE/NL**	0.46	0.8	1.68	0.015
Ommerkanaal	**NL**	0	2	0.5	0.015
Archem TOT	**NL**	0.56	0.49	3.25	0.015
Dalfsen	**NL**	0.46	0.8	1.68	0.015

The calibration results for each station are summarised in Table 14. No observed discharge data for station Dalfsen was available for the calibration period. Therefore, it is omitted from this overview.

Table 14: Performance metric scores per station for calibrated model.

Station		NS_{inv}	NS_w	RVE	OF
Wettringen	**GE**	0.36	0.84	- 36 %	0.44
Bilk	**GE**	0.14	0.70	- 49 %	0.28
Gronau	**GE**	0.25	0.63	- 40 %	0.31
Ohne	**GE**	0.47	0.82	- 40 %	0.46
Neuenhaus	**GE**	0.49	0.16	- 42 %	0.23
Lage Gesamt	**GE**	0.15	0.39	- 29 %	0.21
Osterwald	**GE**	-0.16	0.65	21 %	0.20
Emlichheim	**GE**	0.39	0.28	- 28 %	0.26
De Haandrik	**NL**	-0.14	0.23	- 28 %	0.03
Ane Gramsbergen	**NL**	0.00	0.59	65 %	0.18
Ommen	**NL**	-0.14	0.50	2 %	0.18
Ommerkanaal	**NL**	-0.01	0.44	41 %	0.15
Archem TOT	**NL**	0.54	0.38	- 13 %	0.41

The performance of the model, as evaluated by the multi-objective function (OF), ranges from 0.20 to 0.46 for the German stations and from 0.03 to 0.41 for the Dutch stations. Overall, the performance of the model in the German part of the catchment can be considered satisfactory, while it is generally less reliable in the Dutch part, with most stations showing unsatisfactory results with scores below 0.2.

In general, the scores for NS_{inv} (which evaluates low flows) are lower than those for NS_w (focused on high flows), indicating that the model struggles more with accurately simulating low flow conditions compared to high flow events. This difference is particularly evident in the Dutch part of the basin, where NS_{inv} scores are generally lower. Additionally, there are significant variations in RVE scores, with

most stations showing a substantial deviation in total flow volume, indicating either over- or underestimation of discharge volume over the calibration period.

The OF scores also reveal some patterns: the German stations generally perform better, with higher OF scores, than those in the Dutch section of the basin. A notable exception is the Archem TOT station, which performs well compared to other Dutch stations, achieving a higher OF score. This may be related to the fact that Archem TOT aggregates data from two discharge stations, which could introduce uncertainties or inaccuracies in the observed time series, although the exact reason remains unclear.

To illustrate the differences in performance between high-scoring stations, Figure 23 and Figure 24 present hydrographs for Archem TOT and Ohne, respectively, both of which achieved relatively high OF scores but for different reasons. The hydrographs of the calibration period for all stations can be found in Appendix E.

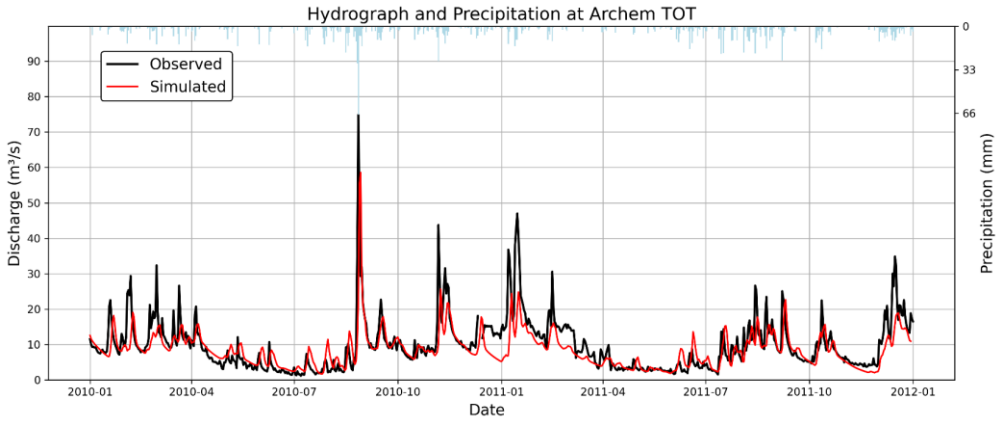

Figure 23: Observed and simulated discharges from 2010-2011 at station Archem TOT.

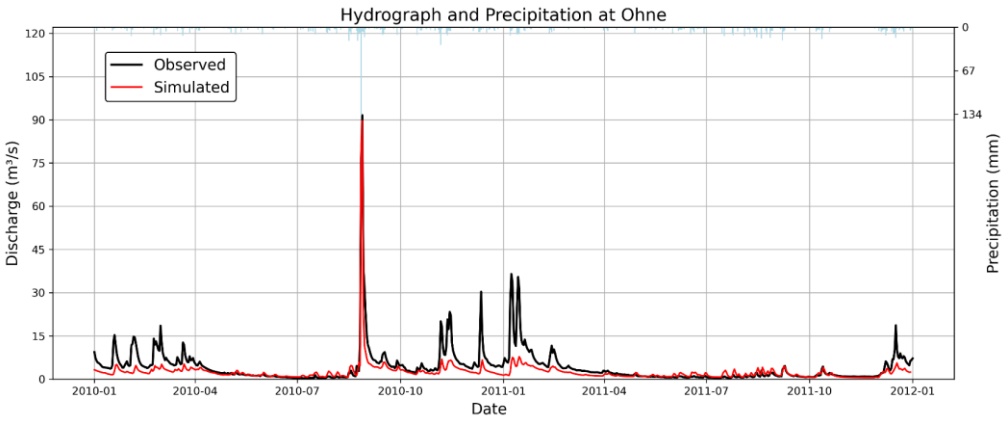

Figure 24: Observed and simulated discharges from 2010-2011 at station Ohne.

Archem TOT benefits from a relatively lower RVE value, contributing to its balanced objective function score. The absence of extremely low flows near zero results in a more moderate NS_{inv} score, as there are less discrepancies in low flow simulation. However, the 2010 peak event is less accurately simulated at Archem TOT, reflected in a lower NS_w score. This suggests that while total volume and low flow conditions are reasonably represented, the model struggles to capture peak discharge events at this station.

The model achieves a high NS_w score at Ohne, as the significant peak discharge event in 2010 is well simulated. However, RVE shows a larger value, with the model either over- or underestimating total discharge volume over the period. The NS_{inv} score is also lower compared to Archem TOT, likely due to the inaccuracies in simulating extremely low flows close to zero. Finally, it results in a higher objective function score due to the more accurate representation of the 2010 peak flow despite the issues with low flow and total volume accuracy.

These results show that although the German stations tend to score higher on average, there are individual exceptions. The variation in OF scores between stations reflects different strengths in simulating peak flows versus maintaining an accurate water balance, as seen at Archem TOT and Ohne. The differences between the performance metrics highlight the challenges of achieving consistent accuracy with the model in both high and low flow conditions across the catchment.

4.1.3. Validation

Table 15 presents the OF scores for each station during the validation years and the calibration scores for easy comparison. Overall, the validation results show considerable variation between stations, with some showing relatively stable performance over both calibration and validation years, while others show more pronounced fluctuations. Stations like Wettringen and Emlichheim show relatively stable OF values over different periods, suggesting robust model performance at these sites under varying hydrological conditions. In contrast, stations like Bilk and Gronau show larger fluctuations in their scores, including some negative values in certain years (e.g. Bilk in 2012 and 2018), indicating challenges in accurately capturing the low flows.

Table 15: Objective function values per station for validation periods and calibration.

Station		1998	2012-2013	2018	2023	Calibration
Wettringen	**GE**	0.26	0.22	0.17	0.31	0.44
Bilk	**GE**	0.18	-0.14	-0.24	0.15	0.28
Gronau	**GE**	0.27	0.16	-0.09	0.22	0.31
Ohne	**GE**	0.26	0.23	-	0.33	0.46
Neuenhaus	**GE**	0.24	0.09	-	0.16	0.23
Lage Gesamt	**GE**	0.28	0.22	-	-	0.21
Osterwald	**GE**	0.21	0.22	-	-0.01	0.20
Emlichheim	**GE**	0.27	0.27	0.34	0.43	0.26
De Haandrik	**NL**	-	0.07	-0.03	0.23	0.03
Ane Gramsbergen	**NL**	-	0.12	-	0.69	0.18
Ommen	**NL**	-	0.25	0.11	0.45	0.18
Ommerkanaal	**NL**	-	0.13	0.03	0.01	0.15
Archem TOT	**NL**	0.51	-0.75	-	0.70	0.41
Dalfsen	**NL**	0.09	0.22	0.23	0.48	-

For a closer look at model performance in both German and Dutch sub-catchments, Figure 25 presents hydrographs for Archem TOT (NL) and Ohne (GE) in the validation period 2012-2013, allowing for a comparison with the calibration results. Although Ohne achieves a higher overall OF score (0.23) compared to Archem TOT (-0.75) in this period, this difference is primarily due to the poor NS_{inv} score at Archem TOT (-2.05) compared to Ohne (0.38), indicating significant challenges in simulating low flows at this station. The hydrographs of the validation periods for all stations can be found in Appendix E, together with all performance metric scores per station and validation period.

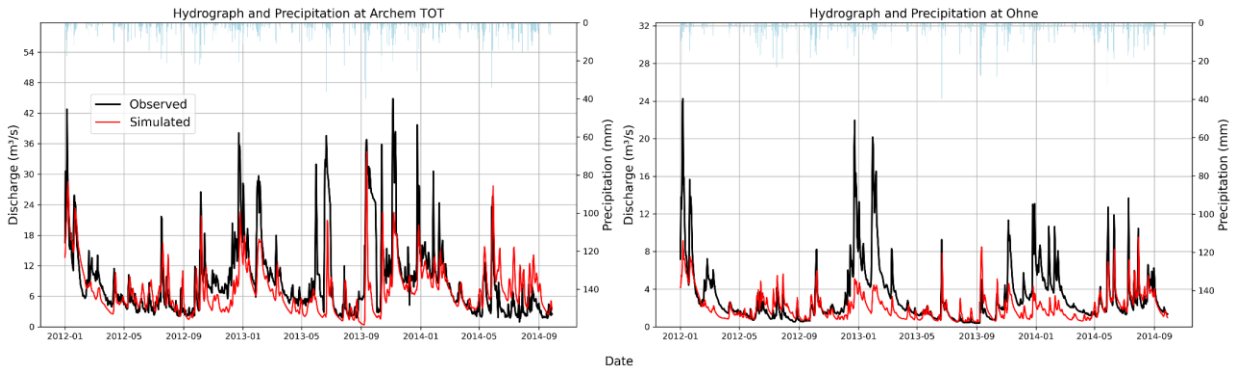

Figure 25: Observed and simulated discharges for dry years 2012-2013 at station Archem TOT and Ohne.

In the 2012-2013 validation period, the model performance varies significantly between Archem TOT and Ohne. During this period, Archem TOT struggles with accurately simulating low flows during the summer periods, contributing to a notably low OF score. This poor fit in the low-flow periods suggests limitations in the model's ability to capture baseflow dynamics at Archem TOT. In contrast, Ohne performed more consistently during both high and low flows in 2012-2013. The OF score for Ohne reflects relatively good performance, mainly due to better baseflow simulation during low flow periods compared to Archem TOT. However, the hydrograph shows notable discrepancies in the simulation of peak flows, indicating limitations in capturing high-flow dynamics. The better representation of baseflow at Ohne contributes to its relatively higher OF score.

4.2. The effects of NBS in the Vecht catchment using LISFLOOD-OS

First, the results for the afforestation scenarios are presented, starting with the artificial rain events, followed by the Limburg 2021 extreme rain event, and ending with the water balance components. The results for the soil improvement scenarios are then discussed in the same order.

4.2.1. Afforestation

4.2.1.1. Artificial rain events

The artificial rain events evaluated the impact of various afforestation scenarios under uniform rainfall events in summer and winter conditions, with results highlighting differences in peak discharge behaviour between seasons and rainfall intensities.

Figure 26 illustrates the simulated hydrographs for the Regge sub-catchment at the Archem TOT station under a uniform two-day rainfall event of 100 mm/day (200 mm total) under summer (a) and winter (b) conditions.

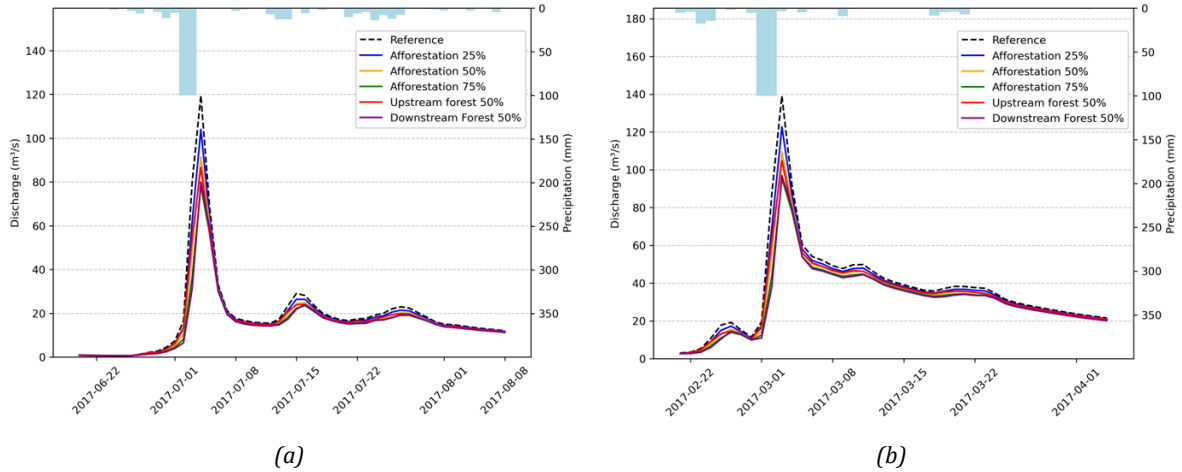

Figure 26: Hydrographs at Archem TOT for afforestation scenarios under summer (a) and winter (b) conditions with a uniform 2-daily rain event of 100 mm/day.

The hydrographs demonstrate a higher peak discharge in winter compared to summer (20 m³/s higher). The elevated soil moisture levels in winter are likely to be the reason that the soil cannot take up as much of the precipitation, resulting in increased discharge to the river. Despite this difference, afforestation scenarios consistently reduce the heights of peak flows, demonstrating their influence on runoff reduction. Furthermore, during winter, relatively high river discharges tend to persist for longer, whereas in summer, the river flow decreases more rapidly to lower levels following the rainfall event.

Additionally, station-specific effects were observed, with notable variations in afforestation impacts across locations. For instance, at station Emlichheim (Appendix G1), the impact of afforestation was considerably smaller during the winter peak, reflecting the spatial variability in runoff dynamics across the Vecht catchment. This variation is probably due to the location of station Emlichheim, where higher winter baseflows from upstream sub-catchments reduce the relative impact of afforestation compared to Archem TOT.

Figure 27 quantifies the effects of afforestation on peak discharge reduction, minimum 7-day average discharge (MAM7), and mean discharge for two rainfall intensities (80 mm and 200 mm) in both summer and winter.

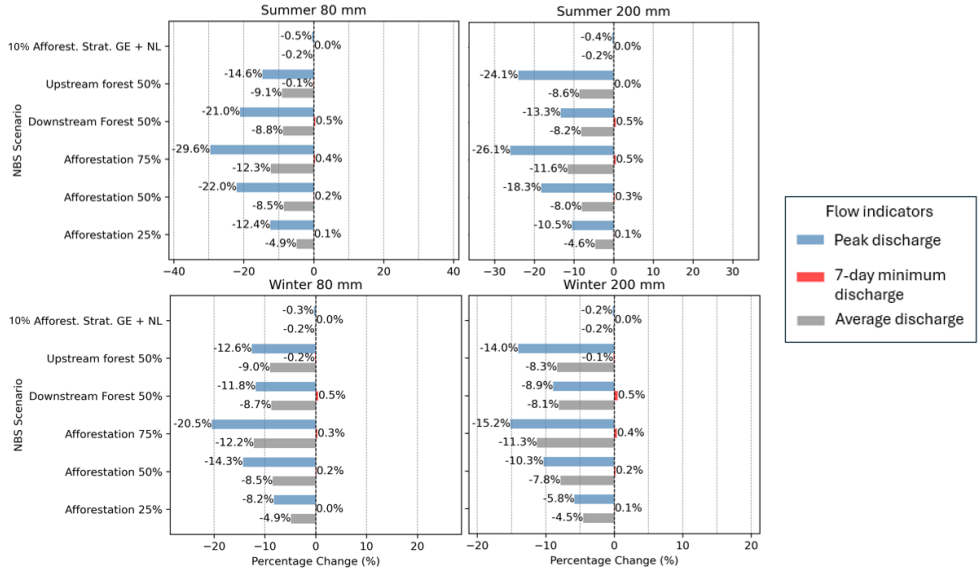

Figure 27: Modelled effects of afforestation scenarios at Dalfsen under summer (top) and winter (bottom) conditions for 2 different rain events; peak daily discharge is based on the discharge waves caused by the 2-daily rain events at the beginning of July (summer) and March (winter); MAM 7 and mean discharge are based on the period 2017 and 2018.

Realistic afforestation strategies, such as the 10% combined afforestation strategy for Germany (GE) and the Netherlands (NL), demonstrated negligible effects on the flow indicators. The largest simulated reduction in peak discharge for this strategy was less than 0.5%, observed during the summer 80 mm rainfall scenario. Since separate strategies targeting only GE or NL individually showed even smaller effects, these were excluded from further figures.

Afforestation had the most significant impact on reducing peak discharges, particularly under summer conditions. For example, the 75% afforestation scenario resulted in a peak flow reduction of nearly 30% during the 80 mm summer event, compared to a 20% reduction under the same rainfall intensity in winter. These results highlight the potential of large-scale afforestation to mitigate flood peaks. However, the impact of afforestation on low flows, as measured by the minimum 7-day average discharge (MAM7), was negligible across all scenarios, with changes consistently below 0.5%. This suggests that the additional water infiltrating into the soil under afforestation does not contribute significantly to base flow during dry periods.

The effects of afforestation on average discharge were consistent across rainfall scenarios, showing reductions of nearly 5% for the 25% afforestation scenario and up to 12% for the 75% afforestation scenario. However, variations in the effectiveness of afforestation were observed depending on rainfall

intensity. In scenarios characterised by higher rainfall (200 mm), the overall effectiveness of afforestation generally declined compared to the 80 mm rainfall events. An exception to this trend was observed for the upstream forest scenario, where effectiveness slightly increased under the 200 mm event. This discrepancy is likely due to localised, unrealistically simulated hydrological dynamics in the sub-catchment Ane Gramsbergen.

In summary, while large-scale afforestation shows potential for reducing peak discharges, realistic afforestation strategies, such as the 10% catchment coverage scenario for Germany and the Netherlands combined, are insufficient to produce meaningful reductions in high flows or increases in low flows.

4.2.1.2. Limburg 2021 event

To evaluate the effects of afforestation on high flows during a realistic extreme rainfall event, the precipitation data of the extreme event in Limburg 2021 was applied to the Vecht catchment. The rainfall event was centred on three sub-catchment areas (Regge, Dinkel, and De Haandrik). Hydrographs are shown for two locations: the 2021 event centred on the Dinkel sub-catchment is shown for station De Haandrik (Figure 28a), and the 2021 event centred on the Regge sub-catchment is shown for station Archem TOT (Figure 28b). The simulation for the 2021 event centred on the De Haandrik sub-catchment was excluded due to extremely high discharge estimations from the Ane Gramsbergen sub-catchments, which distorted the results."

The dashed yellow, orange, and red lines in the figures represent the first, second, and third warning levels. The warning levels have different meanings at the different stations because they are obtained through different organisations with each their own policies on these warning levels. However, they provide a general indication of the severity of peak discharges.

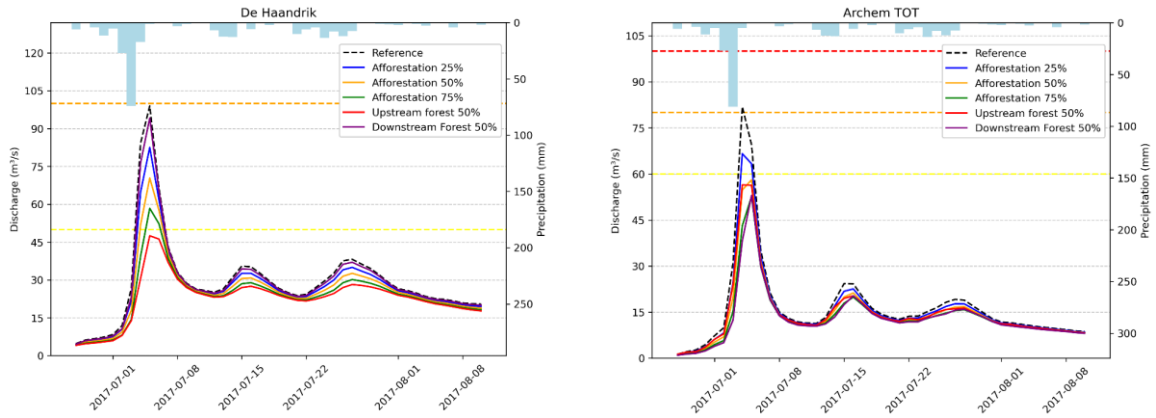

Figure 28: Hydrographs during the 2021 rain event for afforestation scenarios; (a) with peak rain event in Dinkel sub-catchment & (b) with peak rain event in Regge sub-catchment; dashed yellow, orange and red lines are first, second and third warning levels.

At De Haandrik (Figure 28a), a clear trend is visible across the afforestation scenarios. Downstream forest had the least impact, as it lies outside the contributing area upstream of the station. Scenarios with 25%, 50%, and 75% afforestation exhibited progressively larger peak flow reductions, with the upstream forest scenario achieving the most significant modelled reduction of nearly 50 m³/s. Beyond the immediate peak, afforestation scenarios also reduced elevated discharges during the following days, highlighting their influence on moderating high flow conditions.

At Archem TOT (Figure 28b), the effects of the afforestation scenarios were more comparable. The 50% afforestation and upstream forest scenarios resulted in similar peak reductions, while the 75% afforestation and downstream forest scenarios achieved slightly larger reductions. The differences between scenarios were less pronounced than at De Haandrik, and the influence of afforestation on elevated discharges in the days following the event was more limited.

The Limburg 2021 event analysis demonstrates the potential of afforestation to reduce peak flows, primarily when implemented upstream of critical locations. However, the magnitude of the effect varies between sub-catchments and discharge stations, reflecting the spatial dynamics of afforestation effects in the Vecht catchment.

4.2.1.3. Water balance components

Figure 29 presents the annual totals (mm/year) for the modelled water balance components across the reference and afforestation scenarios. These totals are calculated for all grid-cells upstream of the Dalfsen station, covering the period from 2017 to 2018d. The results are based on the meteorological scenario involving a 2-daily rainfall event of 40 mm/day during summer.

The choice of summer or winter scenarios and the intensity of rainfall events had minimal influence on the annual water balance components. However, surface runoff and upper zone outflow in 2017 showed some sensitivity to larger rainfall events. That year, larger rainfall events led to higher surface runoff values and increased upper zone outflow, reflecting the direct relationship between precipitation intensity and these components. This effect persisted slightly into 2018a but diminished in subsequent years. This pattern is illustrated in Appendix G2 as well, which presents the same results for an alternative meteorological scenario.

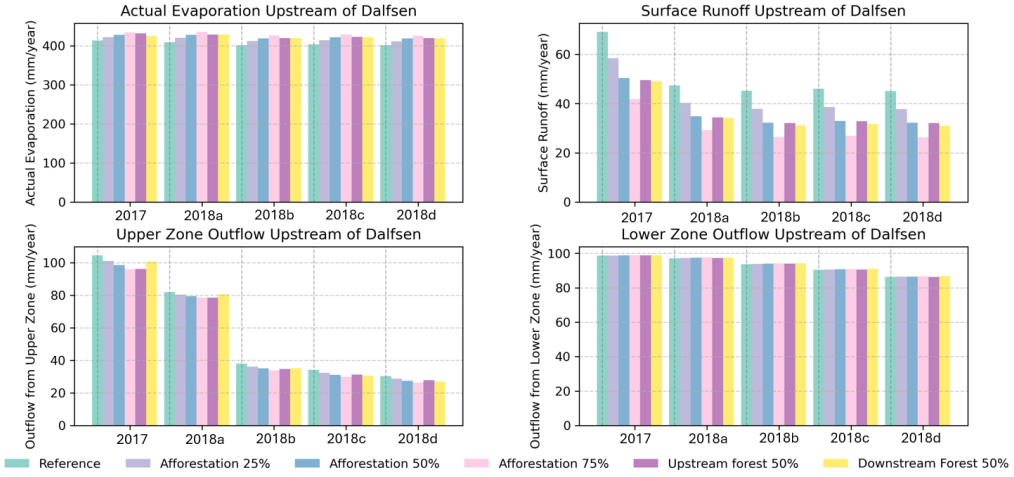

Figure 29: Annual totals of modelled water balance components per afforestation scenario; computed for area upstream of Dalfsen.

Across all afforestation scenarios, the modelled actual evaporation increased compared to the reference scenario, reflecting the additional vegetation and associated evapotranspiration demands. This increase was relatively consistent across years, with a slight decrease over time, likely due to decreasing water availability in the later years of the simulation.

The annual totals of the modelled surface runoff showed a pronounced decrease in the afforestation scenarios with respect to the reference, especially in 2017, a year characterised by the 80 mm rainfall event. This reduction can be attributed to increased infiltration and interception capacity introduced by the afforestation measures. In the subsequent dry years (2018a–2018d), surface runoff showed a repetitive pattern in line with the repeated meteorological conditions of 2018.

The modelled upper zone outflow showed the largest decreases over the simulation period, influenced by both the NBS and the meteorological conditions. In 2017, the modelled outflow reached over 100 mm, but by 2018d, this had reduced to approximately 30 mm. This significant decline is largely due to the cumulative effect of successive dry years reducing water availability in the upper zone, exacerbated by increased evaporation associated with afforestation. This decrease was more pronounced than in the modelled outflow of the lower zone, which decreased from around 100 mm in 2017 to approximately 85 mm in 2018d. An interesting anomaly was observed between 2018a and 2018b, where upper zone outflow differed significantly between these years, a pattern not reflected in the lower zone outflow. This discrepancy may indicate variations in short-term water availability in the upper soil layers, which appear to be sensitive to immediate meteorological conditions.

Figure 30 illustrates the relative changes (%) in water balance components for the afforestation scenarios compared to the reference scenario, calculated for 2017–2018d.

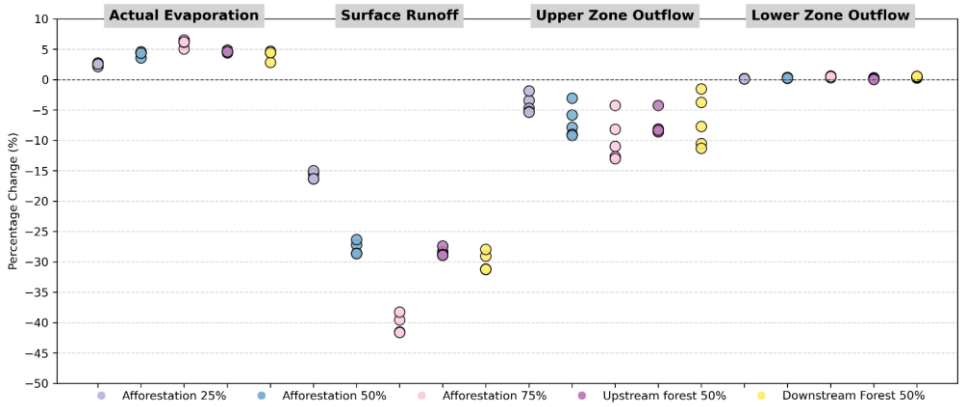

Figure 30: Modelled relative change in water balance components due to afforestation; computed for area upstream of Dalfsen; multiple dots represent percentage change in 2017 – 2018d.

The modelled actual evaporation consistently increased across all scenarios, with the highest increase of 7% observed under 75% afforestation. Each 25% increase in afforestation contributed approximately 2.5% additional evaporation, reflecting the role of vegetation in transpiration and water exchange with the atmosphere.

The modelled surface runoff shows significant reductions, ranging from 15% in the 25% afforestation scenario to 40% in the 75% afforestation scenario. This result highlights the effectiveness of increased vegetation cover in reducing direct runoff by increasing infiltration and evapotranspiration. Surface runoff showed the most significant response to afforestation among the water balance components.

Modelled outflow from the upper zone also decreased across all afforestation scenarios. However, there was considerable variability from year to year, with reductions becoming less pronounced during drier years. Under these conditions, less water is available in the upper zone so that runoff returns closer to the levels observed in the no afforestation scenario. This suggests that the influence of afforestation on the upper soil zone decreases as water availability declines. In contrast, modelled lower zone outflow showed negligible relative changes across all scenarios. This suggests that afforestation had limited effects on deeper groundwater contributions to streamflow, highlighting the minimal interaction between surface processes and the lower groundwater zone.

In summary, the afforestation scenarios significantly altered the distribution of water within the catchment, primarily by increasing actual evaporation and reducing surface runoff. Upper zone outflow showed significant changes, with a pronounced decline under drier conditions, largely driven by the cumulative impact of consecutive dry years. This effect was enhanced by the additional evaporation caused by afforestation. The effect on lower zone runoff remained minimal, suggesting that deeper hydrological components were unaffected by afforestation.

4.2.2. Improving soil conditions

4.2.2.1. Artificial rain events

The hydrographs in Figure 31 illustrate the impact of soil improvement scenarios at station Archem TOT for summer (a) and winter (b) peaks caused by a 2-day uniform rain event of 40 mm/day (totalling 80 mm).

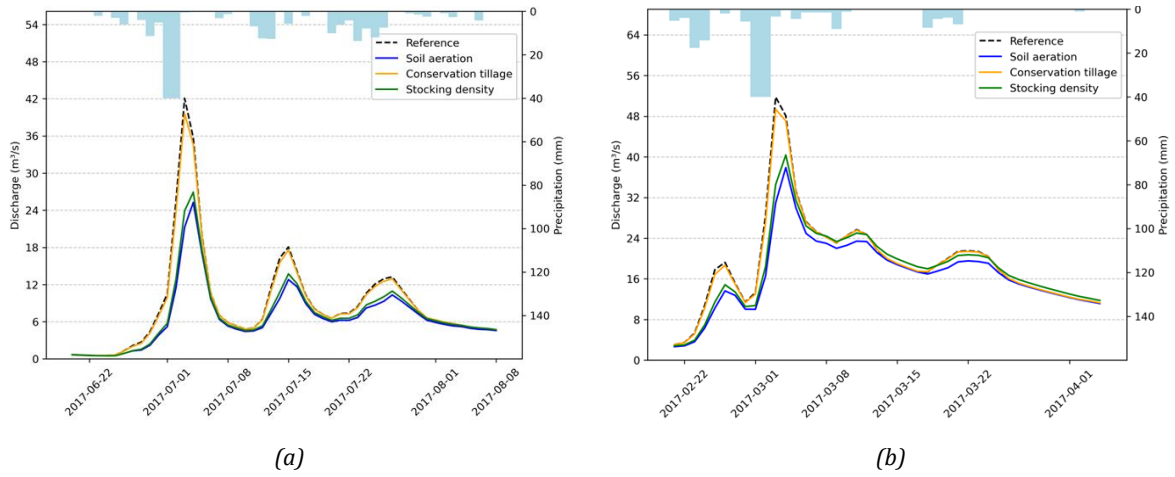

(a) *(b)*

Figure 31: Hydrographs at Archem TOT for soil improvement scenarios under summer (a) and winter (b) conditions with a uniform 2-daily rain event of 40 mm/day.

The results show that soil aeration and stocking density scenarios lead to similar reductions in peak discharge, with modelled decreases of approximately 12 m³/s in summer and slightly lower reductions of 10 m³/s in winter. Conservation tillage has a negligible effect at this station, which aligns with its primary influence in the German part of the catchment, as observed at Emlichheim (Appendix G1).

The pattern of seasonal differences is consistent with the afforestation scenarios: summer peaks drop more quickly, while winter discharges remain elevated for longer periods. In addition, the effect of soil improvement measures on flows following subsequent rain events is more pronounced in summer than in winter, probably because the winter soil remains saturated, further reducing infiltration potential.

Figure 32 presents the effects of soil improvement scenarios on peak flow reduction, minimum average 7-day discharge (MAM7), and average discharge under summer (left) and winter (right) conditions for a 2-day rain event totalling 200 mm (100 mm/day).

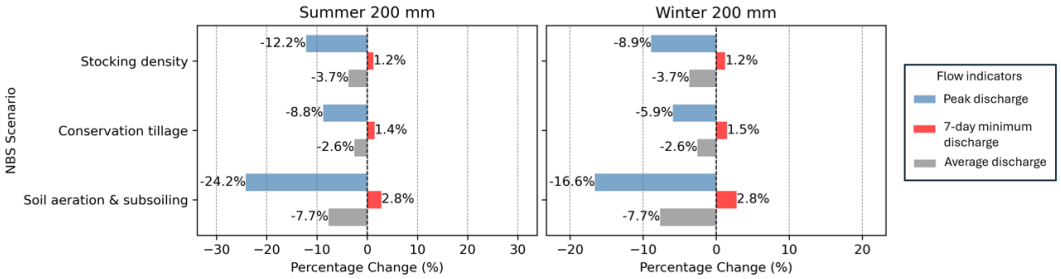

Figure 32: Modelled effects of soil improvement scenarios at Dalfsen under summer (left) and winter (right) conditions for 2-daily rain event of 100 mm/day.

Similar to the afforestation scenarios, the peak flow reduction shows the most significant response. The percentage increase in MAM7 for soil improvement scenarios is slightly larger compared to afforestation scenarios. However, the changes are minimal in absolute terms due to the low baseflow conditions. For example, the most significant increase in MAM7 is 2.8%, equal to only 0.3 m³/s.

Seasonal differences persist, with soil aeration and subsoiling showing effects on peak flow reduction nearly 10% greater in summer than in winter. The 80 mm and 150 mm rainfall events follow the same trends and are therefore not shown.

4.2.2.2. Limburg 2021 event

Figure 33 presents hydrographs at station De Haandrik for a peak event in the Dinkel sub-catchment (Figure 33a) and at station Archem TOT for a peak event in the Regge sub-catchment (Figure 33b).

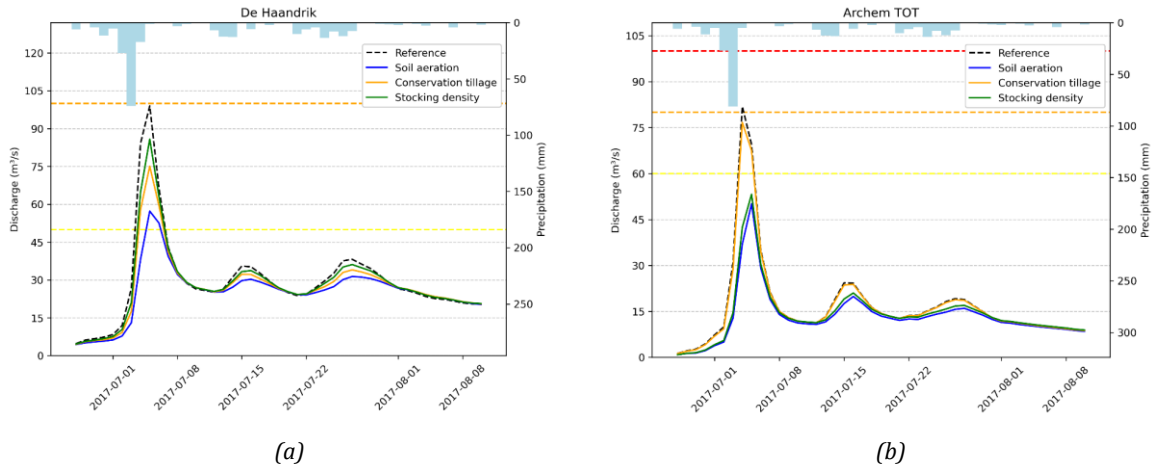

Figure 33: Hydrographs during 2021 rain event for soil improvement scenarios; with peak rain event in Dinkel sub-catchment (a) & with peak rain event in Regge sub-catchment (b); dashed yellow, orange and red lines are first, second and third warning levels.

At the De Haandrik station (Figure 33a), conservation tillage achieved a modelled peak flow reduction of approximately 25 m³/s, while soil aeration and subsoiling achieved a much larger reduction of 45 m³/s. The effect of reduced stocking density was minimal at this site as this measure is mainly applied in the Dutch part of the catchment. Notably, the impact of soil aeration was comparable to the peak reductions observed in the 75% afforestation scenario. The measures also contributed to small reductions in flow during the higher flows observed in the days following the peak event.

The results varied at the Archem TOT station (Figure 30b) according to where the measures were implemented. Conservation tillage showed minimal impact, reflecting its focus on the German parts of the catchment. Both stocking density and soil aeration & subsoiling reduced modelled peak flows by about 30 m³/s, with no significant difference between these measures. Similar to De Haandrik, the effects of these measures persisted over the following days, slightly reducing the discharges from subsequent rainfall events.

The Limburg 2021 event showed that soil improvement measures can reduce peak flows during extreme rainfall, but their performance varies across the catchment. Despite differences in implementation and regional focus, these measures contribute to flood mitigation.

4.2.2.3. Water balance components

Figure 34 presents the annual totals (mm/year) for the reference and soil improvement scenarios. These results are based on the same meteorological scenario as the afforestation analysis, which includes a 2-day rain event of 40 mm/day during the summer.

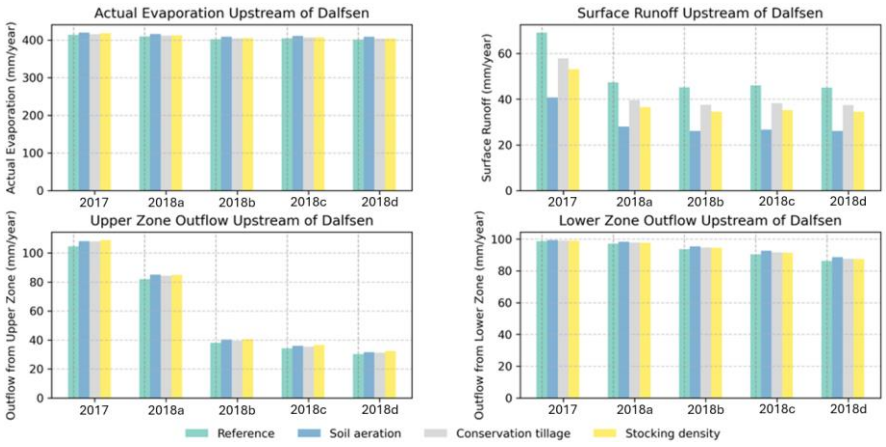

Figure 34: Annual totals of modelled water balance components per soil improvement scenario; computed for area upstream of Dalfsen.

The results show minimal differences in the modelled actual evaporation across the scenarios, with slight decreases over the years. Modelled surface runoff shows the most significant differences between scenarios, consistently lower in all soil improvement scenarios and stabilising after 2017 due to the repetition of 2018's meteorological conditions. In contrast to the afforestation scenarios, soil improvement scenarios show slightly higher modelled upper and lower zone outflow compared with the reference scenario. Upper zone outflow decreases after 2017, but soil improvement measures maintain slightly higher outflow in drier years. Lower zone outflow also decreases in the drier years but shows modest increases compared to the reference during periods of low water availability. This contrasts with the patterns observed under afforestation.

Figure 35 highlights the relative changes (%) in water balance components for the soil improvement scenarios compared to the reference scenario.

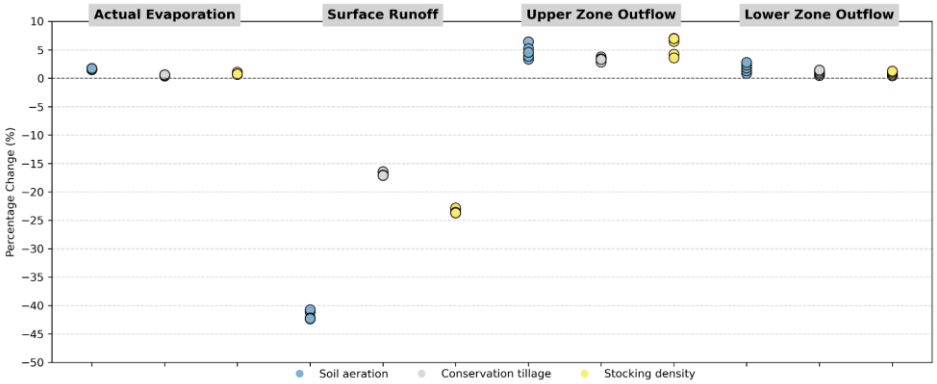

Figure 35: Modelled relative change in water balance components as a result of soil improvement measures; computed for area upstream of Dalfsen; multiple dots represent percentage change in years 2017 – 2018d.

A slight increase is observed in modelled actual evaporation, reflecting the limited influence of soil improvement measures on evapotranspiration. The most significant reductions are seen in modelled surface runoff, with up to 40% decreases for soil aeration and subsoiling. Stocking density and conservation tillage result in smaller reductions, with decreases of approximately 23% and 17%, respectively. On the other hand, the modelled outflow from the upper zone increases by 3% to 7%, likely due to enhanced infiltration allowing more water to infiltrate into the upper zone.

The modelled lower zone outflow shows the most substantial increase under soil aeration measures, with a maximum of approximately 3%. Conservation tillage and stocking density measures exhibit smaller increases in lower zone outflow, ranging from 0% to 2%.

5. Discussion

This chapter discusses the limitations of the data, model, and methods used in this study and their potential impact on the results. The results are interpreted in the context of the existing literature, highlighting how they align or differ from previous research.

5.1. Limitations in data, model and methods

5.1.1. Limitations in data

Precipitation data were derived from the E-OBS raster dataset, which interpolates station-based observations to create spatially distributed data. While E-OBS is a relatively reliable source, its interpolation process can under-represent localised rain events, particularly when these occur between stations. Such gaps can lead to inaccuracies in discharge simulations for events with high spatial variability. Precipitation measurements differed from E-OBS data, probably due to data processing. Nevertheless, rainfall data from the Vecht basin are unlikely to be incomplete due to its dense network of stations (Cornes et al., 2018). Previous comparisons by Cazemier (2024b) with alternative datasets, such as ERA-5 and RADOLAN, further support the suitability of E-OBS for this region despite its limitations.

This study relied on observed discharge data from various measurement stations in the Vecht basin to calibrate and validate the LISFLOOD-OS model. However, discrepancies in the recorded discharge values across different stations introduced uncertainties in the analysis. For example, despite De Haandrik being located downstream of Emlichheim, discharge values at De Haandrik were often recorded as lower than those at Emlichheim. In this case, the observed discharges at Emlichheim were considered more reliable, as they aligned better with the cumulative flows from upstream stations. Such inconsistencies indicate potential errors in measurement or data handling that could affect the reliability of the model's performance metrics. Additionally, stations such as Archem TOT and Lage Gesamt combine data from several stations, which may introduce errors. This data aggregation increases uncertainty, especially if stations malfunction or have errors not immediately identified.

5.1.2. Limitations in model

Although LISFLOOD-OS incorporates spatially distributed and partially physically-based process representations (van der Knijff et al., 2010), its process representations often fall short of fully capturing the complexities of hydrological systems. Van der Knijff et al. (2010) highlights that the model uses simplified descriptions to balance computational efficiency and data availability, leading to compromises in physical accuracy. For example, while the physically based nature of the model is beneficial for simulating the effects of nature-based solutions, the limited physical detail required workarounds to represent certain NBS effects adequately. This limitation reduces the reliability of simulations involving detailed hydrological interventions as introduced by the NBS.

LISFLOOD-OS does not simulate upward vertical soil moisture movement (capillary rise) or deep groundwater systems. Using the percolation loss flux (GW_{loss}) as a calibration parameter to correctly simulate lower zone discharge rates introduces additional uncertainty. Although it was necessary to include GW_{loss} in the calibration to align baseflow simulations with observed discharges, it may inaccurately represent actual baseflow generation processes, as there is no evidence of significant groundwater losses in the Vecht catchment.

The relatively coarse resolution of the input data is also a limitation. The static input maps were primarily derived from the EFAS database at 1.5 km resolution, while the meteorological inputs were derived from the 7 km resolution E-OBS dataset. Although these maps were interpolated to a finer 200 m × 200 m grid for use in the model, this process cannot fully capture the spatial variability within smaller areas, particularly for heterogeneous land use patterns. While this may affect runoff generation or infiltration at smaller scales, the effect on overall discharges is unlikely to be significant.

LISFLOOD-OS models only the natural hydrological response of the catchment, excluding contributions from non-natural sources such as canals and sewage treatment plants. While this exclusion has minimal impact during high flow winter periods, it will likely lead to an underestimation of discharges during low flow summer periods when human-induced water inputs can be a significant proportion of the total flow.

The daily time step used in this study has limitations in capturing peak discharge dynamics during high flow events. Hourly discharge data often show higher peaks than daily averages, particularly in sub-catchments with rapid hydrological responses. This discrepancy is most evident during intense rainfall events and can lead to an underestimation of peak flow magnitudes. However, this limitation is less critical during low flow periods as flow tends to be relatively stable throughout the day.

The calibrated model performed better in simulating the more natural flow regime of the German part of the Vecht catchment than the heavily regulated Dutch sections. This limitation is consistent with the findings of Dankers et al. (2007), who analysed LISFLOOD-OS simulations of the 2002 flood event in the Danube at Bratislava. Their study revealed a systematic overestimation of peak flows. Van der Knijff et al. (2010) attributed this overestimation to the inability of LISFLOOD-OS to account for hydraulic structures such as sluices, weirs, and artificial channels, which significantly alter the natural flow regime. The results of this study for the regulated Dutch Vecht may not fully capture the potential effects of NBS due to the model's reduced accuracy in simulating the local discharge dynamics.

5.1.3. Limitations in methods

The calibration of LISFLOOD-OS was performed manually, resulting in acceptable values for the multi-objective function. However, manual calibration has inherent limitations in the systematic optimisation of parameters. Automatic calibration methods could overcome the challenges of manual calibration. They streamline parameter optimisation and reduce resource requirements, achieving greater accuracy in hydrological model calibration (Nandi & Janga Reddy, 2021). LISFLOOD-OS includes an automated calibration tool that uses a genetic algorithm (DEAP) to optimise parameters across inter-station regions systematically. While this tool was not used in this study, it might have improved calibration efficiency and simulation accuracy. The observed underestimation of peak flows in the used reference scenarios is considered to have affected the assessment of the impact of NBS on absolute peak flows.

The model calibration process used a multi-objective function with three performance metrics: NS_w, NS_{inv} and RVE. This approach aimed to balance the performance of the model for both high and low flows. However, greater emphasis on RVE during calibration may have been more appropriate as it directly reflects the accuracy of the water balance - including key processes such as infiltration, evaporation and runoff - which are central to assessing the impact of NBS.

The calibration and validation results showed significant deviations in the RVE, with average errors of ±30% and outliers exceeding 70%. These large discrepancies indicate potential inaccuracies in representing the water balance across the catchment. As a result, the ability to assess absolute flow changes due to NBS is reduced, and the results primarily reflect trends rather than precise values of flow extremes.

The parameterisation of the effects of NBS was based on literature that primarily focused on field experiments and small-scale studies. While these studies provided valuable insights into the effects of measures such as afforestation and soil improvement on soil properties, their results showed considerable variability. This variability was particularly evident in saturated hydraulic conductivity and soil water-holding capacity, which often differed significantly between studies. In addition, the depth of the soil layers considered in these studies was limited. For afforestation, effects were generally only measured to a depth of 1 m, while for soil improvement measures, measurements rarely exceeded 20 cm. However, in LISFLOOD-OS, the soil layers are divided into three depths, with the second layer extending to a depth of 140 cm. Due to the lack of data for deeper layers, adjustments for saturated hydraulic conductivity and soil moisture content were extrapolated from surface level results. This extrapolation is subject to uncertainty as the actual effect of NBS at these depths remains unclear. Furthermore, during the parameterisation process, adjustments were consistently made to the same parameters—such as saturated hydraulic conductivity—regardless of the specific NBS being implemented. This raises the question of whether such uniform adjustments adequately reflect the varying impacts of different NBS.

5.2. Interpretation of results

The results of this study are interpreted and compared to existing literature to provide context and evaluate their implications for understanding the effects of nature-based solutions on high and low flows.

5.2.1. Model performance

Performance of LISFLOOD-OS for the Vecht

The LISFLOOD-OS model showed mixed performance in simulating discharges within the Vecht catchment. During calibration, the NS_w was above 0.5 on average across stations, which is in the "satisfactory" range (Motovilov et al., 1999). However, inverse Nash-Sutcliffe efficiencies were often below 0.36, indicating 'unsatisfactory' performance at low flows. The RVE showed large variations, averaging ±30%, reflecting significant inaccuracies in the water balance simulation.

During validation, performance varied between different validation periods. In years with extreme peak discharges like 1998 and 2023, NS_{inv} scores improved, with some stations scoring above 0.6. In contrast, performance for dry years like 2018 severely decreased, with many stations scoring NS_{inv} below 0. This highlights the model's limited ability to simulate low flows during dry periods while performing reasonably well for high flow dynamics in wet conditions.

Comparison with other LISFLOOD-OS applications

In most studies, different performance metrics are used, making direct comparisons with the results of this study challenging. Therefore, the performance of LISFLOOD-OS for the Vecht catchment was evaluated using Nash-Sutcliffe efficiency (NSE) as a common benchmark and compared to other studies that applied the model in different catchments. For example, van der Knijff et al. (2010) reported average NSE scores of around 0.7 for the Elbe catchment, while Silva Peixoto et al. (2024) achieved similar results for the Madeira catchment. These scores are significantly higher than the NS_w and NS_{inv} scores in this study. In contrast, Gai et al. (2019), who applied LISFLOOD-OS to the Wei River catchment in China, reported a wider range of NSE values, including some negative values and averages closer to 0.5. This variability is more in line with the performance observed for the Vecht catchment.

Comparison with Wflow sbm in the Vecht catchment

The performance of LISFLOOD-OS was compared with that of the Wflow sbm model applied to the same Vecht catchment in a parallel study by Cazemier (2024b). Table 16 shows the observed and simulated average discharges and the objective function (OF) values for both models during the calibration period. Wflow sbm consistently achieved higher OF values at most stations, reflecting better overall model performance. For example, at the Emlichheim station, Wflow sbm achieved an OF of 0.76 compared to 0.26 for LISFLOOD-OS. In addition to higher OF values, Wflow sbm generally simulated average discharges closer to the observed values, whereas LISFLOOD-OS tended to underestimate flows at most stations. This suggests that LISFLOOD-OS may under-represent the runoff generation in the catchment. This trend of better performance of Wflow sbm was also observed during the validation periods, where it consistently achieved higher OF values than LISFLOOD-OS.

Table 16: Observed and simulated average discharges and objective function values over calibration period for both LISFLOOD-OS and Wflow sbm at all stations. Green indicates better model performance compared to other model, red indicates worse, and orange indicates equal performance.

Station	Average discharge [m³/s]			Objective function value	
	Observed	LISFLOOD-OS	Wflow sbm	LISFLOOD-OS	Wflow sbm
Wettringen	1.9	1.2	1.9	0.44	0.54
Bilk	2.1	1.1	2.2	0.28	0.58
Gronau	1.9	1.2	2.2	0.31	0.51
Ohne	4.4	2.7	4.5	0.46	0.73
Neuenhaus	7.6	4.4	7.5	0.23	0.60
Lage Gesamt	7.2	5.3	6.2	0.21	0.66

Table continues on the next page

Station	Average discharge [m³/s]			Objective function value	
	Observed	LISFLOOD-OS	Wflow sbm	LISFLOOD-OS	Wflow sbm
Osterwald	1.3	1.6	2.1	0.20	-0.27
Emlichheim	18.0	13.1	17.3	0.26	0.76
De Haandrik	17.3	13.3	17.4	0.03	0.38
Ane Gramsbergen	5.1	8.3	5.0	0.18	0.28
Ommen	23.8	24.8	25.8	0.18	0.49
Ommerkanaal	2.4	3.5	1.4	0.15	0.22
Archem TOT	9.7	8.7	13.6	0.41	0.15
Dalfsen	-	37.5	41.7	-	-

5.2.2. Effects of nature-based solutions on high and low flows

Afforestation

The effects of afforestation on peak flow reduction reported in this study are consistent with the existing literature but show different magnitudes. The modelled peak discharge reductions in this study are consistent with the findings of Penning et al. (2024), who reported reductions of up to 60-70% for frequent, less extreme events but only 30% for more extreme events with 80% afforestation. Gai et al. (2019) documented a 14% reduction in peak flows in a forested scenario, which is less pronounced than the results found in this study for larger-scale afforestation scenarios. In contrast, the impact of afforestation on low flow (MAM7) is negligible in this study, with changes consistently below 0.5%. These results are in contrast to the findings of Farley et al. (2005) and Gai et al. (2019), who observed decreases in low flows of up to 60% in pine plantations and 85% in afforestation scenarios, respectively. Such differences highlight the dependence of the low-flow effects on the type and age of the forest and the model structure. The 12% average streamflow reductions for 75% afforestation is more in line with the Gai et al. (2019) average, demonstrating afforestation's potential. However, Buechel et al. (2022) observed smaller reductions, suggesting effects may vary.

The effects of afforestation on water balance components in this study are consistent with findings in the wider literature, particularly concerning increases in evapotranspiration and reductions in surface runoff. In the Vecht catchment, afforestation scenarios led to consistent increases in modelled actual evaporation. Similar trends are observed by Hoang & Hughes (2024), where evapotranspiration increased between 22% and 48% following significant land use conversion to pine plantations. The reductions in surface runoff modelled in this study, ranging from 15% to 40%, are comparable to the findings by Farley et al. (2005), who observed reductions of up to 50% in 20-year-old forest plantations. However, other studies show more variable results. Buechel et al. (2022) report seasonal differences, with runoff reductions occurring mainly in winter, spring and autumn but with potential increases in summer due to higher soil saturation.

Regarding subsurface hydrology, this study found that afforestation decreased upper zone outflow significantly, particularly in wetter years, while impacts on lower zone outflow were minimal. In contrast, Hoang & Hughes (2024) reported an increase in lateral flow and a consistent but uncertain decrease in groundwater flow. While the results differ in the direction of changes in shallow subsurface flow, both studies highlight that afforestation predominantly affects surface and shallow subsurface hydrological processes, with minimal and less consistent effects on deeper groundwater dynamics.

Soil aeration and subsoiling

This study demonstrated that soil aeration and subsoiling significantly reduced peak discharges, with reductions of approximately 24% in summer and 17% in winter under a 200 mm rainfall scenario. These reductions are consistent with findings in the literature, which consistently highlight the ability of aeration to increase infiltration and reduce surface runoff. For example, DeLaune et al. (2013) reported runoff reductions of up to 57% after aeration. Soil aeration and subsoiling resulted in a 2.8% increase in low flow. This aligns with the increased infiltration and soil water storage capacity reported by Smith (2012) who documented increases in soil water storage capacity, showing the potential of aeration to enhance subsurface flow.

The reduction in surface runoff observed in this study illustrates the potential of soil aeration to improve water retention and reduce annual runoff volumes. This is consistent with the findings of DeLaune et al. (2013) and Douglas et al. (1998), who highlighted the role of aeration in improving soil structure and macropore connectivity. However, as noted in the literature, these effects can vary significantly depending on site-specific conditions and are often short-lived. For example, DeLaune et al. (2013) reported that runoff volumes returned to baseline within six weeks due to sediment accumulation and natural re-compaction of soils. It is important to note that these temporal effects are not represented in this study, as the parameter settings in LISFLOOD-OS remain static over time. The small increases in subsurface outflow are consistent with the literature on increased infiltration and water redistribution.

Conservation tillage

This study found that conservation tillage reduced peak discharges by up to 9% in summer under a 200 mm rainfall scenario. This is consistent with the findings of He et al. (2009), who reported improved infiltration rates and macroporosity in no-till systems, leading to better water retention and slower runoff generation. However, some studies suggest that the effects of conservation tillage may be inconsistent. For example, Deasy et al. (2014) found that minimum tillage can increase runoff and peak flow generation in certain contexts, particularly during intense rainfall events.

The potential of conservation tillage to improve soil water retention and reduce annual runoff is illustrated by the reduction in surface runoff observed in this study. These results are consistent with those of Fér et al. (2020), who demonstrated higher soil water retention capacity under no-till systems compared to conventional tillage. While this study found slight increases in upper and lower zone outflow, suggesting increased subsurface water movement, these changes were modest. The observed modest increases in subsurface outflow lack direct support from the literature, indicating a gap in understanding the effects of conservation tillage on subsurface hydrology.

Stocking density

The reduction in peak flows observed in this study is consistent with findings in the literature emphasising the benefits of reduced grazing pressure on infiltration and surface runoff. Heathwaite et al. (1990) demonstrated that heavily grazed grasslands produced almost 12 times more runoff than ungrazed fields, highlighting the significant role of grazing pressure on runoff dynamics. Similarly, Marshall et al. (2014) observed that ungrazed plots had shallower rising limbs and smaller runoff peaks than grazed plots.

The increase in subsurface outflow observed in this study is supported by studies reporting increased infiltration associated with reduced grazing (Daniel et al., 2002). While direct comparisons are difficult due to variability and site-specific conditions, the literature shows that reduced grazing intensity can improve infiltration and reduce peak runoff.

5.2.3. Cross-model evaluation of NBS: LISFLOOD-OS and Wflow sbm in the Vecht basin

Parametrisation of nature-based solutions

The exact parameterisation of NBS differs between LISFLOOD-OS and Wflow sbm due to differences in model structure and land use representation. In LISFLOOD-OS, each grid-cell can contain multiple land use types represented as fractions, whereas Wflow sbm assigns a single dominant land use type to each grid-cell. Both models link dominant land use types to hydrological processes. Cells with dense vegetation in both models emphasise the importance of evaporation and transpiration, but how these processes are parameterised differs.

A key difference lies in the treatment of Leaf Area Index (LAI): LISFLOOD-OS uses 10-day average LAI values that vary by land use fraction and includes this only for the forest, irrigated agriculture and 'other' land use fractions. In contrast, Wflow sbm uses monthly LAI values specific to all included land use types.

The representation of soil structure also varies substantially. Wflow sbm assumes a single 2-meter soil layer of uniform depth across the catchment. At the same time, LISFLOOD-OS incorporates three distinct soil layers of variable depth, allowing for differential parameter adjustment over depths of up to 28 meters. This layered structure in LISFLOOD-OS allows a more detailed parameterisation of NBS effects on processes such as infiltration, which vary with soil depth. Finally, the adjustment of Manning's

roughness coefficients in forested areas highlights another difference. LISFLOOD-OS uses a maximum roughness of 0.14 s $m^{-1/3}$ in forested areas, while Wflow sbm uses significantly higher values, ranging from 0.4 to 0.6 s $m^{-1/3}$. This difference reflects the models' different approaches to representing surface roughness and its influence on surface runoff.

Comparison of afforestation effects in LISFLOOD-OS and Wflow sbm

Figure 36 a & Figure 36 b highlight the key differences between the discharge waves generated by LISFLOOD-OS (a) and Wflow sbm (b).

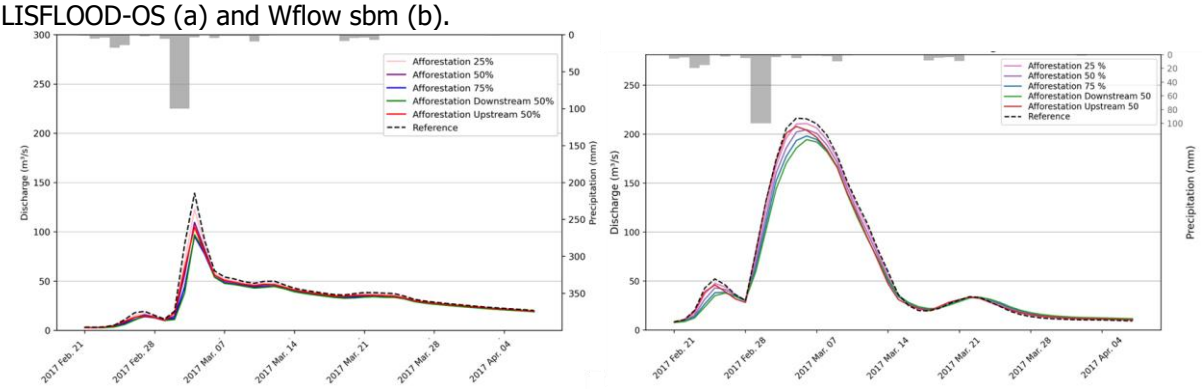

(a) *(b)*

Figure 36: Hydrographs at Archem TOT for afforestation scenarios under winter conditions with a uniform 2-daily rain event of 100 mm/day in LISFLOOD-OS (a) and Wflow sbm (b).

A significant difference is observed in the magnitude of the simulated peak discharges between the two models. In the reference scenario, LISFLOOD-OS simulates a peak discharge of approximately 140 m³/s at Archem TOT, while Wflow sbm estimates a substantially higher peak of around 220 m³/s. This discrepancy of ±70 m³/s represents approximately 50% of the LISFLOOD-OS peak discharge. This difference highlights the tendency of LISFLOOD-OS to underestimate discharges in the Vecht catchment, as also observed during the calibration and validation phases.

In LISFLOOD-OS, the peak discharge decreases rapidly, while in Wflow sbm, the high flows persist for several days before gradually decreasing. This difference is probably due to the different flow routing methods used by the two models. Wflow sbm uses the local inertial method, which accounts for backwater effects (influence of downstream conditions on upstream flow) and flood wave attenuation (reduction of flood peak magnitude as it moves downstream). In contrast, LISFLOOD-OS uses the kinematic wave approach, simplifying flow routing by neglecting these effects, resulting in faster peak dissipation.

For smaller rainfall events, such as the 80 mm scenario, the relative reductions in peak discharge are comparable between the models. For heavier rainfall events or during wet winter conditions, the reduction in peak discharge is less pronounced in Wflow sbm compared to LISFLOOD-OS. This trend suggests that soil saturation occurs earlier in Wflow sbm, probably due to differences in how the two models parameterise the soil layers.

When examining changes in average discharge, both models show similar trends, with comparable relative reductions across afforestation scenarios. These consistent trends indicate that both models effectively capture the effect of afforestation on average discharges, primarily driven by increased evaporation in forested areas. There is a notable difference when examining the impact on minimum 7-day average discharge. Wflow sbm shows a more pronounced relative increase in low flows than LISFLOOD-OS. Nevertheless, the absolute increases in MAM7 remain small in both models, with maximum increases of less than 0.25 m³/s in all afforestation scenarios. This underscores the limited impact of afforestation on enhancing baseflow.

6. Conclusion and Recommendations

6.1. Conclusion

RQ1 - What is the performance of the LISFLOOD-OS model in simulating high and low flows in the Vecht catchment during historical extreme events?

The LISFLOOD-OS model exhibited acceptable performance in the simulation of high and low flows in the Vecht catchment. Calibration results showed satisfactory performance for high flows, as indicated by the relatively higher NS_w scores, but relatively poor performance for low flows, reflected in low NS_{inv} scores. Large deviations in RVE (±30% on average, with some outliers >70%) indicate problems in representing the water balance, which undermines the ability to simulate absolute discharge volumes reliably. Validation showed better performance during wet years, but further limitations emerged for dry periods and low flows. The model performed notably better in the less-regulated German part of the catchment than in the Dutch part, where human interventions added complexity that was challenging to capture through calibration. Compared to other applications of LISFLOOD-OS in larger catchments, performance was significantly lower in the Vecht catchment.

RQ2 - How can measures within the NBS groups land use & cover changes and improving soil conditions be integrated into the LISFLOOD-OS hydrological model?

A limited set of NBS was considered suitable for application in the Vecht catchment and modelling with LISFLOOD-OS. Afforestation and soil improvement measures such as soil aeration, conservation tillage and reduced stocking density were selected based on their feasibility and hydrological relevance at the catchment scale. These NBS were integrated into LISFLOOD-OS by parameterising changes in soil hydraulic properties, surface roughness and land use fractions. Uncertainties in the character and exact values of the parameters modified to model the NBS introduce variability in the hydrological effects of the NBS, thereby affecting the accuracy and reliability of the modelled results.

RQ3 - What are the effects of the nature-based solutions on high and low flows in the Vecht catchment according to LISFLOOD-OS under extreme wet and dry conditions?

Realistic afforestation scenarios, such as 10% afforestation in the Dutch and German parts of the catchment, showed minimal hydrological effects, highlighting that substantial effects require large-scale implementation. Larger afforestation scenarios showed significant reductions in peak flows, particularly during summer events, due to increased infiltration and evapotranspiration. However, the benefits of afforestation for low flows were negligible in all scenarios, suggesting that while large-scale afforestation is effective in mitigating high flow events, its contribution to improving drought resilience is limited.

Soil improvement measures, which are more feasible for widespread implementation on agricultural land, had notable effects on both high and low flows. These measures, particularly soil aeration and subsoiling, reduced peak flows by increasing infiltration through improved soil structure. Compared to afforestation, these measures also showed slightly greater benefits for low flows, reflecting their influence on subsurface water retention and outflow. Conservation tillage and stocking density adjustments showed smaller but meaningful effects, highlighting their potential as complementary strategies in agricultural areas.

Aim - To quantify the effects of the nature-based solution groups land use & cover changes and improving soil conditions on high and low stream flows in the Vecht catchment under extreme wet and dry conditions, using the LISFLOOD-OS distributed hydrological model.

This study has shown that NBS can influence extreme flow conditions in the Vecht catchment. Still, the magnitude of the effect is highly dependent on the scale and location of implementation. Afforestation and soil improvement measures both showed significant potential to reduce high flows. While afforestation had minimal impact on low flows, soil improvement measures showed slightly greater benefits, highlighting their potential to address both high and low flow challenges.

However, practical limitations such as the feasibility of large-scale implementation, uncertainties in parameterisation and the limited accuracy of the LISFLOOD-OS model, especially for simulating low flows, limit the applicability of the results. The results highlight the importance of balancing ambitious measures such as afforestation with more pragmatic and scalable measures such as soil improvement strategies to increase hydrological resilience in the Vecht catchment.

6.2. Recommendations

6.2.1. Practical recommendations

Discrepancies between observed discharges at various stations in the Vecht catchment, together with missing discharge measurements, introduced uncertainties that affected model calibration and validation in this study. Ensuring robust and standardised discharge datasets would improve model calibration and validation, thereby indirectly enhancing the reliability of model outputs and providing a more solid foundation for evaluating NBS. It is recommended that standardised protocols for discharge measurements are implemented across the catchment to ensure accuracy and consistency across stations and time periods. In addition, while the EFAS maps used in this study provided a reasonable basis for modelling, higher quality datasets tailored to the study area could further improve the reliability of the simulations. Investment in more detailed input data, such as high-resolution soil maps, would allow more accurate assessments of NBS effects. Furthermore, the LISFLOOD-OS model for the Vecht catchment does not currently include inputs from non-natural sources, such as canal discharges and wastewater flows. Including these would improve the accuracy of the simulations, especially during low flow conditions.

Calibration of the model to balance accurate simulation of discharges with a more appropriate representation of water balance components could improve the reliability of results. Metrics such as infiltration, evaporation, and runoff generation should be prioritised during calibration while ensuring the model reproduces observed high and low flows reliably. Therefore, it is recommended to prioritise the RVE during calibration, as this metric provides critical insights into the water balance and can help address discrepancies in the simulated flow volumes. In addition, moving from a daily to an hourly timestep could significantly improve the simulation of short-duration peak flows during extreme events. While the daily timestep is fine for general trends, high flow events often occur over hours. Moving to finer temporal resolutions would help to represent such events.

Expanding the range of NBS that can be represented in hydrological models requires dynamic land use representation and higher spatial resolutions. Dynamic land use maps would allow models to capture temporal variations, critical for accurately simulating long-term NBS effects. Similarly, improving the spatial resolution will ensure that localised interventions such as buffer strips or small-scale afforestation can be effectively modelled. Field measurements are also crucial to better understand the impact of NBS in specific regions. It is recommended that local measurements are taken to better parameterise NBS measures and reduce reliance on overly generalised assumptions. Finally, it is recommended to couple LISFLOOD-OS with hydrodynamic or groundwater models, as this would allow a better assessment of how NBS affect surface hydrology and subsurface dynamics, providing a more comprehensive perspective on catchment-scale water management strategies.

6.2.2. Recommendations for future research

This study assessed the impact of nature-based solutions on high and low flows using simplified meteorological scenarios, including uniform 2-day rainfall events and a historically dry year. While these scenarios provided valuable insights, future research should adopt more realistic approaches that reflect potential future climate conditions. Investigating the effectiveness of NBS under climate change scenarios, such as those outlined in the KNMI'23 framework (Bessembinder et al., 2023), could provide critical insights into their ability to mitigate the impacts of heavier rainfall and prolonged droughts. Examining shifts in seasonal rainfall patterns and changes in the intensity and frequency of events will help to assess the long-term resilience of NBS in the face of climate variability.

The comparison of LISFLOOD-OS with Wflow-sbm provided a clearer understanding of model strengths and limitations in simulating the effects of NBS. Additional cross-model evaluations can identify discrepancies in simulated impacts and assess the robustness of results between different modelling

frameworks. This can guide the selection of the most appropriate modelling approach for specific catchments or research objectives, thereby increasing confidence in hydrological predictions. Beyond model comparisons, a multi-model ensemble approach could be used to simulate NBS effects, combining the strengths of different models to provide a more comprehensive and reliable representation of hydrological impacts.

The combined effects of different NBS on hydrological processes and their feasibility for large-scale implementation require further investigation. While studies often analyse individual measures, the combination of measures can lead to synergistic benefits or unforeseen conflicts. Understanding these interactions at different scales could optimise the design of NBS strategies. In addition, future research should integrate socio-economic considerations such as land use conflicts, financial constraints and stakeholder priorities. By addressing both hydrological and practical implementation challenges, more actionable NBS strategies can be developed.

Bibliography

Adnan, M., Badi, W., Dereczynski, C., Di Luca, A., Ghosh, S., Iskandar, I., Kossin, J., Lewis, S., Otto, F., Pinto, I., Satoh, M., Vicente-Serrano, S. M., Wehner, M., & Zhou, B. (2023). Weather and Climate Extreme Events in a Changing Climate. In *Climate Change 2021 – The Physical Science Basis* (pp. 1513–1766). Cambridge University Press. https://doi.org/10.1017/9781009157896.013

Agriculture and Horiculture Development Board. (2024, November 22). *Field drainage: The importance of soil health*. https://ahdb.org.uk/knowledge-library/field-drainage-the-importance-of-soil-health

Akhtar, M., Ahmad, N., & Booij, M. J. (2009). Use of regional climate model simulations as input for hydrological models for the Hindukush-Karakorum-Himalaya region. *Hydrology and Earth System Sciences*, *13*(7), 1075–1089. https://doi.org/10.5194/hess-13-1075-2009

Arnold, J. G., & Fohrer, N. (2005). SWAT2000: current capabilities and research opportunities in applied watershed modelling. *Hydrological Processes*, *19*(3), 563–572. https://doi.org/10.1002/hyp.5611

Aston, A. R. (1979). Rainfall interception by eight small trees. *Journal of Hydrology*, *42*, 383–396.

Ávila, L., Silveira, R., Campos, A., Rogiski, N., Gonçalves, J., Scortegagna, A., Freita, C., Aver, C., & Fan, F. (2022). Comparative Evaluation of Five Hydrological Models in a Large-Scale and Tropical River Basin. *Water (Switzerland)*, *14*(19). https://doi.org/10.3390/w14193013

Beersma, J., Hakvoort, H., Jilderda, R., Overeem, A., & Versteeg, R. (2019). *Neerslagstatistiek en-reeksen voor het waterbeheer 2019* (Tech. Rep.). Amersfoort: STOWA

Beillouin, D., Schauberger, B., Bastos, A., Ciais, P., & Makowski, D. (2020). Impact of extreme weather conditions on European crop production in 2018: Random forest - Yield anomalies. *Philosophical Transactions of the Royal Society B: Biological Sciences*, *375*(1810). https://doi.org/10.1098/rstb.2019.0510

Berrang-Ford, L., Siders, A. R., Lesnikowski, A., Fischer, A. P., Callaghan, M. W., Haddaway, N. R., Mach, K. J., Araos, M., Shah, M. A. R., Wannewitz, M., Doshi, D., Leiter, T., Matavel, C., Musah-Surugu, J. I., Wong-Parodi, G., Antwi-Agyei, P., Ajibade, I., Chauhan, N., Kakenmaster, W., … Abu, T. Z. (2021). A systematic global stocktake of evidence on human adaptation to climate change. *Nature Climate Change*, *11*(11), 989–1000. https://doi.org/10.1038/s41558-021-01170-y

Bessembinder, J., Bintanja, R., van Dorland, R., Homan, C., Overbeek, B., Selten, F., & Siegmund, P. (2023). *KNMI'23 klimaat scenario's voor Nederland*.

Beven, K., & Freer, J. (2001). A dynamic TOPMODEL. *Hydrological Processes*, *15*(10), 1993–2011. https://doi.org/10.1002/hyp.252

Bezak, N., Kovačević, M., Johnen, G., Lebar, K., Zupanc, V., Vidmar, A., & Rusjan, S. (2021). Exploring options for flood risk management with special focus on retention reservoirs. *Sustainability (Switzerland)*, *13*(18). https://doi.org/10.3390/su131810099

Bruijn de, K., & Maas, B. (2023). *Methode voor bovenregionale stresstesten voor grootschalige neerslag Ten behoeve van een landelijk uniform beeld* (Tech. Rep.). Delft: Deltares.

Bruijn de, K., & Slager, K. (2021). *Wat als "de waterbom" elders in Nederland was gevallen?* (Tech. Rep.). Delft: Deltares.

Buechel, M., Slater, L., & Dadson, S. (2022). Hydrological impact of widespread afforestation in Great Britain using a large ensemble of modelled scenarios. *Communications Earth & Environment*, *3*(1), 6. https://doi.org/10.1038/s43247-021-00334-0

Burges-Gamble, L., Ngai, R., Wilkinson, M., Nisbe, T., Pontee, N., Harvey, R., Kipling, K., Addy, S., Rose, S., Maslen, S., Jay, H., Nicholson, A., Page, T., Jonczyk, J., & Quinn, P. (2018). *Working with Natural Processes-Evidence Directory SC150005*. https://www.gov.uk/government/organisations/environment-agency/about/research.

Burgess, C. P., Chapman, R., Singleton, P. L., & Thom, E. R. (2000). Shallow mechanical loosening of a soil under dairy cattle grazing: Effects on soil and pasture. *New Zealand Journal of Agricultural Research*, *43*(2), 279–290. https://doi.org/10.1080/00288233.2000.9513428

Büttner, G., & Kosztra, B. (2011). *Manual of CORINE Land Cover changes EEA subvention 2011 Project Manager*. (Tech. Rep.).

Cazemier, W. (2024a). *The effect of nature-based solutions on high and low flows in hydrological models in the Vecht catchment*. (Unpublished doctoral dissertation). University of Twente, Enschede.

Cazemier, W. (2024b). *The effects of nature-based solutions on high and low flows in the Vecht using hydrological model Wflow sbm*. (Thesis). Deltares, Delft.

Centraal Bureau Statistiek. (2024, March 29). *Landbouw; gewassen, dieren en grondgebruik naar gemeente*. https://opendata.cbs.nl/#/CBS/nl/dataset/80781ned/barv?ts=1731336659231

Chen, D., Rojas, M., Samset, B. H., Cobb, K., Diongue Niang, A., Edwards, P., Emori, S., Faria, S. H., Hawkins, E., Hope, P., Huybrechts, P., Meinshausen, M., Mustafa, S. K., Plattner, G.-K., & Tréguier, A.-M. (2023). Framing, Context, and Methods. In I. P. on C. C. (IPCC) (Ed.), *Climate Change 2021 – The Physical Science Basis: Working Group I Contribution to the Sixth Assessment Report of the Intergovernmental Panel on Climate Change* (pp. 147–286). Cambridge University Press. https://doi.org/DOI: 10.1017/9781009157896.003

Chow, V. T., Maidment, D. R., & Mays, L. M. (1988). *Applied Hydrology*. McGraw-Hill.

Copernicus Emergency Management Service. (2023, June 7). *European Flood Awareness System*. https://european-flood.emergency.copernicus.eu/en

Copernicus, & World Meteorological Organization. (2022, October 31). *Copernicus: Temperatures in Europe increase more than twice global average; Europe presents a live picture of a warming world*. https://climate.copernicus.eu/copernicus-temperatures-europe-increase-more-twice-global-average-europe-presents-live-picture#:~:text=Temperatures%20over%20Europe%20have%20warmed,to%20accelerating%20sea%20level%20rise.

Cornes, R. C., van der Schrier, G., van den Besselaar, E. J. M., & Jones, P. D. (2018). An Ensemble Version of the E-OBS Temperature and Precipitation Data Sets. *Journal of Geophysical Research: Atmospheres*, *123*(17), 9391–9409. https://doi.org/10.1029/2017JD028200

Danáčová, M., Földes, G., Labat, M. M., Kohnová, S., & Hlavčová, K. (2020). Estimating the effect of deforestation on runoin small mountainous basins in slovakia. *Water (Switzerland)*, *12*(11). https://doi.org/10.3390/w12113113

Daniel, J. A., Potter, K., Altom, W., Aljoe, H., & Stevens, R. (2002). Long term granzing density impacts on soil compaction. *Transactions of the ASAE*, *45*(6). https://doi.org/10.13031/2013.11442

Dankers, R., Christensen, O. B., Feyen, L., Kalas, M., & de Roo, A. (2007). Evaluation of very high-resolution climate model data for simulating flood hazards in the Upper Danube Basin. *Journal of Hydrology*, *347*(3–4), 319–331. https://doi.org/10.1016/j.jhydrol.2007.09.055

De Roo, A. P. J., Wesseling, C. G., & Van Deursen, W. P. A. (2000). Physically based river basin modelling within a GIS: The LISFLOOD model. *Hydrological Processes*, *14*(11–12), 1981–1992. https://doi.org/10.1002/1099-1085(20000815/30)14:11/12<1981::aid-hyp49>3.0.co;2-f

Deasy, C., Titman, A., & Quinton, J. N. (2014). Measurement of flood peak effects as a result of soil and land management, with focus on experimental issues and scale. *Journal of Environmental Management*, *132*, 304–312. https://doi.org/10.1016/j.jenvman.2013.11.027

DeLaune, P. B., Sij, J. W., & Krutz, L. J. (2013). Impact of soil aeration on runoff characteristics in dual-purpose no-till wheat systems. *Journal of Soil and Water Conservation*, *68*(4), 315–324. https://doi.org/10.2489/jswc.68.4.315

Deltares. (2021). *Wflow.jl*. https://deltares.github.io/Wflow.jl/dev/

Dormaar, J. F., Smoliak, S., & Willms, W. D. (1989). Vegetation and Soil Responses to Short-Duration Grazing on Fescue Grasslands. *Journal of Range Management*, *42*(3), 252. https://doi.org/10.2307/3899484

Douglas, J. T., Koppi, A. J., & Crawford, C. E. (1998). Structural improvement in a grassland soil after changes to wheel-traffic systems to avoid soil compaction. *Soil Use and Management*, *14*(1), 14–18. https://doi.org/10.1111/j.1475-2743.1998.tb00604.x

Drewry, J. J., Lowe, J. A. H., & Paton, R. J. (2000). Effect of subsoiling on soil physical properties and pasture production on a Pallic Soil in Southland, New Zealand. *New Zealand Journal of Agricultural Research*, *43*(2), 269–277. https://doi.org/10.1080/00288233.2000.9513427

Dunn, A. M., Julien, G., Ernst, W. R., Cook, A., Doe, K. G., & Jackman, P. M. (2011). Evaluation of buffer zone effectiveness in mitigating the risks associated with agricultural runoff in Prince Edward Island. *Science of the Total Environment*, *409*(5), 868–882. https://doi.org/10.1016/j.scitotenv.2010.11.011

Dwarakish, G. S., & Ganasri, B. P. (2015). Impact of land use change on hydrological systems: A review of current modeling approaches. *Cogent Geoscience*, *1*(1), 1115691. https://doi.org/10.1080/23312041.2015.1115691

Eliasson, S., & Larsson, M. (2006). *The influence of land-use change, root abundance and macropores on saturated infiltration rate.* (Thesis). Lund Institute of Technology, Lund. https://lup.lub.lu.se/luur/download?func=downloadFile&recordOId=1325506&fileOId=1325507

European Centre for Disease Prevention and Control. (2021). *Extreme rainfall and catastrophic floods in western Europe*.

European Environment Agency. (2022). *Economic losses and fatalities from weather and climate-related events in Europe*. https://www.eea.europa.eu/publications/economic-losses-and-fatalities-from

Farley, K. A., Jobbágy, E. G., & Jackson, R. B. (2005). Effects of afforestation on water yield: A global synthesis with implications for policy. *Global Change Biology*, *11*(10), 1565–1576. https://doi.org/10.1111/j.1365-2486.2005.01011.x

Fér, M., Kodešová, R., Hroníková, S., & Nikodem, A. (2020). The effect of 12-year ecological farming on the soil hydraulic properties and repellency index. *Biologia*, *75*(6), 799–807. https://doi.org/10.2478/s11756-019-00373-1

Ferreira, C. S. S., Kalantari, Z., Hartmann, T., & Pereira, P. (2021). *Introduction: Nature-Based Solutions for Flood Mitigation* (pp. 1–7). https://doi.org/10.1007/698_2021_776

Feyen L. (2005). *Calibration of the LISFLOOD Model for Europe: Current Status and Way Forward.* EUR 22125 EN. 2005. JRC32044. https://publications.jrc.ec.europa.eu/repository/handle/JRC32044

Gai, L., Nunes, J. P., Baartman, J. E. M., Zhang, H., Wang, F., de Roo, A., Ritsema, C. J., & Geissen, V. (2019). Assessing the impact of human interventions on floods and low flows in the Wei River Basin in China using the LISFLOOD model. *Science of the Total Environment*, *653*, 1077–1094. https://doi.org/10.1016/j.scitotenv.2018.10.379

Ghorai, D., Bhunia, G. S., & Shit, P. K. (2022). *Automatic Strahler's Stream Order Computing on Digital Stream Network Dataset* (pp. 407–415). https://doi.org/10.1007/978-3-030-79634-1_18

Gochis, D. J., Barlage, M., Cabell, R., Casali, M., Dugger, A., FitzGerald, K., McAllister, M., McCreight, J., RafieeiNasab, A., Lead, L., Sampson, K., Yates, D., & Zhang, Y. (2020). *The WRF Hydro modeling system technical description, (Version 5.2.0). NCAR Technical Note.* . 2020.

Haasnoot, M., & Diermanse, F. (2022). *Analyse van bouwstenen en adaptatiepaden voor aanpassen aan zeespiegelstijging in Nederland* (Tech. Rep.). Delft: Deltares.

Han, S., & Kuhlicke, C. (2019). Reducing Hydro-Meteorological Risk by Nature-Based Solutions: What Do We Know about People's Perceptions? In *Water (Switzerland)* (Vol. 11, Issue 12). MDPI. https://doi.org/10.3390/w11122599

He, J., Wang, Q., Li, H., Tullberg, J. N., McHugh, A. D., Bai, Y., Zhang, X., McLaughlin, N., & Gao, H. (2009). Soil physical properties and infiltration after long-term no-tillage and ploughing on the Chinese Loess Plateau. *New Zealand Journal of Crop and Horticultural Science*, *37*(3), 157–166. https://doi.org/10.1080/01140670909510261

Heathwaite, A. L., Burt, T. P., & Trudgill, S. T. (1990). Land-use controls on sediment production in a lowland catchment, south-west England. In J. Boardman, I. Foster, & J. Dearing (Eds.), *Soil erosion on agricultural land* (pp. 70–86). John Wiley and Sons.

Heinrichs, J., Kuhn, T., Pahmeyer, C., & Britz, W. (2021). Economic effects of plot sizes and farm-plot distances in organic and conventional farming systems: A farm-level analysis for Germany. *Agricultural Systems*, *187*. https://doi.org/10.1016/j.agsy.2020.102992

Hersbach, H., Bell, B., Berrisford, P., Biavati, G., Horányi, A., Muñoz Sabater, J., Nicolas, J., Peubey, C., Radu, R., Rozum, I., Schepers, D., Simmons, A., Soci, C., Dee, D., & Thépaut, J.-N. (2024, October 4). *ERA5 hourly data on single levels from 1940 to present.* Copernicus Climate Change Service (C3S) Climate Data Store (CDS). https://cds.climate.copernicus.eu/datasets/reanalysis-era5-single-levels?tab=overview

Hoang, L., & Hughes, A. (2024). Modelling the hydrological impact of afforestation in hill country catchments in New Zealand. *Journal of Hydrology: Regional Studies*, *51*, 101620. https://doi.org/10.1016/j.ejrh.2023.101620

Horel, Á., Tóth, E., Gelybó, G., Kása, I., Bakacsi, Z., & Farkas, C. (2015). Effects of Land Use and Management on SoilHydraulic Properties. *Open Geosciences*, *7*(1). https://doi.org/10.1515/geo-2015-0053

Hundecha, Y., & Bárdossy, A. (2004). Modeling of the effect of land use changes on the runoff generation of a river basin through parameter regionalization of a watershed model. *Journal of Hydrology*, *292*(1–4), 281–295. https://doi.org/10.1016/j.jhydrol.2004.01.002

Information und Technik Nordrhein-Westfalen. (2024). *Landwirtschaftlich genutzte Fläche nach Hauptnutzungs- und Kulturarten sowie Hauptfruchtarten*. https://statistik.nrw/wirtschaft-und-umwelt/land-und-forstwirtschaft/bodennutzung-und-ernte/landwirtschaftlich-genutzte-flaeche-nach-hauptnutzungs-und-kulturarten-sowie-hauptfruchtarten#

Jaiswal, R. K., Ali, S., & Bharti, B. (2020). Comparative evaluation of conceptual and physical rainfall–runoff models. *Applied Water Science*, *10*(1). https://doi.org/10.1007/s13201-019-1122-6

Jeuken, A., Ray, P., Penning, E., Bouaziz, L., Tracy, J., Wi, S., McEvoy, S., Taner, Ü., & Hegnauer, M. (2023). Challenges for upscaling hydrological effectiveness of nature-based solution for adaptation to climate change in watersheds. *Aquatic Ecosystem Health & Management*, *26*(2), 19–32. https://doi.org/10.14321/aehm.026.02.019

Ji, H. K., Mirzaei, M., Lai, S. H., Dehghani, A., & Dehghani, A. (2023). The robustness of conceptual rainfall-runoff modelling under climate variability – A review. In *Journal of Hydrology* (Vol. 621). Elsevier B.V. https://doi.org/10.1016/j.jhydrol.2023.129666

Joint Research Centre. (2022, July 18). *Droughts in Europe in July 2022: almost half of the EU +UK territory at risk*. https://joint-research-centre.ec.europa.eu/jrc-news-and-updates/droughts-europe-july-2022-almost-half-eu-uk-territory-risk-2022-07-18_en

Joint Research Centre. (2024a). *LISFLOOD model documentation*. https://ec-jrc.github.io/lisflood-model/2_01_stdLISFLOOD_overview/

Joint Research Centre. (2024b). *LISFLOOD user guide*. https://ec-jrc.github.io/lisflood-code/

Joint Research Centre. (2024c, April 14). *LISFLOOD hydrological model*. 9-11-2023. https://web.jrc.ec.europa.eu/policy-model-inventory/explore/models/model-lisflood/

Joint Research Centre. (2024d, October 8). *CEMS-EFAS opendata*. https://jeodpp.jrc.ec.europa.eu/ftp/jrc-opendata/CEMS-EFAS/

Journée, M., Goudenhoofdt, E., Vannitsem, S., & Delobbe, L. (2023). Quantitative rainfall analysis of the 2021 mid-July flood event in Belgium. *Hydrology and Earth System Sciences*, *27*(17), 3169–3189. https://doi.org/10.5194/hess-27-3169-2023

Klein, A., & Van der Vat, M. (2024). *Scoping Study of the Vecht, Berkel and Oude IJssel river basins* (Tech. Rep.). JCAR-ATRACE.

Koks, E. E., Van Ginkel, K. C. H., Van Marle, M. J. E., & Lemnitzer, A. (2022). Brief communication: Critical infrastructure impacts of the 2021 mid-July western European flood event. *Natural Hazards and Earth System Sciences*, *22*(12), 3831–3838. https://doi.org/10.5194/nhess-22-3831-2022

Kumar, P., Debele, S. E., Sahani, J., Rawat, N., Marti-Cardona, B., Alfieri, S. M., Basu, B., Basu, A. S., Bowyer, P., Charizopoulos, N., Gallotti, G., Jaakko, J., Leo, L. S., Loupis, M., Menenti, M., Mickovski, S. B., Mun, S. J., Gonzalez-Ollauri, A., Pfeiffer, J., … Zieher, T. (2021). Nature-based solutions efficiency evaluation against natural hazards: Modelling methods, advantages and limitations. In *Science of the Total Environment* (Vol. 784). Elsevier B.V. https://doi.org/10.1016/j.scitotenv.2021.147058

Landesamt für Statistik Niedersachsen. (2023). *Landwirtschaftliche Bodennutzung in Niedersachsen - Ergebnisse*. https://www.statistik.niedersachsen.de/landwirtschaft_forstwirtschaft_fischerei/landwirtschaft_in_niedersachsen/bodennutzung/landwirtschaftliche-bodennutzung-in-niedersachsen-ergebnisse-209478.html#:~:text=Landesamt%20f%C3%BCr%20Statistik%20Niedersachsen%20(LSN)&text=Im%20Jahr%202023%20wurden%20in,als%20Fl%C3%A4chen%20f%C3%BCr%20Dauerkulturen%20bewirtschaftet.

Le Moine, N. (2008). *Le bassin versant de surface vu par le souterrain: une voie d'amélioration des performance et du réalisme des modéles pluie–débit?* (Thesis). Université Pierre et Marie Curie, Paris.

Leegwater, I. (2024). *Investigating the effects of nature-based solutions in the Vecht river basin* (Unpublished doctoral dissertation). University of Twente, Enschede.

Li, H., Liao, X., Zhu, H., Wei, X., & Shao, M. (2019). Soil physical and hydraulic properties under different land uses in the black soil region of Northeast China. *Canadian Journal of Soil Science*, *99*(4), 406–419. https://doi.org/10.1139/cjss-2019-0039

Lindström, G., Johansson, B., Persson, M., Gardelin, M., & Bergström, S. (1997). Development and test of the distributed HBV-96 hydrological model. *Journal of Hydrology*, *201*(1–4), 272–288. https://doi.org/10.1016/S0022-1694(97)00041-3

Lozano-Baez, S. E., Cooper, M., Frosini de Barros Ferraz, S., Ribeiro Rodrigues, R., Castellini, M., & Di Prima, S. (2019). Recovery of Soil Hydraulic Properties for Assisted Passive and Active Restoration: Assessing Historical Land Use and Forest Structure. *Water*, *11*(1), 86. https://doi.org/10.3390/w11010086

Marshall, M. R., Ballard, C. E., Frogbrook, Z. L., Solloway, I., McIntyre, N., Reynolds, B., & Wheater, H. S. (2014). The impact of rural land management changes on soil hydraulic properties and runoff processes: results from experimental plots in upland UK. *Hydrological Processes*, *28*(4), 2617–2629. https://doi.org/10.1002/hyp.9826

Maulé, C. P., & Reed, W. B. (1993). Infiltration under no-till and conventional tillage systems in Saskatchewan. *Canadian Agricultural Engineering*, *35*(3), 165–173.

McCullough, Parker, Robinson, & Auvermann. (2001). Hydraulic conductivity, bulk density, moisture content, and electrical conductivity of a new sandy loam feedlot surface. *Applied Engineering in Agriculture*, *17*(4). https://doi.org/10.13031/2013.6471

Merriam, R. A. (1960). A note on the interception loss equation. *Journal of Geophysical Research*, *65*(11), 3850–3851. https://doi.org/10.1029/JZ065i011p03850

Ministerie van Landbouw; Natuur en Voedselkwaliteit. (2020). *Bos voor de toekomst* (Tech. Rep.) https://nl.chm-cbd.net/sites/nl/files/2021-05/Bos%2Bvoor%2Bde%2Btoekomst_Uitwerking%2Bambities%2Ben%2Bdoelen%2Blandelijke%2BBossenstrategie%2Ben%2Bbeleidsagenda%2B2030.pdf

Mohr, S., Ehret, U., Kunz, M., Ludwig, P., Caldas-Alvarez, A., Daniell, J. E., Ehmele, F., Feldmann, H., Franca, M. J., Gattke, C., Hundhausen, M., Knippertz, P., Küpfer, K., Mühr, B., Pinto, J. G., Quinting, J., Schäfer, A. M., Scheibel, M., Seidel, F., & Wisotzky, C. (2023). A multi-disciplinary analysis of the exceptional flood event of July 2021 in central Europe - Part 1: Event description and analysis. *Natural Hazards and Earth System Sciences*, *23*(2), 525–551. https://doi.org/10.5194/nhess-23-525-2023

Mosbahi, M., Kassouk, Z., Benabdallah, S., Aouissi, J., Arbi, R., Mrad, M., Blake, R., Norouzi, H., & Béjaoui, B. (2023). Modeling Hydrological Responses to Land Use Change in Sejnane Watershed, Northern Tunisia. *Water*, *15*(9), 1737. https://doi.org/10.3390/w15091737

Motovilov, Y. G., Gottschalk, L., Engeland, K., & Rodhe, A. (1999). Validation of a distributed hydrological model against spatial observations. *Agricultural and Forest Meteorology*, *98–99*, 257–277. https://doi.org/10.1016/S0168-1923(99)00102-1

Nandi, S., & Janga Reddy, M. (2021). *Parameter Estimation of a Macroscale Hydrological Model Using an Adaptive Differential Evolution* (pp. 243–255). https://doi.org/10.1007/978-3-030-58051-3_17

Penning, E., Klein, A., Asselman, N., De Louw, P., Kaandorp, V., Van Geest, G., Kingma, V., & Schoonderwoerd, E. (2024). *Sponswerking van Landschappen in Nederland* (Tech. Rep.). Delft: Deltares.

Provincie Drenthe. (2021). *Drentse bomen-en bossenstrategie, uitwerking van de landelijke bossenstrategie* (Tech. Rep.) (https://www.provincie.drenthe.nl/publish/pages/131355/drentse_bomen_en_bossenstrategie.pdf

Pushpalatha, R., Perrin, C., Moine, N. Le, & Andréassian, V. (2012). A review of efficiency criteria suitable for evaluating low-flow simulations. *Journal of Hydrology*, *420–421*, 171–182. https://doi.org/10.1016/j.jhydrol.2011.11.055

Raška, P., Bezak, N., Ferreira, C. S. S., Kalantari, Z., Banasik, K., Bertola, M., Bourke, M., Cerdà, A., Davids, P., Madruga de Brito, M., Evans, R., Finger, D. C., Halbac-Cotoara-Zamfir, R., Housh, M., Hysa, A., Jakubínský, J., Solomun, M. K., Kaufmann, M., Keesstra, S., … Hartmann, T. (2022). Identifying barriers for nature-based solutions in flood risk management: An interdisciplinary overview using expert community approach. *Journal of Environmental Management*, *310*. https://doi.org/10.1016/j.jenvman.2022.114725

Ruangpan, L., Vojinovic, Z., Di Sabatino, S., Leo, L. S., Capobianco, V., Oen, A. M. P., McClain, M. E., & Lopez-Gunn, E. (2020). Nature-based solutions for hydro-meteorological risk reduction: a state-of-the-art review of the research area. *Natural Hazards and Earth System Sciences*, *20*(1), 243–270. https://doi.org/10.5194/nhess-20-243-2020

Silva Peixoto, J. da, Ernesto de Moraes, M. A., Garcia, K., Broedel, E., Cuartas, A., & Nova da Cruz, P. P. (2024). Performance analysis of the lisflood hydrological model in a flood event in the madeira river basin. *International Journal of Hydrology*, *8*(2), 38–42. https://doi.org/10.15406/ijh.2024.08.00372

Sitterson, J., Knightes, C., Parmar, R., Wolfe, K., Avant, B., Overview, A., & Muche, M. (2018). An Overview of Rainfall-Runoff Model Types. *International Congress on Environmental Modelling and Software*, 41. https://scholarsarchive.byu.edu/iemssconference/2018/Stream-C/41/

Slager, K., & Kwadijk, J. (2023). *JCAR-ATRACE: Joint Cooperation programme for Applied scientific Research on flood and drought risk management in regional river basins* (Tech. Rep.). Delft: Deltares.

Slavíková, L., Hartmann, T., & Thaler, T. (2021). Paradoxes of financial schemes for resilient flood recovery of households. *Wiley Interdisciplinary Reviews: Water*, *8*(2). https://doi.org/10.1002/wat2.1497

Smakhtin, V. U. (2001). Low flow hydrology: a review. *Journal of Hydrology*, *240*(3–4), 147–186. https://doi.org/10.1016/S0022-1694(00)00340-1

Smith, K. A. (2012). *Evaluation of land management impacts on low flows in northern England*, Durham theses, Durham University. http://etheses.dur.ac.uk/3501/

Snel, K. A. W., Witte, P. A., Hartmann, T., & Geertman, S. C. M. (2020). The shifting position of homeowners in flood resilience: From recipients to key-stakeholders. In *Wiley Interdisciplinary Reviews: Water* (Vol. 7, Issue 4). John Wiley and Sons Inc. https://doi.org/10.1002/wat2.1451

Strahler, A. N. (1952). Hypsometric (area-altitude) analysis of erosional topography. *GSA Bulletin*, *63*(11), 1117–1142. https://doi.org/10.1130/0016-7606(1952)63[1117:HAAOET]2.0.CO;2

Stroosnijder, L. (1982). Simulation of the soil water balance. In F. W. T. Penning de Vries & H. H. van Laar (Eds.), *Simulation of plant growth and crop production* (pp. 175–193).

Stroosnijder, L. (1987). Soil evaporation: test of a practical approach under semi-arid conditions. *Netherlands Journal of Agricultural Science*, *35*(3), 417–426. https://doi.org/10.18174/njas.v35i3.16736

Supit, I., Hooijer, A. A., & van Diepen, C. A. (1994). *System Description of the WOFOST 6.0 Crop Simulation Model Implemented in CGMS Volume 1: Theory and Algorithms* (Tech. Rep.). Joint Research Centre

Ten Berge, A. (2024). *Robustness of hydrological models for simulating impact of climate change on high and low streamflow in the Lesse* (Thesis). University of Twente, Enschede.

Toreti, A., Masante, D., Acosta Navarro, J., Bavera, D., Cammalleri, C., De Felice, M., de Jager, A., Di Ciollo, C., Hrast Essenfelder, A., Maetens, W., Magni, D., Mazzeschi, M., & Spinoni, J. (2022). *Drought in Europe July 2022*. https://doi.org/10.2760/014884

Tradowsky, J. S., Philip, S. Y., Kreienkamp, F., Kew, S. F., Lorenz, P., Arrighi, J., Bettmann, T., Caluwaerts, S., Chan, S. C., De Cruz, L., de Vries, H., Demuth, N., Ferrone, A., Fischer, E. M., Fowler, H. J., Goergen, K., Heinrich, D., Henrichs, Y., Kaspar, F., … Wanders, N. (2023). Attribution of the heavy rainfall events leading to severe flooding in Western Europe during July 2021. *Climatic Change*, *176*(7), 90. https://doi.org/10.1007/s10584-023-03502-7

Trautmann, T., Koirala, S., Carvalhais, N., Güntner, A., & Jung, M. (2021). *The importance of vegetation to understand terrestrial water storage variations*. 1089–1109. https://doi.org/10.5194/hess-2021-394

United Nations Environment Programme. (2022). Resolution adopted by the United Nations Environment Assembly on 2 March 2022. 5/5. Nature-based solutions for supporting sustainable development. *United Nations Environment Assembly of the United Nations Environment Programme* .

University of Washington Computational Hydrology Group. (2021). *Variable Infiltration Capacity (VIC) Macroscale Hydrologic Model*. https://vic.readthedocs.io/en/master/

van der Knijff, J. M., Younis, J., & de Roo, A. P. J. (2010). LISFLOOD: A GIS-based distributed model for river basin scale water balance and flood simulation. *International Journal of Geographical Information Science*, *24*(2), 189–212. https://doi.org/10.1080/13658810802549154

van Dijk, S., & van Wijk, F. (2022). *Bossenstrategie Overijssel* (Tech. Rep.). Provincie Overijssel, Zwolle.

van Genuchten, M. Th. (1980). A Closed-form Equation for Predicting the Hydraulic Conductivity of Unsaturated Soils. *Soil Science Society of America Journal*, *44*(5), 892–898. https://doi.org/10.2136/sssaj1980.03615995004400050002x

Van Zanten, B., Gutierrez Goizueta, G., Brander, L., Gonzalez Reguero, B., Griffin, R., Kapur Macleod, K., Alves, A., Midgley, A., Diego Herrera, L., & Jongman, B. (2023). *Assessing the Benefits and Costs of Nature-Based Solutions for Climate Resilience: A Guideline for Project Developers* (Tech. Rep.). World Bank, Washington, DC.

Viviroli, D., Zappa, M., Gurtz, J., & Weingartner, R. (2009). An introduction to the hydrological modelling system PREVAH and its pre- and post-processing-tools. *Environmental Modelling & Software*, *24*(10), 1209–1222. https://doi.org/10.1016/j.envsoft.2009.04.001

Von Hoyningen-Huene, J. (1981). Die Interzeption des Niederschlags in landwirtschaftlichen Pflanzenbeständen (Rainfall interception in agricultural plant stands). *Arbeitsbericht Deutscher Verband Für Wasserwirtschaft Und Kulturbau, DVWK*, 63.

Waterschap Drents Overijsselse Delta. (2021). *Maatregelen voor een Delta met toekomst* (Tech. Rep.). Waterschap Drents Overijsselse Delta, Zwolle.

Yamazaki, D., Ikeshima, D., Sosa, J., Bates, P. D., Allen, G. H., & Pavelsky, T. M. (2019). MERIT Hydro: A High-Resolution Global Hydrography Map Based on Latest Topography Dataset. *Water Resources Research*, *55*(6), 5053–5073. https://doi.org/10.1029/2019WR024873

Yao, S. x., Zhao, C. c., Zhao, X. M., Wang, S. y., Li, Y. j., & Tian, L. n. (2015). Effects of land use on soil saturated hydraulic conductivity of Horqin Sand Land. *Proceedings of the 2015 International Forum on Energy, Environment Science and Materials*. https://doi.org/10.2991/ifeesm-15.2015.220

Yoosefdoost, I., Bozorg-Haddad, O., Singh, V. P., & Chau, K. W. (2022). Hydrological Models. In *Springer Water* (pp. 283–329). Springer Nature. https://doi.org/10.1007/978-981-19-1898-8_8

Zabret, K., & Šraj, M. (2015). Can urban trees reduce the impact of climate change on storm runoff? *Urbani Izziv*, *26*, S165–S178. https://doi.org/10.5379/urbani-izziv-en-2015-26-supplement-011

Zhao, R. J., & Liu, X. R. (1995). The Xinanjiang model. In V. P. Singh (Ed.), *Computer models of watershed hydrology* (pp. 215–232).

Zimmermann, B., Elsenbeer, H., & De Moraes, J. M. (2006). The influence of land-use changes on soil hydraulic properties: Implications for runoff generation. *Forest Ecology and Management*, *222*(1–3), 29–38. https://doi.org/10.1016/j.foreco.2005.10.070

Appendices

Appendix A – Hydrological processes in LISFLOOD-OS

The following sections give a detailed description of each individual process included in LISFLOOD-OS.

Meteorological forcing

LISFLOOD-OS is driven by the following meteorological variables: precipitation intensity ($P\ \left[\frac{mm}{day}\right]$), potential evapotranspiration of a closed canopy ($ET0\ \left[\frac{mm}{day}\right]$), potential evaporation from bare soil ($ES0\ \left[\frac{mm}{day}\right]$), potential evaporation from open water ($EW0\ \left[\frac{mm}{day}\right]$), and average 24-hour temperature ($T_{avg}\ [°C]$). $ET0$, $ES0$, and $EW0$ are calculated externally, and a pre-processing application (LISVAP) is available to compute these values from standard meteorological data (van der Knijff et al., 2010).

Snow melt and frost

In LISFLOOD-OS, when the average daily temperature falls below 1°C, all precipitation is considered snow, accumulating on the soil surface until it melts. While LISFLOOD-OS can calculate snow accumulation and snowmelt, these processes are not highly relevant to the study area, so their detailed description is omitted from this report.

Interception

Interception is estimated using the storage-based approach of Aston (1979) and Merriam (1960), using two parameters (Equation 5).

$$Int = S_{max} \cdot \left[1 - e^{\frac{-k \cdot R \cdot \Delta t}{S_{max}}}\right] \qquad \text{[Eq. 5]}$$

Where $Int\ [mm]$ is the interception per time step, $S_{max}\ [mm]$ is the maximum interception, $R\ \left[\frac{mm}{day}\right]$ is the rainfall intensity and the factor $k[-]$ accounts for the density of the vegetation. S_{max} is calculated using empirical Equation 6 (Von Hoyningen-Huene, 1981), where $LAI\ \left[\frac{m^2}{m^2}\right]$ is the average Leaf Area Index of each pixel.

$$\begin{cases} S_{max} = 0.935 + 0.498 \cdot LAI - 0.00575 \cdot LAI^2 & [LAI > 0.1] \\ S_{max} = 0 & [LAI \leq 0.1] \end{cases} \qquad \text{[Eq. 6]}$$

And k is related to LAI following Equation 7.

$$k = 0.046 \cdot LAI \qquad \text{[Eq. 7]}$$

The interception at each timestep cannot exceed the rainfall amount. It can also not exceed the interception storage capacity defined as the difference between S_{max} and the accumulated amount of water that is stored as interception, $Int_{cum}\ [mm]$.

Evaporation of intercepted water

The evaporation of water intercepted by vegetation, $EW_{int}\ [mm]$, occurs at the same rate as it would from an open water surface, $EW0\ \left[\frac{mm}{day}\right]$. However, the maximum amount of evaporation during each time step $EW_{max}\ [mm]$ is proportional to the fraction of the pixel covered by vegetation as described in Equation 8 (Supit et al., 1994).

$$EW_{max} = EW0 \cdot [1 - e^{-\kappa_{gb} \cdot LAI}] \cdot \Delta t \qquad \text{[Eq. 8]}$$

Where the constant $\kappa_{gb}[-]$ is the extinction coefficient for global solar radiation. The actual amount of evaporation EW_{int} is limited by the amount of water stored on the leaves Int_{cum} (Equation 9).

$$EW_{int} = \min\left(EW_{max} \cdot \Delta t, Int_{cum}\right) \qquad \text{[Eq. 9]}$$

Water that is not lost as evaporation from the interception storage falls to the soil because of leaf drainage, which is modelled as a linear reservoir (Equation 10).

$$D_{int} = \frac{1}{T_{int}} \cdot Int_{cum} \cdot \Delta t \quad \text{[Eq. 10]}$$

Where D_{int} $[mm]$ is the amount of leaf drainage per timestep and T_{int} $[days]$ is a the residence time constant of the interception store.

Water available for infiltration and direct runoff

In the permeable fraction of each pixel, the amount of water available for infiltration, W_{av} $[mm]$ is calculated using Equation 11 (Supit et al., 1994).

$$W_{av} = R \cdot \Delta t + M + D_{int} - Int \quad \text{[Eq. 11]}$$

Where R $\left[\frac{mm}{day}\right]$ is rainfall and M $[mm]$ is snowmelt. No infiltration takes place in the 'direct runoff fraction' of each cell. Therefore, the direct runoff R_d $[mm]$ per timestep is calculated as described by Equation 12.

$$R_d = f_{dr} \cdot (R \cdot \Delta t + M - IntercSealed) + WaterFraction \cdot (R \cdot \Delta t + M - EW0) \quad \text{[Eq. 12]}$$

Where $IntercSealed$ $[mm]$ is the water retained by the depressions of the impervious surfaces and not immediately available to generate direct runoff. It is important to note that the water available for infiltration, W_{av}, is only valid in the permeable fraction of each cell, whereas the direct runoff, R_d, is computed for the full pixel (permeable + direct runoff areas).

Water uptake by plant roots and transpiration

Water uptake and transpiration by vegetation and direct evaporation from the soil are two separate processes in the model. This section describes the computation of the roots water uptake to support plant transpiration. The maximum transpiration per timestep T_{max} $[mm]$ is described by Equation 13.

$$T_{max} = k_{crop} \cdot ET0 \cdot \left[1 - e^{-\kappa_{gb} \cdot LAI}\right] \cdot \Delta t - EW_{int} \quad \text{[Eq. 13]}$$

Where k_{crop} $[-]$ is a crop coefficient describing the ration between the potential evapotranspiration rate and the potential evaporation rate of a specific crop. $ET0$ $\left[\frac{mm}{day}\right]$ is the potential evapotranspiration rate. The actual transpiration rate is dependent on the amount of available soil moisture. The model uses a reduction factor to simulate this effect, this R_{WS} is computed as described by Equation 14.

$$R_{WS} = \frac{w_1 - w_{wp1}}{w_{crit1} - w_{wp1}} \quad \text{[Eq. 14]}$$

Where $w_1[mm]$ is the amount of soil moisture in the superficial and upper soil layers, w_{wp1} $[mm]$ is the amount of soil moisture at wilting point and w_{crit1} $[mm]$ is the critical amount of soil moisture. When soil moisture levels reach lower levels than the critical point the plants start closing their stomata and water uptake is reduced. The value of w_{crit1} is dependent on soil and crop types and computed as described by Equation 15.

$$w_{crit1} = (1 - p) \cdot \left(w_{fc1} - w_{wp1}\right) + w_{wp1} \quad \text{[Eq. 15]}$$

Where w_{fc1} $[mm]$ is the amount of soil moisture at field capacity, and p is the soil water depletion fraction. The actual transpiration T_a $[mm]$ is now computed as described by Equation 16. The amount of moisture in the superficial soil layer 1a and the upper soil layer 1b are updated after computing the actual transpiration.

$$T_a = R_{WS} \cdot T_{max} \quad \text{[Eq. 16]}$$

Evaporation from the soil surface

The maximum amount of evaporation from the soil surface is equal to the maximum evaporation from a shaded soil surface, ES_{max} $[mm]$ which is computed as (Equation 17):

$$ES_{max} = ES0 \cdot e^{\left(\frac{-\kappa_{gb} \cdot LAI}{\Delta t}\right)} \quad \text{[Eq. 17]}$$

Where $ES0\ \left[\frac{mm}{day}\right]$ is the potential evaporation rate from bare soil surface. The actual evaporation from the soil depends on soil moisture availability near the soil surface, with decreasing evaporation rates as the topsoil is drying. The model simulates this using a reduction factor, which is a function of the number of days since the last rain storm, as described by Equation 18 (Stroosnijder, 1987) & (Stroosnijder, 1982).

$$ES_a = ES_{max} \cdot \left(\sqrt{D_{slr}} - \sqrt{D_{slr} - 1}\right) \quad \text{[Eq. 18]}$$

Where $D_{slr}\ [days]$ is the number of days since the last rain event. The actual evaporation from the soil is always the smallest value out of Equation 18 and the available amount of moisture in the soil. The actual soil evaporation is extracted from the superficial soil layer and, subsequently, from the upper soil layer. The amount of moisture in in the superficial and upper soil layers is then updated.

Preferential bypass flow

During extreme rainfall events, the model simulates preferential flow, where water bypasses the soil matrix and drains directly into the groundwater. At each time step, a portion of the water available for infiltration W_{av} bypasses the soil matrix. It goes directly to the groundwater, following a power function based on the saturation level of the superficial and upper soil layers. This results in an equation that is somewhat similar to the excess soil water equation as used in the HBV model (Lindström et al., 1997) The amount of preferential flow per timestep, $D_{pref,gw}\ [mm]$, is computed as (Equation 19):

$$D_{pref,gw} = W_{av} \cdot \left(\frac{w_1}{w_{s1}}\right)^{c_{pref}} \quad \text{[Eq. 19]}$$

Where $c_{pref}\ [-]$ is an empirical shape parameter, and at increasing values for c_{pref} the percentage of preferential flow is decreasing. Preferential flow is only simulated in the permeable fraction of each pixel and becomes increasingly important as the soil gets wetter.

Infiltration capacity

The infiltration capacity of the soil is estimated using the Xinanjiang model (Zhao & Liu, 1995), which assumes that the fraction of a grid-cell contributing to surface runoff is related to the total amount of soil moisture, and that this relationship can be described by a non-linear distribution factor. The saturated fraction A_s of the permeable fraction of each pixel is computed as described by Equation 20.

$$A_s = 1 - \left(1 - \frac{w_1}{w_{s1}}\right)^b \quad \text{[Eq. 20]}$$

Where $w_{s1}\ [mm]$ and $w_1\ [mm]$ are the maximum and actual amounts of moisture in the superficial and upper soil layers. $b\ [-]$ is an empirical non-dimensional shape parameter. The potential infiltration capacity $INF_{pot}\ [mm]$ is a function of w_{s1} and A_s as described by Equation 21.

$$INF_{pot} = \frac{w_{s1}}{b+1} \cdot (1 - A_s)^{\frac{b+1}{b}} \quad \text{[Eq. 21]}$$

Actual infiltration and surface runoff

The actual infiltration $INF_{act}\ [mm]$ is now calculated as described by Equation 22.

$$INF_{act} = \min\left(INF_{pot}, W_{av} - D_{pref,gw}\right) \quad \text{[Eq. 22]}$$

The amount of actual infiltration is added to the superficial and upper soil layers. Finally, the surface runoff $R_s\ [mm]$ is computed as (Equation 23):

$$R_s = R_d + (1 - f_{dr}) \cdot \left(W_{av} - D_{pref,gw} - INF_{act}\right) \quad \text{[Eq. 23]}$$

Where $R_d\ [mm]$ is the direct runoff generated in the pixel's 'direct runoff fraction' (f_{dr}). After the infiltration calculations the amount of moisture in the upper soil layer is updated.

Soil moisture redistribution

The moisture fluxes out of the subsoil and between the upper and lower soil layers are based on the simplifying assumption that the flow of soil moisture is entirely gravity-driven. Starting from Darcy's law

for 1-D vertical flow rate, where $q\ \left[\frac{mm}{day}\right]$ is the flow rate out of the soil (e.g. superficial, upper or lower soil layer) as described by Equation 24.

$$q = -K(\theta) \cdot \left[\frac{\partial h(\theta)}{\partial z} - 1\right] \quad \text{[Eq. 24]}$$

Where $K(\theta)\ \left[\frac{mm}{day}\right]$ is the hydraulic conductivity as a function of the volumetric moisture content of the soil $\theta\ \left[\frac{mm}{day}\right]$, and $\frac{\partial h(\theta)}{\partial z}$ is the matric potential gradient. Hydraulic conductivity and soil moisture status is further described by the Van Genuchten equation (van Genuchten, 1980). Here, Equation 25 describes the Van Genuchten equation in terms of mm water slice instead of volume fractions.

$$K(w) = K_s \cdot \sqrt{\left(\frac{w - w_r}{w_s - w_r}\right)} \cdot \left\{1 - \left[1 - \left(\frac{w - w_r}{w_s - w_r}\right)^{\frac{1}{m}}\right]^m\right\}^2 \quad \text{[Eq. 25]}$$

Where $K_s\ \left[\frac{mm}{day}\right]$ is the saturated conductivity of the soil, and w, w_r and w_s are the actual, residual and maximum amounts of soil moisture in the soil respectively (all in [mm]). Parameter m is calculated from the soil texture-related pore size index, λ. The computation of m is done as described by Equation 26.

$$m = \frac{\lambda}{\lambda + 1} \quad \text{[Eq. 26]}$$

Subsurface flow

LISFLOOD-OS simulates groundwater storage and flow using two parallel linear reservoirs, following a method similar to the HBV-96 model (Lindström et al., 1997). The upper reservoir represents faster runoff, which includes rapid groundwater and subsurface flow through large soil pores, while the lower reservoir represents slower groundwater movement that contributes to base flow. The outflow from the upper zone to the channel, $Q_{uz}\ [mm]$, is calculated as described by Equation 27.

$$Q_{uz} = \frac{1}{T_{uz}} \cdot UZ \cdot \Delta t \quad \text{[Eq. 27]}$$

Where $T_{uz}\ [days]$ is the reservoir constant of the upper zone, and $UZ\ [mm]$ the amount of water that is stored in the upper zone. The amount of water stored in the upper zone is computed as follows (Equation 28):

$$UZ = D_{ls,uz} + D_{pref,uz} - D_{uz,lz} \quad \text{[Eq. 28]}$$

Where $D_{ls,uw}\ [mm]$ is the flux from the lower soil layer to the groundwater, $D_{pref,uz}\ [mm]$ is the amount of preferential flow and $D_{uz,lz}\ [mm]$ is the amount of water that percolates from the upper to the lower zone. Outflow from the lower zone to the channel is then computed by (Equation 29):

$$Q_{lz} = \frac{1}{T_{lz}} \cdot LZ \cdot \Delta t \quad \text{[Eq. 29]}$$

Where $T_{lz}\ [days]$ is the reservoir constant of the lower zone, and $LZ\ [mm]$ the amount of water stored in the lower zone. The amount of water stored in the lower zone is computed as follows (Equation 30):

$$LZ = D_{uz,lz} - TotalAbstractionFromGroundwater - D_{loss} \quad \text{[Eq. 30]}$$

Where $TotalAbstractionFromGroundwater\ [mm]$ is the water abstracted from the lower zone to comply with domestic, industrial, irrigation and livestock demand. $D_{loss}\ [mm]$ is percolation from the groundwater zone, this water never rejoins the channel and is lost beyond the catchment boundaries or to deep groundwater systems.

Surface- and subsurface runoff routing

Routing in LISFLOOD-OS takes place in two stages. First, the runoff generated in each pixel is routed to the nearest downstream channel. Surface runoff is routed using a four-point implicit finite difference method based on the kinematic wave equations (Chow et al., 1988). Subsurface runoff, including water from the upper and lower groundwater zones, is routed to the nearest downstream channel pixel within

one time step. Finally, the water in each channel pixel is routed through the channel network, again using the four-point implicit finite-difference solution of the kinematic wave equations. The basic equations used are the equations of continuity (Equation 31) and momentum (Equation 32).

$$\frac{\partial Q_{sr}}{\partial x} + \frac{\partial A_{sr}}{\partial t} = q_{sr} \qquad \text{[Eq. 31]}$$

Where Q_{sr} $\left[\frac{m^3}{s}\right]$ is the surface runoff, A_{sr} $[m^2]$ is the cross-sectional area of the flow and q_{sr} $\left[\frac{m^2}{s}\right]$ is the amount of lateral inflow per unit flow length.

$$\rho \cdot g \cdot A_{sr} \cdot (S_0 - S_f) = 0 \qquad \text{[Eq. 32]}$$

Where ρ $\left[\frac{kg}{m^3}\right]$ is the density of the flow, g $\left[\frac{m}{s^2}\right]$ is the gravity acceleration, S_0 is the topographical gradient and S_f is the friction gradient.

Appendix B – Discharge data

Table B 1: Discharge station data availability and corresponding sources.

Station name	**From**	**Until**	**Source(s)**
Bilk	GE	1975-01-11	2024-05-31	Deltares (1975-2017), NRW (1996-2024)
Wettringen	GE	1975-01-11	2024-05-31	Deltares (1975-2017), NRW (1996-2024)
Ohne	GE	1968-01-02	2024-04-30	Deltares (1968-2017), FEWS (2019-2024)
Gronau	GE	1996-01-11	2024-05-31	NRW (1996-2024)
Lage I	GE	1963-01-03	2017-12-31	NLWKN
Lage II	GE	1963-01-03	2017-12-31	NLWKN
Lage III	GE	1972-01-04	2017-12-31	NLWKN
Lage Gesamt	GE	1963-01-03	2017-12-31	NLWKN
Dinkel	GE	2020-01-05	2023-11-06	FEWS (2020-2023)
Neuenhaus	GE	1950-01-01	2024-05-31	NLWKN, FEWS (2020-2024)
Osterwald	GE	1963-01-11	2024-05-31	NLWKN, FEWS (2020-2024)
Emlichheim	GE	1950-01-01	2024-05-31	NLWKN, FEWS (2017-2024), Waterboard Vechtstromen (Christmas 23/24)
De Haandrik	NL	2007-01-01	2024-05-28	Waterboard Vechtstromen
Ane Gramsbergen	NL	2005-07-15	2024-05-31	Deltares (2005-2016), FEWS (2020-2024), Waterboard Vechtstromen (Christmas 23/24)
ST Hardenberg	NL	1997-07-01		Deltares
ST Marienberg	NL	1997-07-01		Deltares
ST Junne	NL	1989-01-01		Deltares
Ommen	NL	2001-10-14	2024-05-31	Deltares (2001-2015), RWS (2015-2024), Waterboard Vechtstromen (Christmas 23/24)
Ommerkanaal	NL	2001-10-14	2024-05-31	Deltares (2001-2015), RWS (2015-2024), Waterboard Vechtstromen (Christmas 23/24)
Archem TOT	NL	1996-01-01	2017-12-04	Deltares (1996-2017), FEWS (2022-2024)
DM Dalfsen	NL	2012-12-06	2024-05-13	Waterboard Drents Overijsselse Delta

Appendix C – Static maps in LISFLOOD-OS model

All EFAS maps were retrieved from the Joint Research Centre open database (Joint Research Centre, 2024d). Wflow sbm maps for the Vecht were retrieved from MERIT Hydro (Yamazaki et al., 2019).

Table C 1: Overview of static maps used in LISFLOOD-OS model.

Map name	**Description**	**Units; range**	**Interpolation method**	**Source**
General maps				
Mask map	Boolean map that defines model boundaries	Units: -; Range: NoData or 1		User-defined
Land use mask	Boolean map for land use calculations	Units: -; Range: NoData or 1		User-defined
Pixel length	Map with grid-cell (pixel) length along the latitude	Units: -; Range: >0		User-defined
Pixel area	Map with grid-cell (pixel) area	Units: m^2; Range: >0		User-defined
Topography maps				
Local drain direction map	Local drain direction map - flow directions from each grid-cell to its steepest downslope neighbour;	Units: -; Values: 1,2,3,4,5,6,7,8,9	-	Wflow sbm
Gradient map	Slope gradient	Units: -; Range: >0	Cubic	EFAS
Elevation standard deviation	Standard deviation of elevation (altitude difference elevation within a grid-cell)	Units: -; Range: >=0	Cubic	EFAS
Land use maps				
Fraction of inland water	Inland water fraction for each grid-cell	Units: -; Range: [0-1]	Nearest-neighbour	EFAS
Fraction of sealed surfaces	Urban surface fraction for each grid-cell	Units: -; Range: [0-1]	Nearest-neighbour	EFAS
Fraction of forest	Forest fraction for each grid-cell	Units: -; Range: [0-1]	Nearest-neighbour	EFAS
Fraction of irrigated crops	Irrigated crop (except rice) fraction for each grid-cell	Units: -; Range: [0-1]	Nearest-neighbour	EFAS
Fraction of rice	Irrigated rice fraction for each grid-cell	Units: -; Range: [0-1]	Nearest-neighbour	EFAS
Fraction of other land use type	Other (e.g. agricultural areas, non-forested natural areas, pervious surface of urban areas) land cover type (not mentioned above) fraction for each grid-cell	Units: -; Range: [0-1]	Nearest-neighbour	EFAS
Land use depending maps				
Crop coefficient	Averaged (by time and ecosystem type) crop coefficient for forest/ irrigated crops/ other land cover type	Units: -; Range: 0.20 .. 1.08	Cubic	EFAS
Crop group number	Averaged (by time and ecosystem type) crop group number for forest/ irrigated crops/ other land cover type	Units: -; Range: 1 .. 5	Cubic	EFAS

Table continues on the next page

Map name	**Description**	**Units; range**	**Interpolation method**	**Source**
Continuation of Land use depending maps				
Manning's coefficient	Averaged (by ecosystem type) Manning's roughness coefficient for forest/ irrigated crops/ other land cover type	Units: $m^{1/3}$ s^{-1}; Range: 0.015 .. 0.200	Cubic	EFAS
Soil depth	Forested/ other (non-forested) area soil depth for soil layer 1 (surface layer)/ 2 (middle layer)/ 3 (bottom layer)	Units: mm; Range: ≥ 50**	Cubic	EFAS
Soil hydraulic properties maps				
Theta saturated	Saturated volumetric soil moisture content for forested/non-forested (others) areas	Units: m^3/m^3; Range: > 0.000 & < 1.000	Cubic	EFAS
Theta residual	Residual volumetric soil moisture content for forested/non-forested (others) areas	Units: m^3/m^3; Range: > 0.000 & < 1.000	Cubic	EFAS
lambda	Pore size index (λ) for forested/non-forested (others) areas	Units: - ; Range: > 0.000 & ≤ 0.42	Cubic	EFAS
Genu Alpha	Van Genuchten parameter (α) for forested/non-forested (others) areas soil	Units: cm^{-1} ; Range: > 0.000 & ≤ 0.055	Cubic	EFAS
K saturated	Saturated conductivity for forested/non-forested (others) areas	Units: mm/day ; Range: > 0.000	Cubic	EFAS
Channel geometry maps				
Channel mask	Boolean map that identifies the channel grid-cells	Units: -; Range: NoData or 1	-	EFAS
Side slope	Channel side slope	Units: m; Range>0	-	EFAS
Channel length	Channel length (value can exceed grid size, to account for meandering rivers)	Units: m; Range>0	-	Wflow sbm
Channel gradient	Channel longitudinal gradient	Units: m/m; Range: [0-1]	Cubic	EFAS
Manning's roughness coefficient	Channels Manning's roughness coefficient	Units: $m^{1/3}$ s^{-1}	Cubic	EFAS
Bottom width	Channel bottom width	Units: m; Range>0	-	User-defined
Floodplain	Width of the area where the surplus of water is distributed when the water level in the channel exceeds the bankfull channel depth	Units: m; Range>0	-	User-defined
Bankfull channel depth	Bankfull channel depth	Units: m; Range>0	Cubic	EFAS

Table continues on the next page

Map name	**Description**	**Units; range**	**Interpolation method**	**Source**
Leaf area index maps				
LAI for forest	10-day average (36 maps in total) Leaf Area Index for closed forested areas (forest fraction per grid-cell ≥ 0.7)	Units: -; Range: 0 ..7	Cubic	EFAS
LAI for irrigated crops	10-day average (36 maps in total) Leaf Area Index for irrigated crop areas (irrigated crop fraction per grid-cell ≥ 0.7)	Units: -; Range: 0 ..7	Cubic	EFAS
LAI for other	10-day average (36 maps in total) Leaf Area Index for mainly other land cover type areas (other land cover type fraction per grid-cell ≥ 0.7)	Units: -; Range: 0 ..7	Cubic	EFAS

Appendix D – Sensitivity analysis

Appendix D1: Parameter values in sensitivity analysis

Table D 1: Parameter values included in sensitivity analysis.

Parameter name	Unit	Min		Default		Max
C_m	mm/(C day)	-	-	-	-	-
b	-	0.01	0.255	0.5	2.75	5
C_{pref}	-	0.5	2.25	4	6	8
T_{uz}	days	0.01	5.005	10	25	40
GW_{perc}	mm/day	0.01	0.405	0.8	1.7	2
T_{lz}	days	40	70	100	550	10000
$LZ_{threshold}$	mm	0	5	10	20	30
GW_{loss}	-	0	0.125	0.25	0.375	0.5
$QSplitMult$	-	0	1	2	11	20
$CalChanMan1$	-	0.5	0.75	1	1.5	2
$CalChanMan2$	-	0.5	0.75	1	3	5
$AdjL_n$	-	-	-	-	-	-
$ResMultQ_{norm}$	-	-	-	-	-	-
α	-	-	-	-	-	-

Appendix D2: Sensitivity analysis results

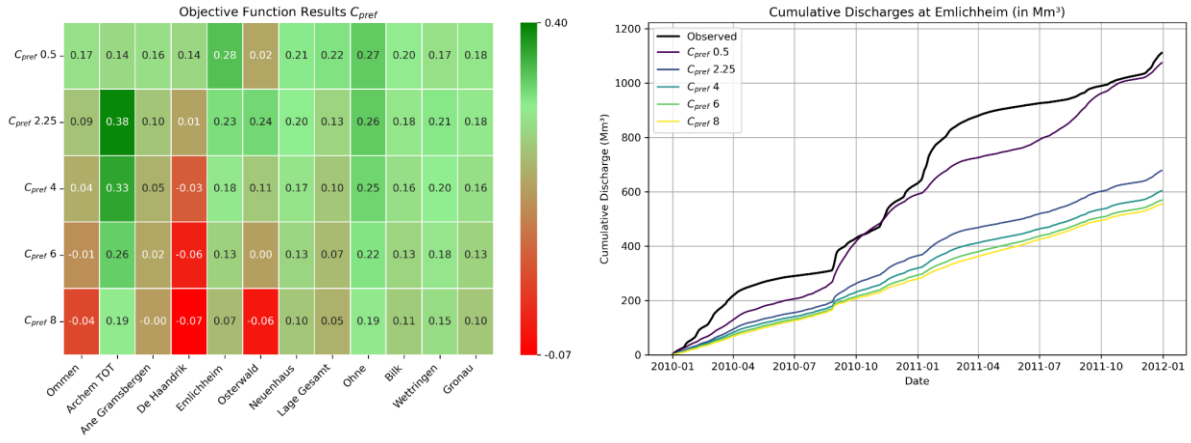

Figure D 1: Objective function values and cumulative discharges at Emlichheim for varying C_{pref} values [-].

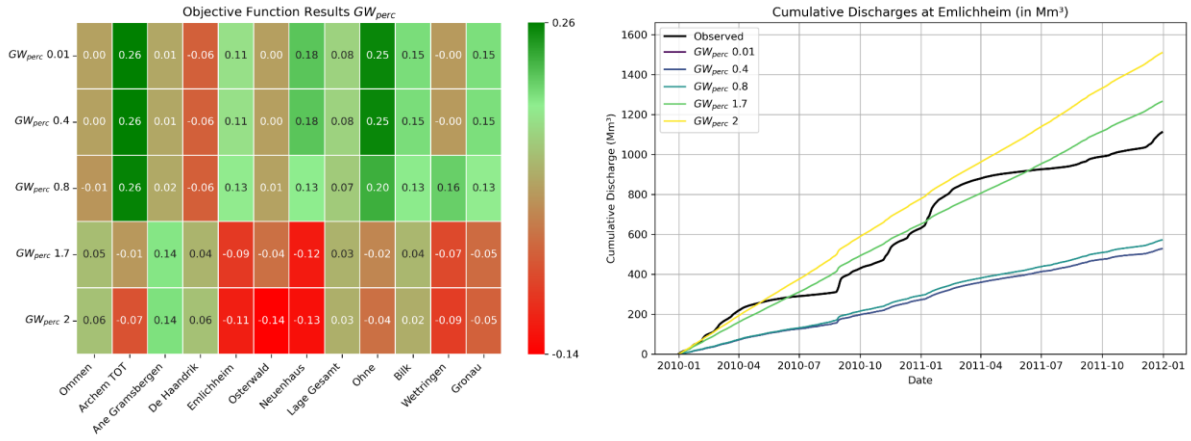

Figure D 2: Objective function values and cumulative discharges at Emlichheim for varying GW_{perc} values [mm/day].

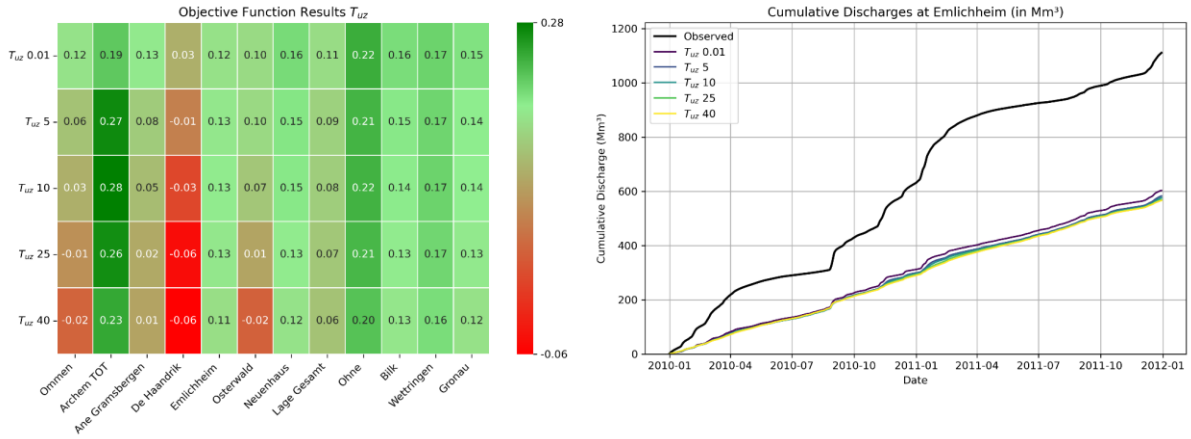

Figure D 3: Objective function values and cumulative discharges at Emlichheim for varying T_{uz} values [days].

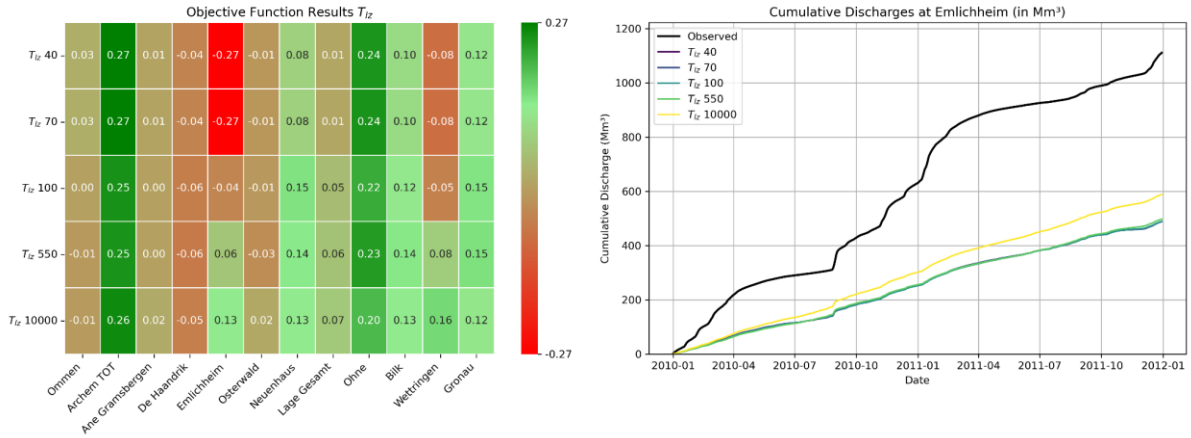

Figure D 4: Objective function values and cumulative discharges at Emlichheim for varying T_{lz} values [days].

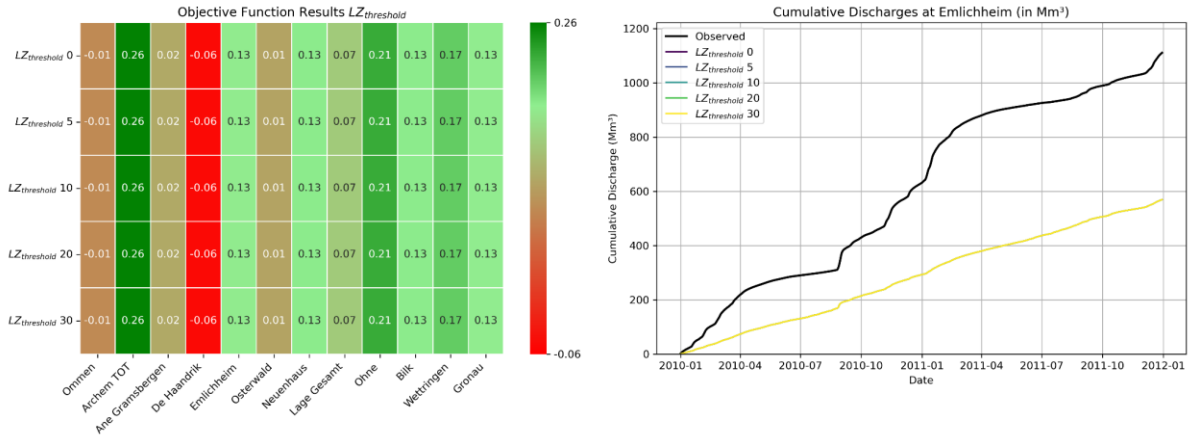

Figure D 5: Objective function values and cumulative discharges at Emlichheim for varying $LZ_{threshold}$ values [mm].

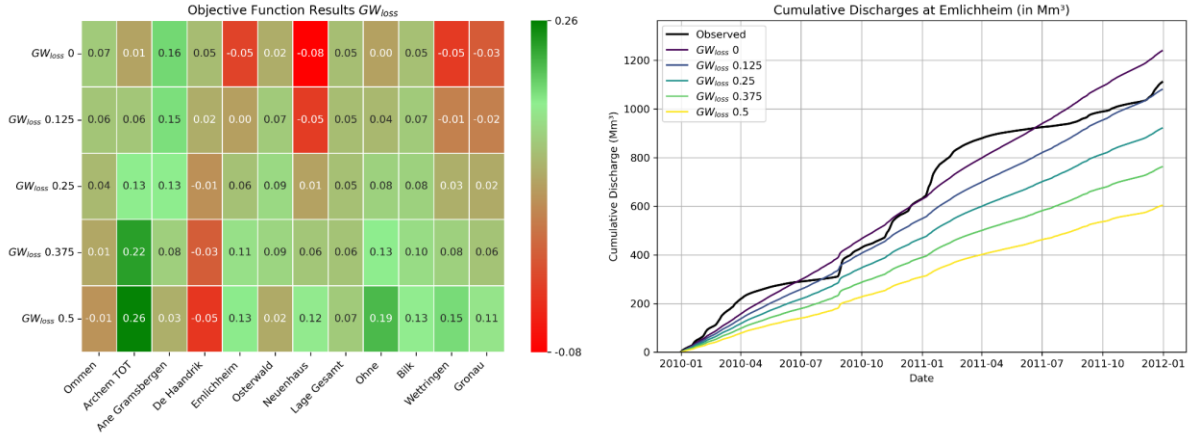

Figure D 6: Objective function values and cumulative discharges at Emlichheim for varying GW_{loss} values [mm/day].

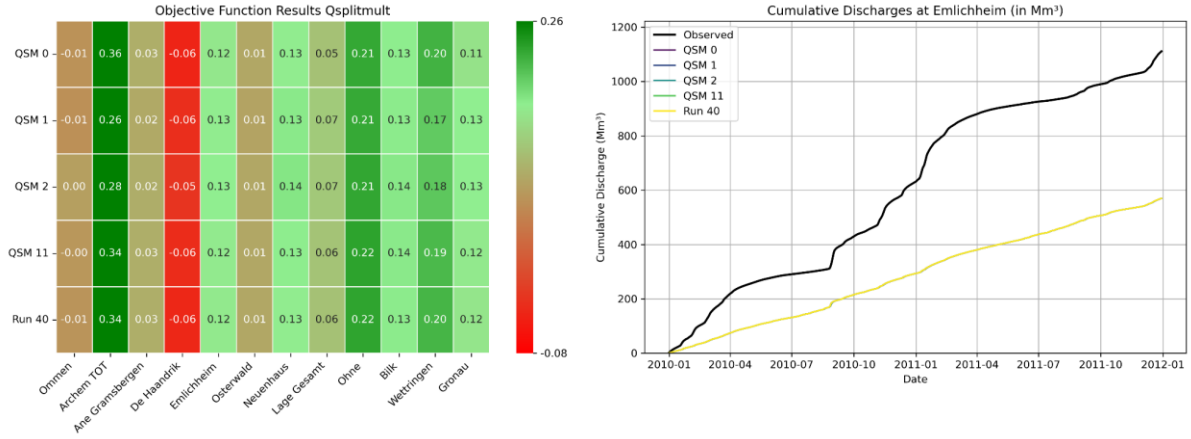

Figure D 7: Objective function values and cumulative discharges at Emlichheim for varying QSplitMult values [-].

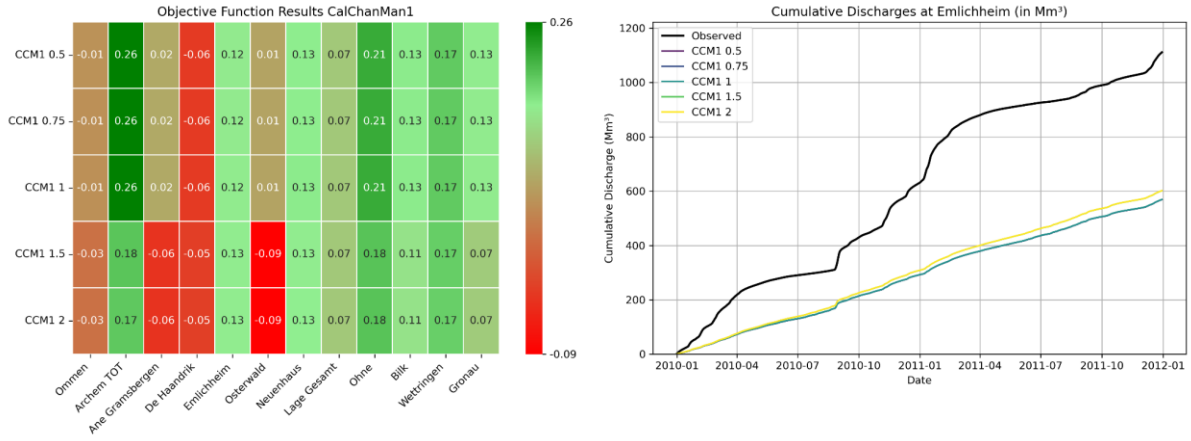

Figure D 8: Objective function values and cumulative discharges at Emlichheim for varying CalChanMan1 values [-].

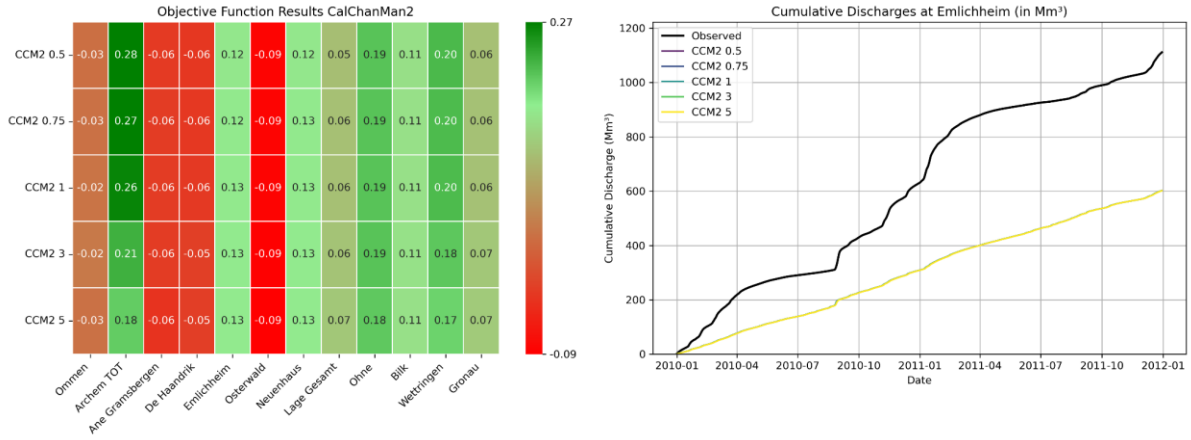

Figure D 9: Objective function values and cumulative discharges at Emlichheim for varying CalChanMan2 values [-].

Appendix E – Calibration and validation

Appendix E1: Calibration hydrographs

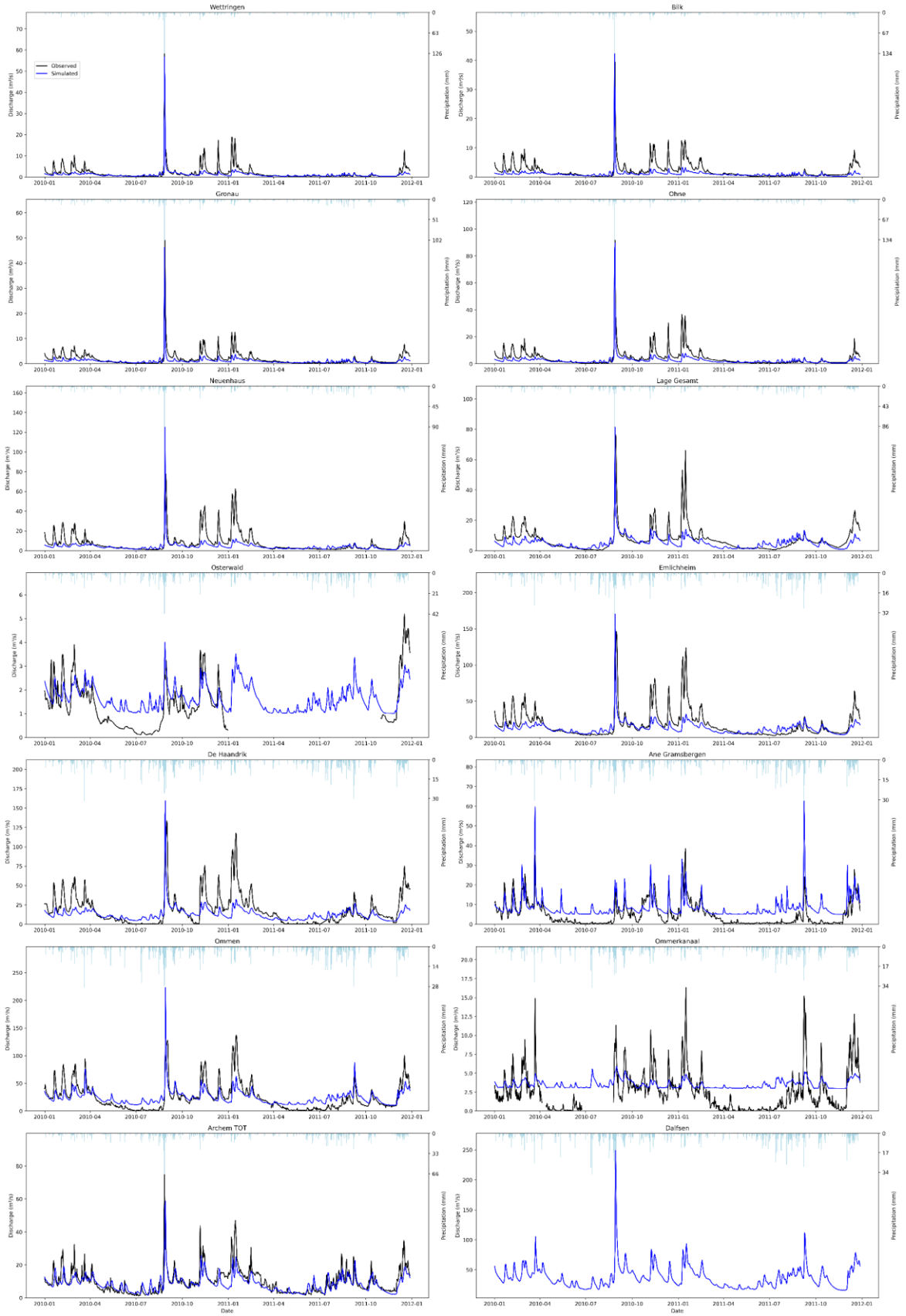

Appendix E2: Hydrographs validation 1998

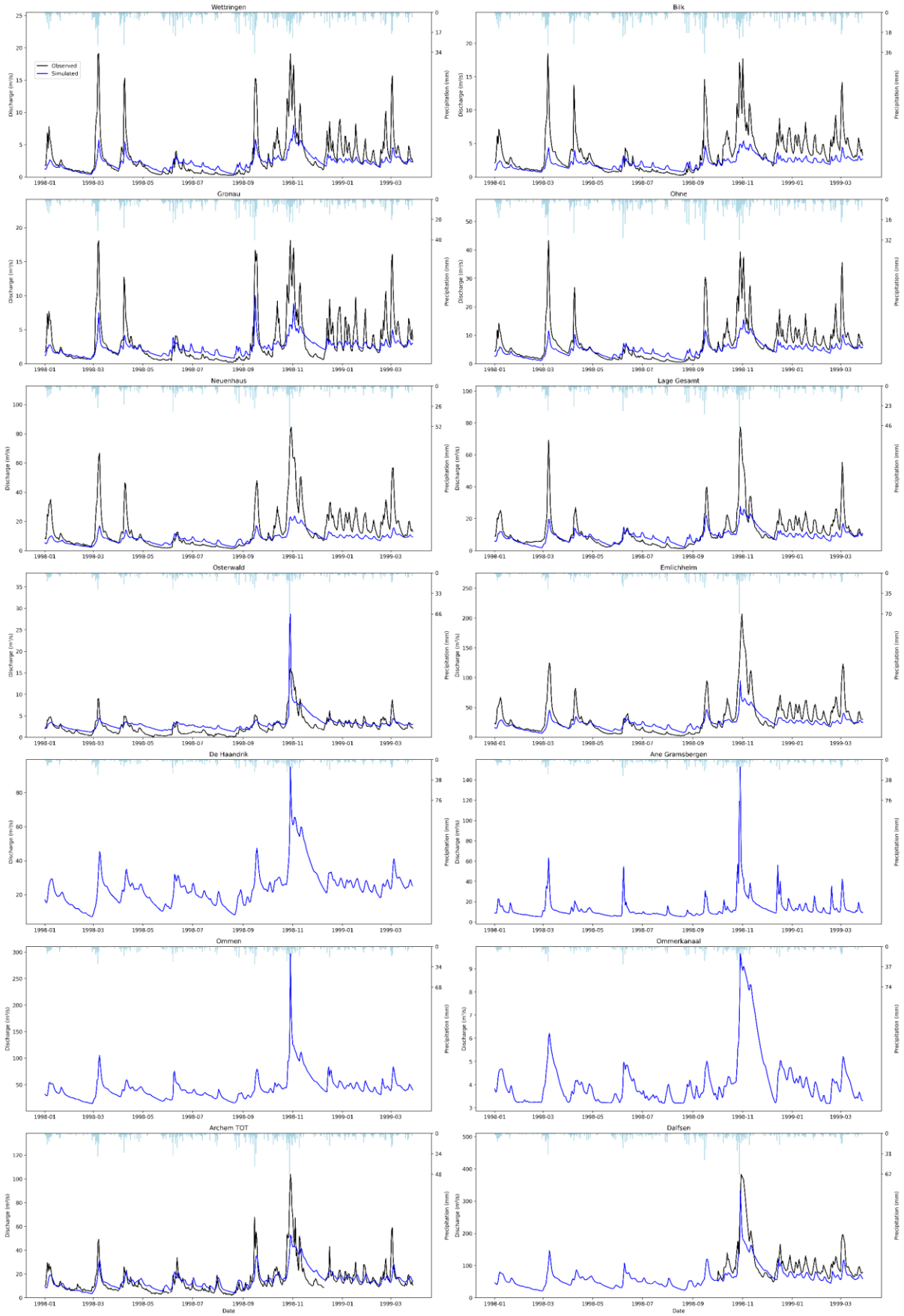

Appendix E3: Hydrographs validation 2012-2013

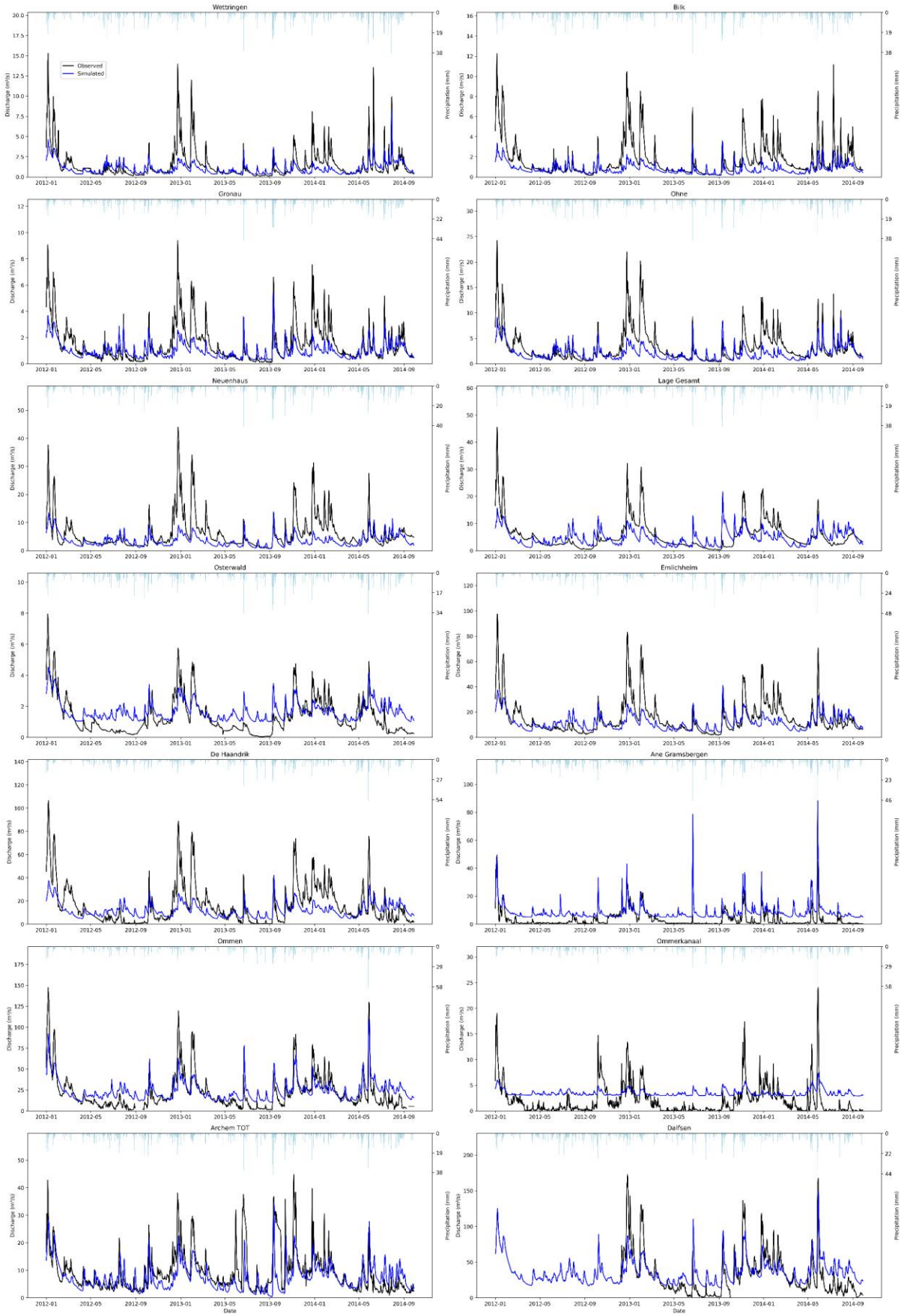

Appendix E4: Hydrographs validation 2018

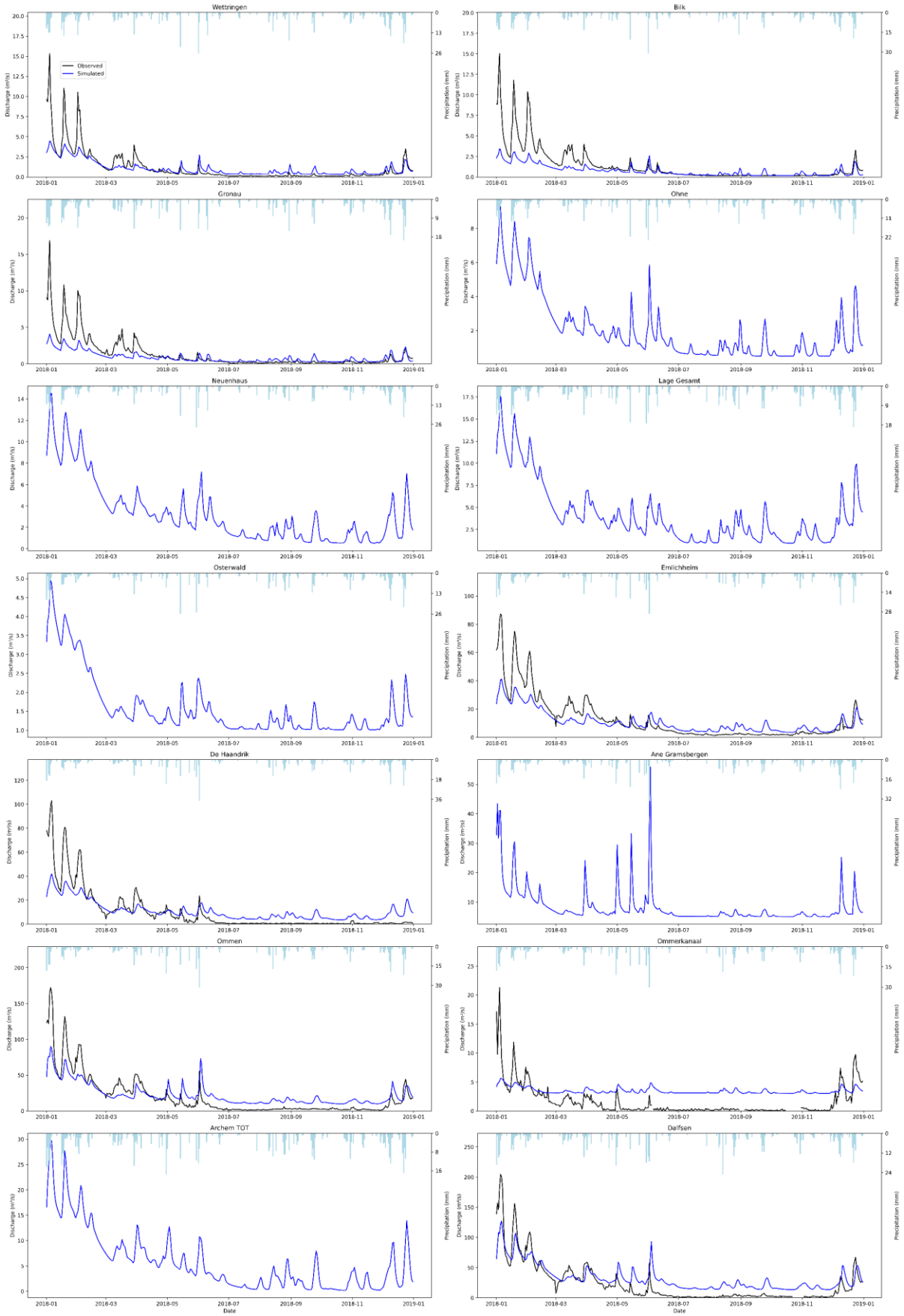

Appendix E5: Hydrographs validation 2023

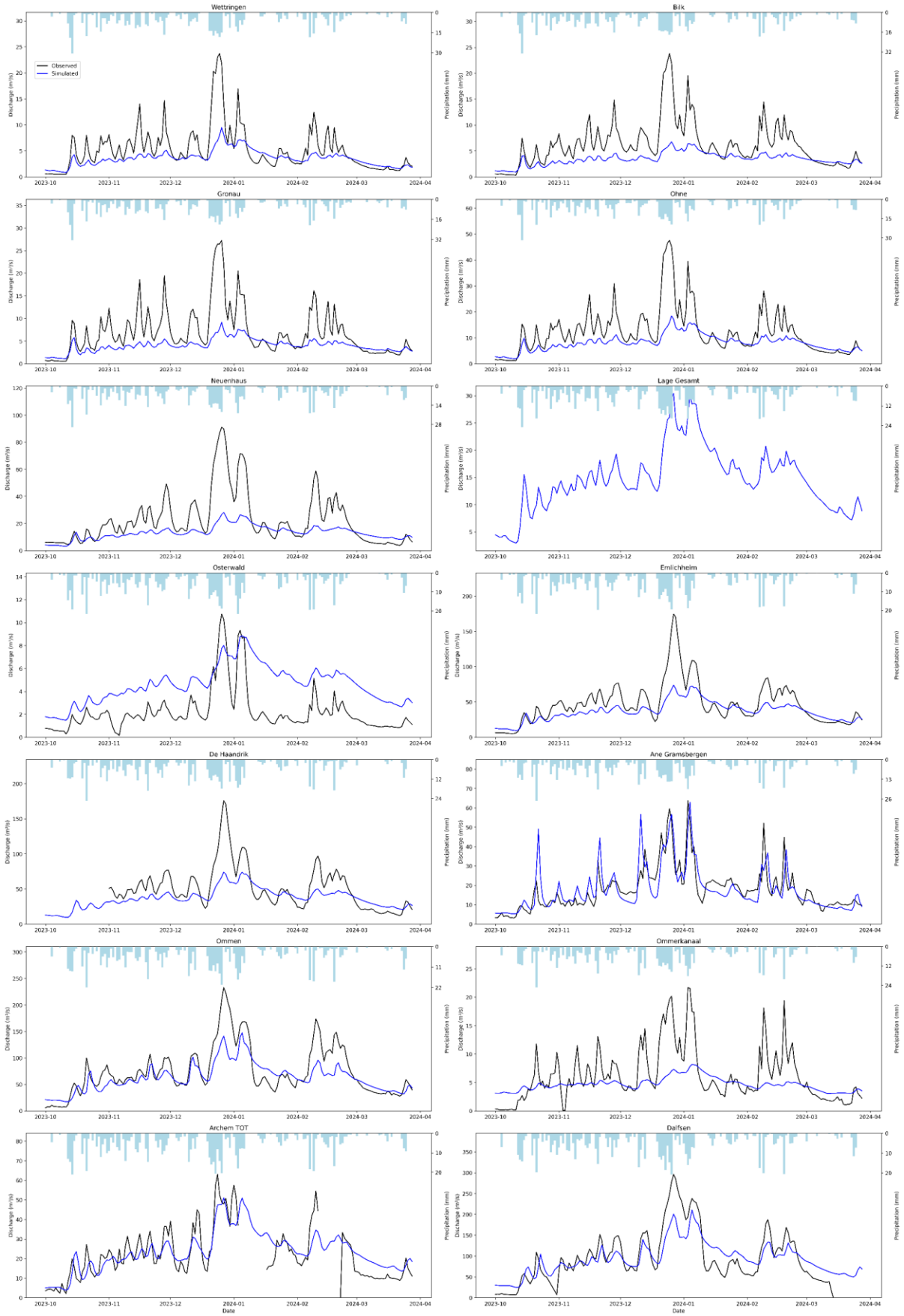

Appendix E6: Performance metric scores validation periods

Table E 1: Performance metric scores per station for validation period 1998.

		1998			
Station		**NS_{inv}**	**NS_w**	**RVE**	**OF**
Wettringen	**GE**	0.39	0.28	- 27 %	0.26
Bilk	**GE**	0.43	0.08	- 39 %	0.18
Gronau	**GE**	0.28	0.37	- 22 %	0.27
Ohne	**GE**	0.42	0.25	- 30 %	0.26
Neuenhaus	**GE**	0.52	0.14	- 39 %	0.24
Lage Gesamt	**GE**	0.34	0.34	- 24 %	0.28
Osterwald	**GE**	-0.04	0.59	27 %	0.21
Emlichheim	**GE**	0.30	0.36	- 25 %	0.27
De Haandrik	**NL**				
Ane Gramsbergen	**NL**				
Ommen	**NL**				
Ommerkanaal	**NL**				
Archem TOT	**NL**	0.44	0.60	2 %	0.51

Table E 2: Performance metric scores per station for validation period 2012-2013.

		2012-2013			
Station		**NS_{inv}**	**NS_w**	**RVE**	**OF**
Wettringen	**GE**	0.29	0.27	- 31 %	0.22
Bilk	**GE**	-0.51	0.07	- 51 %	-0.14
Gronau	**GE**	0.11	0.32	- 33 %	0.16
Ohne	**GE**	0.38	0.23	- 35 %	0.23
Neuenhaus	**GE**	0.16	0.08	- 41 %	0.09
Lage Gesamt	**GE**	0.10	0.39	- 14 %	0.22
Osterwald	**GE**	-0.13	0.70	27 %	0.22
Emlichheim	**GE**	0.32	0.34	- 21 %	0.27
De Haandrik	**NL**	-0.07	0.25	- 24 %	0.07
Ane Gramsbergen	**NL**	-0.05	0.66	150 %	0.12
Ommen	**NL**	-0.12	0.69	15 %	0.25
Ommerkanaal	**NL**	0.00	0.44	76 %	0.13
Archem TOT	**NL**	-2.05	0.26	- 20 %	-0.75

Table E 3: Performance metric scores per station for validation period 2018.

		2018			
Station		**NS_{inv}**	**NS_w**	**RVE**	**OF**
Wettringen	**GE**	-0.11	0.49	- 13 %	0.17
Bilk	**GE**	-0.98	0.29	- 45 %	-0.24
Gronau	**GE**	-0.62	0.36	- 36 %	-0.09
Ohne	**GE**				
Neuenhaus	**GE**				
Lage Gesamt	**GE**				
Osterwald	**GE**				
Emlichheim	**GE**	0.16	0.61	- 15 %	0.34
De Haandrik	**NL**	-0.66	0.59	8 %	-0.03
Ane Gramsbergen	**NL**				
Ommen	**NL**	-0.46	0.69	12 %	0.11
Ommerkanaal	**NL**	-0.30	0.44	108 %	0.03
Archem TOT	**NL**				

Table E 4: Performance metric scores per station for validation period 2023

		2023			
Station		**NS_{inv}**	**NS_w**	**RVE**	**OF**
Wettringen	**GE**	0.61	0.21	- 30 %	0.31
Bilk	**GE**	0.53	-0.10	- 41 %	0.15
Gronau	**GE**	0.61	0.00	- 39 %	0.22
Ohne	**GE**	0.71	0.15	- 31 %	0.33
Neuenhaus	**GE**	0.39	0.06	- 37 %	0.16
Lage Gesamt	**GE**				
Osterwald	**GE**	-0.45	0.42	108 %	-0.01
Emlichheim	**GE**	0.67	0.38	- 20 %	0.43
De Haandrik	**NL**	0.23	0.33	- 19 %	0.23
Ane Gramsbergen	**NL**	0.68	0.72	1 %	0.69
Ommen	**NL**	0.48	0.56	- 14 %	0.45
Ommerkanaal	**NL**	-0.04	0.07	- 21 %	0.01
Archem TOT	**NL**	0.67	0.74	2 %	0.70

Appendix F – Selection and literature review of NBS

Appendix F1: Selection of nature-based solutions

Table F 1 provides an overview of NBS within the groups land use & cover changes and improving soil conditions that have been assessed for feasibility and compatibility with the LISFLOOD-OS model.

Table F 1: Nature-based solutions within groups land use & cover changes and improving soil conditions; adapted from Raška et al. (2022) and Burges-Gamble et al. (2018).

Land use & cover changes	Improving soil conditions
(Re-) forestation	Increasing soil organic matter
Agroforestry	Supporting deep infiltration
Grassing	Reducing soil erosion by vegetation cover
Vegetation filter strips	Soil aeration and subsoiling
Supporting woodland buffer zones and riparian forests	Conservation tillage
Delimiting agricultural floodable land	Stocking density
Multifunctional agriculture	Crop rotation
Landscape features such as hedges and buffer strips	Early sowing winter crops and cover crops

Feasibility in the Vecht catchment was assessed based on the applicability of the measures to current land use practices. Given the large proportion of agricultural land in the catchment (38%), the selected NBS primarily target interventions that can be applied effectively on farmland.

Compatibility with the LISFLOOD-OS model was determined by evaluating whether the effects of the measures could be adequately parameterised within the modelling framework. The spatial resolution of 200 m x 200 m limits the implementation of small-scale, highly localised interventions such as vegetation filter strips. Furthermore, the static nature of the input maps in LISFLOOD-OS means that time-variable measures such as crop rotation could not be incorporated into the scenarios.

Appendix F2: Literature review on the effects of the selected NBS

(Re-) forestation

The parameter adjustments for reforestation were guided by various studies that compared forested areas to pastures, croplands, and other land uses. Reported effects on saturated hydraulic conductivity (ksat in LISFLOOD-OS) varied between studies depending on soil depth, vegetation type, and land use history. Zimmermann et al. (2006) found that ksat in forested areas was 8 times higher than in pastures at 12.5 cm depth and 4 times higher at 20 cm. Similarly, Lozano-Baez et al. (2019) reported a 10-fold increase in ksat for the 0–5 cm layer in forests compared to pastures, while Yao et al. (2015) observed a 3.5-fold increase in ksat across the top 100 cm in pine and poplar forests relative to farmland. Horel et al. (2015) found that ksat of the topsoil in forests was approximately twice as high as in grazing or cropland areas, and Eliasson & Larsson (2006) noted a 1.8-fold increase in ksat for forested soils versus croplands. Additionally, Li et al. (2019) observed ksat increases of 5.4, 2, and 2 times at 20, 60, and 85 cm depths, respectively, in forested soils compared to agricultural areas.

Considering these findings, the following adjustments were applied to the ksat values for newly forested cells:

- ksat in the first soil layer (0–5 cm) was multiplied by a factor of 3, reflecting significant improvements in infiltration observed in new forested areas.
- ksat in the second soil layer (5–140 cm) was multiplied by a factor of 1.5, acknowledging moderate but consistent effects extending into deeper soil.

For Manning's roughness (mannings_f), adjustments were based on the observed maximum roughness in already forest-dominated cells. The maximum roughness value in these cells was 0.14, which was adopted as the new value for all forested cells. This included both existing forest cells with roughness below 0.14 and newly created forest cells. This adjustment to existing forest cells was necessary because the interpolated Manning's roughness values derived from EFAS maps sometimes underestimated roughness in fully forested areas.

Soil aeration and subsoiling

Soil aeration and subsoiling are targeted practices for compacted agricultural soils, aiming to enhance infiltration and soil permeability. Subsoiling breaks up compacted soil at greater depths, enhancing infiltration, while grass aeration targets the topsoil to improve surface drainage with minimal disturbance to the grassland. Figure F 1 illustrates the machinery used for both practices.

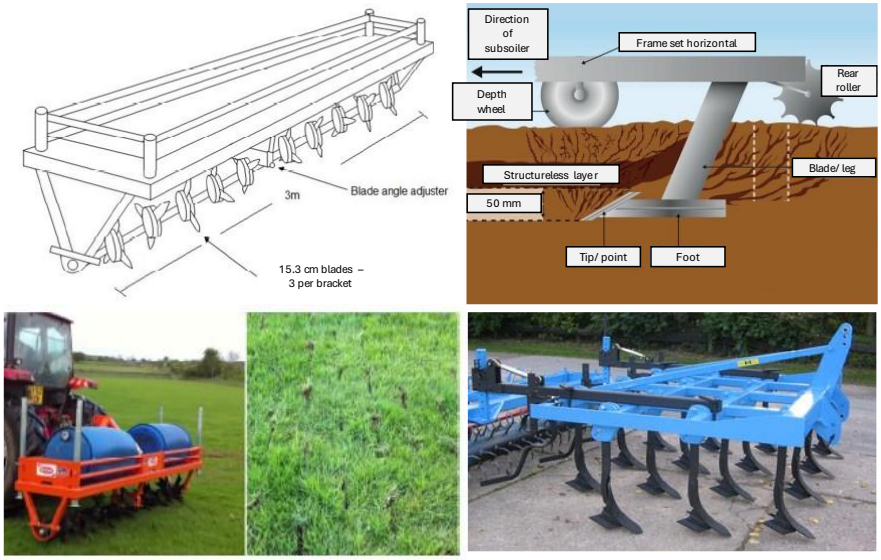

Figure F 1: Schematics and photographs of grassland aerator (left) and subsoiler (right); adapted from Smith (2012) and Agriculture and Horiculture Development Board (2024).

Studies highlight notable effects on saturated hydraulic conductivity (ksat) and saturated soil moisture content (thetas). Drewry et al. (2000) reported that subsoiling increased ksat by a factor of 4 at 5 cm depth and 5.3 at 25 cm depth, while Burgess et al. (2000) observed a 6.8-fold increase in ksat at 15–20 cm depth in aerated soils compared to non-aerated soils. Smith (2012) found that the effects of soil aeration on soil water storage capacity vary widely, with changes ranging from negligible to increases of up to 100%. These findings underscore the variability in impacts but consistently highlight improvements in soil permeability and moisture retention following aeration and subsoiling practices.

Based on these findings, parameter adjustments were determined as follows:

- ksat in the first layer (0–5 cm) was multiplied by a factor of 3 to reflect the significant mechanical disruption in this layer.
- ksat in the second layer (5–140 cm) was multiplied by a factor of 1.4, accounting for changes observed up to 25 cm depth and considering that the machinery typically does not penetrate deeper than approximately 40 cm.
- Saturated soil moisture content (thetas) in the topsoil layer was multiplied by a factor of 1.2, representing a conservative estimate between negligible effects and the maximum reported increases.
- For the second soil layer, thetas was multiplied by a factor of 1.05, reflecting minor changes while ensuring realistic adjustments based on current values.

Conservation tillage

Conservation tillage, which includes practices like reduced ploughing, is designed to minimize soil disturbance, improving soil permeability and infiltration capacity over time. The literature highlights moderate effects on saturated hydraulic conductivity (ksat) and slight increases in soil moisture content (thetas). He et al. (2009) reported a 1.2-fold increase in ksat at 0–15 cm depth and a 4-fold increase at 15–30 cm depth under no-tillage practices compared to conventional tillage, along with increases in thetas by factors of 1.07 at 0–5 cm, 1.05 at 5–10 cm, and 1.11 at 20–30 cm. Similarly, Maulé & Reed (1993) observed a 4.5-fold increase in ksat at 0–10 cm depth and a 2-fold increase at 10–30 cm under no-tillage systems. Fér et al. (2020) further highlighted a 1.4-fold increase in thetas at 5 cm depth

between tillage and conventional tillage practices, emphasizing the positive effects of conservation tillage on soil moisture retention and permeability.

Considering these findings, parameter adjustments were determined as follows:

- ksat in the first soil layer (0–5 cm) was multiplied by a factor of 1.5, reflecting improvements due to reduced soil compaction and enhanced infiltration.
- ksat in the second layer (5–140 cm) was multiplied slightly by a factor of 1.05, acknowledging minimal but notable effects extending into deeper soil.
- thetas in the first layer was multiplied by a factor of 1.1, reflecting modest gains in soil moisture retention.
- thetas in the second layer was adjusted minimally, with a multiplication factor of 1.02, as the impacts of conservation tillage diminish with depth.

These parameter adjustments account for the cumulative benefits of conservation tillage practices while maintaining a realistic representation of their hydrological impacts.

Stocking density

Adjustments to stocking density aim to mitigate the effects of soil compaction caused by livestock grazing. McCullough et al. (2001) observed a 7.5-fold increase in ksat at 15 cm depth after nine months in a highly compacted feedlot, highlighting the substantial effects of extreme grazing intensity. Dormaar et al. (1989) reported a 1.4-fold increase in ksat at 0–6 cm depth when comparing ungrazed areas to short-duration grazing systems. Daniel et al. (2002) examined varying stocking densities and found ksat values 4.1 to 5.3 times lower in low- to high-intensity grazing systems (12.5–50 cows/ha) compared to ungrazed areas.

Considering these findings, the following parameter adjustments were applied:

- ksat in the first soil layer (0–5 cm) was multiplied by a factor of 2, reflecting moderate improvements in infiltration due to reduced compaction from optimized stocking density. This adjustment is higher than for conservation tillage, as grazing impacts are more distributed across the field, whereas tillage primarily affects the wheel tracks.
- ksat in the second layer (5–140 cm) was multiplied slightly by a factor of 1.02, acknowledging the minimal effects of livestock weight at deeper depths.

These parameter adjustments align with previous adjustments made for other NBS measures, maintaining consistency across the LISFLOOD-OS model and reflecting hydrological improvements reported in the literature.

Appendix G – Hydrographs and water balance components

Appendix G1: Hydrographs at Emlichheim

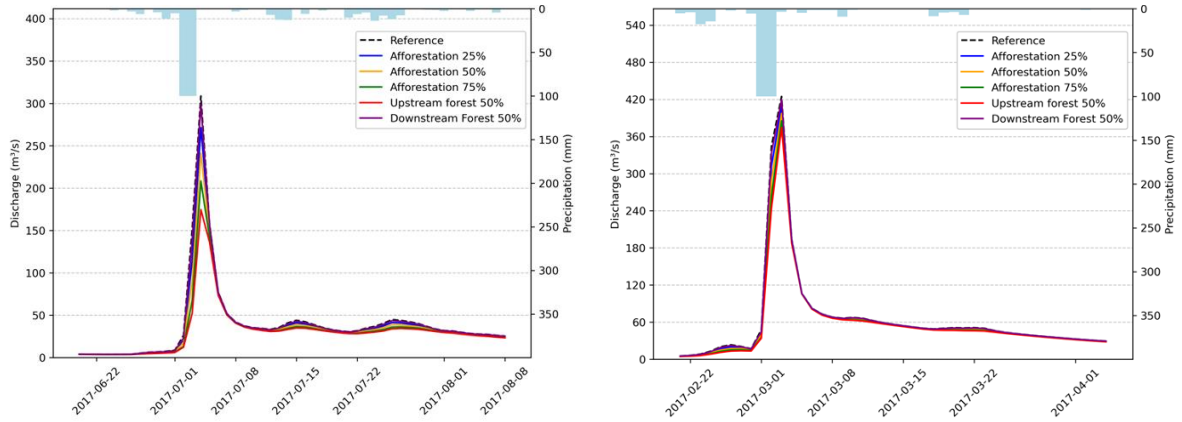

(a) *(b)*

Figure G 1: Hydrographs at Emlichheim for soil improvement scenarios under summer (a) and winter (b) conditions with a uniform 2-daily rain event of 100 mm/day.

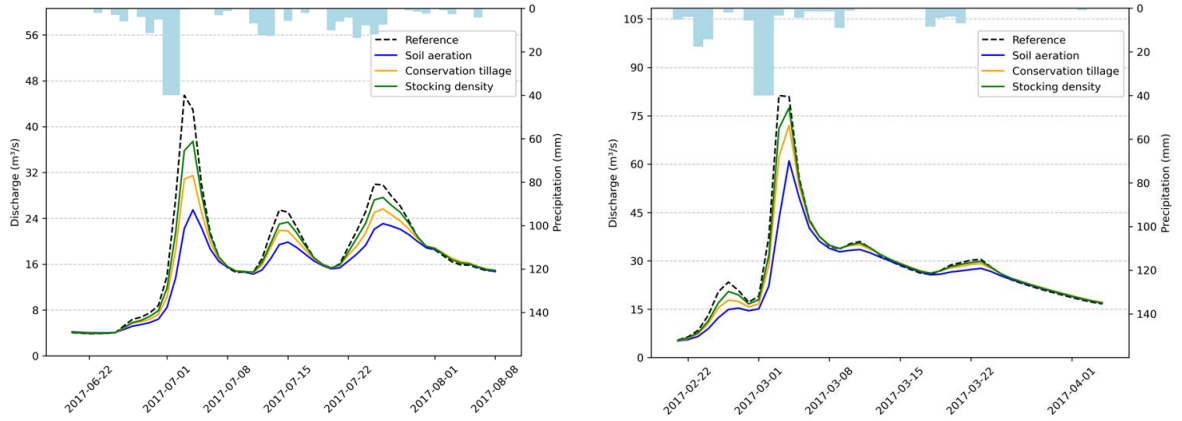

(a) *(b)*

Figure G 2: Hydrographs at Emlichheim for soil improvement scenarios under summer (a) and winter (b) conditions with a uniform 2-daily rain event of 40 mm/day.

Appendix G2: Water balance components

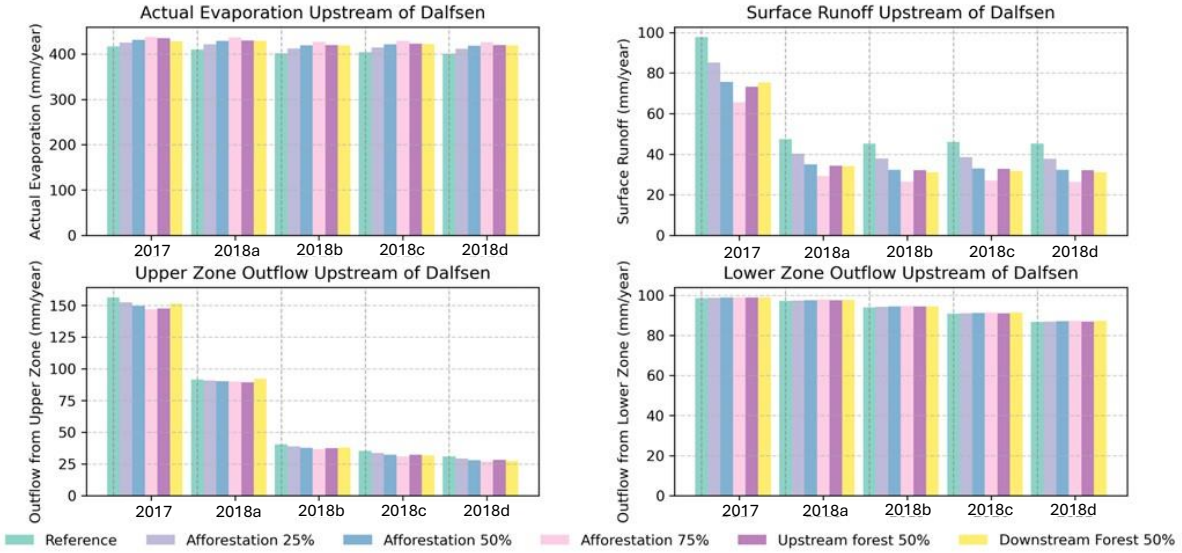

Figure G 3: Modelled water balance components yearly totals per afforestation scenario; computed for 2-daily summer rain peak of 100 mm/day and for area upstream of Dalfsen.